PB87-145645

Establishment of Design Criteria for Optimum Burners for Application to Heavy Fuel Fired Package Boilers. Volume 2 Pilot Scale Tests

Energy and Environmental Research Corp.
Irvine, CA

Prepared for

Environmental Protection Agency
Research Triangle Park, NC

Nov 86

U.S. Department of Commerce
National Technical Information Service
NTIS

PB87-145645

EPA/600/7-86/044b
November 1986

THE ESTABLISHMENT OF DESIGN CRITERIA FOR OPTIMUM BURNERS FOR APPLICATION TO HEAVY FUEL FIRED PACKAGE BOILERS

Volume II. Pilot Scale Tests

by:

G. C. England, D. W. Pershing, and M. P. Heap
Energy and Environmental Research Corporation
18 Mason
Irvine, California 92718-4190

EPA Contract 68-02-3125

Project Officer, W. S. Lanier
U. S. Environmental Protection Agency
Air and Energy Engineering Research Laboratory
Research Triangle Park, North Carolina 27711

AIR AND ENERGY ENGINEERING RESEARCH LABORATORY
OFFICE OF RESEARCH AND DEVELOPMENT
U.S. ENVIRONMENTAL PROTECTION AGENCY
RESEARCH TRIANGLE PARK, NC 27711

REPRODUCED BY
U.S. DEPARTMENT OF COMMERCE
NATIONAL TECHNICAL
INFORMATION SERVICE
SPRINGFIELD, VA. 22161

TECHNICAL REPORT DATA

(Please read Instructions on the reverse before completing)

1. REPORT NO.
EPA/600/7-86/044b

2.

3. RECIPIENT'S ACCESSION NO.
PB87 145645/AS

4. TITLE AND SUBTITLE
The Establishment of Design Criteria for Optimum Burners for Application to Heavy Fuel Fired Package Boilers; Volume II. Pilot Scale Tests

5. REPORT DATE
November 1986

6. PERFORMING ORGANIZATION CODE

7. AUTHOR(S)
G. C. England, D. W. Pershing, and M. P. Heap

8. PERFORMING ORGANIZATION REPORT NO.

9. PERFORMING ORGANIZATION NAME AND ADDRESS
Energy and Environmental Research Corporation
18 Mason
Irvine, California 92714

10. PROGRAM ELEMENT NO.

11. CONTRACT/GRANT NO.
68-02-3125

12. SPONSORING AGENCY NAME AND ADDRESS
EPA, Office of Research and Development
Air and Energy Engineering Research Laboratory
Research Triangle Park, NC 27711

13. TYPE OF REPORT AND PERIOD COVERED
Final; 1980 - 1982

14. SPONSORING AGENCY CODE
EPA/600/13

15. SUPPLEMENTARY NOTES AEERL project officer W. S. Lanier is no longer with the Agency; for details, contact Joseph A. McSorley, Mail Drop 65, 919/541-2920. Volume I is Laboratory Scale Tests.

16. ABSTRACT

The report gives results of a research program to develop low-NOx heavy oil burners for application to industrial package boilers. Volume I documents Phase 1 of the program, bench scale studies which defined optimum conditions for two-stage combustion. This information led to a conceptual two-stage low-NOx burner design. Volume II gives results of pilot scale experiments conducted in two test facilities with nominal capacities of 0.9 and 2.9 MWt, including tests of commercial burners for both firetube and watertube boilers. A wide range of petroleum-, coal-, and shale-derived fuels were investigated. Tests were also conducted with prototype advanced low-NOx burners which demonstrated that NOx emissions below 100 ppm (corrected to 0% O_2) could be achieved almost independently of the bound nitrogen content in the fuel. The conceptual design was successfully scaled from 21 kWt to 0.9 MWt to 2.9 MWt with similar NOx emissions performance.

17. KEY WORDS AND DOCUMENT ANALYSIS

a. DESCRIPTORS		b. IDENTIFIERS/OPEN ENDED TERMS	c. COSATI Field/Group	
Pollution	Combustion	Pollution Control	13B	21B
Burners		Stationary Sources	13A	
Design		Burner Design	14G	
Boilers		Package Boilers		
Nitrogen Oxides		Staged Combustion	07B	
Heavy Oils			11G	

18. DISTRIBUTION STATEMENT
Release to Public

19. SECURITY CLASS (This Report)
Unclassified

20. SECURITY CLASS (This page)
Unclassified

21. NO. OF PAGES
158

22. PRICE

EPA Form 2220-1 (9-73)

PREFACE TO VOLUME II

This final report is the second of two volumes describing the work carried out under EPA Contract 68-02-3125. Volume I includes bench scale (21 kW) experimental results and reviews commercial package boiler/burner designs. Volume II includes results of two pilot scale experiments (1 MW and 3 MW), an overall summary of the results, and conclusions with respect to optimum burner designs.

Preceding page blank

TABLE OF CONTENTS

Section Page

1.0 SUMMARY 1-1

1.1 Background 1-1
1.2 Bench Scale Studies 1-4
1.3 Pilot Scale Studies 1-14

2.0 FIRETUBE BURNER 2-1

2.1 Firetube Boiler Simulator Facility 2-1
2.2 Evaluation of Commercial Burner A 2-3
  2.2.1 Baseline Characterization 2-9
  2.2.2 Fuel Effects 2-28
  2.2.3 Staged Combustion 2-28
2.3 Evaluation of Commercial Burner B 2-33
  2.3.1 Baseline Characterization 2-31
2.4 Experimental Prototype Low-NO_x Oil Burner 2-44
  2.4.1 First-Stage Parameters 2-54
  2.4.2 Second-Stage Parameters 2-70
  2.4.3 Process Parameters 2-77
  2.4.4 Fuel Nitrogen Effects 2-79

3.0 WATERTUBE BURNER STUDIES 3-1

3.1 Small Watertube Simulator (SWS) 3-2
3.2 Commercial Watertube Burner Tests 3-7
  3.2.1 Commercial Watertube Burner Characterization . . 3-9
3.3 Distributed Mixing Burner Tests 3-20
  3.3.1 Experimental Results 3-22
3.4 Advanced Prototype Burner Tests 3-25

4.0 REFERENCES 4-1

Preceding page blank

LIST OF FIGURES

Figure Page

1-1 NO_x emissions and fuel N conversion under unstaged conditions (bench scale) 1-7

1-2 The effect of fuel type and stoichiometry on the production of TFN (XN) for (a) petroleum oils and (b) alternate fuels 1-9

1-3 The effect of fuel bound nitrogen content on exhaust NO_x and TFN (XN) in the primary zone at $SR_1 = 0.7$ (3 percent overall excess O_2) 1-10

1-4 The influence of fuel-rich holdup zone temperature profile on exhaust NO_x 1-12

1-5 CO oxidation and decay of XN species for hot and cool primary zone temperature profiles 1-13

1-6 NO_x versus smoke emissions for (a) commercial watertube burner and (b) distributed mixing burner (3 MW_t) 1-16

1-7 Prototype burners and experimental test furnaces 1-20

1-8 Influence of first-stage stoichiometry on NO_x, CO, and smoke emissions (bench scale and pilot scale, California residual fuel oil) 1-21

1-9 Effect of first-stage residence time on exhaust NO_x emissions and TFN decay for bench scale, small pilot scale (SP), and intermediate pilot scale (IP) staged combustors 1-23

1-10 Effect of fuel nitrogen content on NO_x emissions from (a) all bench scale and pilot scale burners tested and (b) low-NO_x prototype burners 1-25

2-1 Firetube boiler simulator facility 2-2

2-2 (A) Firetube boiler simulator, (B) gas fuel system, (C) liquid fuel system 2-4

2-3 Exhaust sampling system used on firetube boiler simulator 2-6

2-4 Commercial Burner A 2-8

LIST OF FIGURES (Continued)

Figure Page

2-5 Oil nozzle assembly--Commercial Burner A 2-10

2-6 NO_x emissions from Commercial Burner A--effect of excess air and load 2-13

2-7 Smoke emission from Commercial Burner A--effect of turndown 2-15

2-8 Approximate turndown performance for Burner A 2-16

2-9 NO_x emissions from Commercial Burner A--effect of atomizing air pressure 2-17

2-10 Smoke emissions from Commercial Burner A--effect of atomizing air pressure 2-18

2-11 Effect of oil temperature on NO_x emissions from Burner A . . 2-19

2-12 Pressure characteristics of Burner A atomizer 2-21

2-13 Atomizing fluid consumption for Commercial Burner A 2-22

2-14 NO_x emissions from Burner A using steam as the atomizing medium 2-23

2-15 Smoke emissions from Burner A using steam as the atomizing medium 2-24

2-16 Particulate emissions and size distribution from Burner A . 2-25

2-17 Scanning electron micrographs of coarse particulate collected during SASS runs 2-26

2-18 Scanning electron micrographs of fine particulate collected in SASS runs 2-27

2-19 NO_x emissions for various fuels tested with Commercial Burner A 2-29

2-20 Smoke emissions for various fuels tested with Commercial Burner A 2-30

2-21 NO_x emissions versus fuel nitrogen content--Burner A 2-31

LIST OF FIGURES (Continued)

Figure Page

2-22 Effect of staged air addition on NO_x emissions from Commercial Burner A 2-32

2-23 Commercial Burner B 2-34

2-24 Atomizing air requirements of Burner B atomizer 2-35

2-25 NO_x emissions from Burner B as a function of heat release rate 2-37

2-26 Smoke emissions from Burner B as a function of load 2-38

2-27 Effect of atomizing air pressure on NO_x emissions from Burner B 2-39

2-28 Effect of atomizing air pressure on smoke emissions from Burner B 2-40

2-29 NO_x emissions for several fuels fired in Burner B 2-41

2-30 Smoke emissions for several fuels fired in Burner B 2-42

2-31 NO_x emissions from Burner B versus load for distillate, residual, and alternate fuel oils 2-43

2-32 Prototype firetube boiler test burner 2-47

2-33 Spray characteristics of commercial atomizers used in prototype burner 2-49

2-34 Premixer assembly for experimental prototype burner 2-51

2-35 Small pilot scale burner configurations evaluated on SWS facility 2-52

2-36 Effect of SR_1 upon NO_x emissions 2-55

2-37 Effect of SR_1 upon CO and smoke emissions 2-56

2-38 Effect of load upon NO_x emissions (staged and unstaged) . . 2-57

2-39 Effect of load on minimum NO_x and smoke emissions 2-58

2-40 Influence of primary zone length on NO_x emissions 2-60

LIST OF FIGURES (Continued)

Figure Page

2-41 Effect of atomizer type and pressure upon NO_x and smoke emissions (0.59 MW_{th}) 2-61

2-42 Influence of atomizing fluid on NO_x emissions 2-63

2-43 Influence of primary and secondary air swirl on NO_x emissions 2-64

2-44 Effect of primary fuel/air mixing on NO_x emissions with short primary zone residence time 2-65

2-45 Detailed measurements at first-stage exit--California oil at 0.59 MW_{th} (2 x 10^6 Btu/hr) 2-67

2-46 Detailed measurements at first-stage exit--California oil at 0.88 MW_{th} (3 x 10^6 Btu/hr) 2-68

2-47 Detailed measurements at first-stage exit--propane at 0.88 MW_{th} (3 x 10^6 Btu/hr) 2-69

2-48 Effect of rapid secondary air injection upon NO_x and smoke emissions (0.59 MW_{th}) 2-71

2-49 Effect of exhaust O_2 upon NO_x and smoke emissions 2-72

2-50 Influence of interstage heat extraction on NO_x 2-74

2-51 Comparison of NO_x emissions in Firetube Simulator and Small Watertube Simulator 2-75

2-52 Impact of furnace environment on emissions performance . . . 2-76

2-53 Effect of flue gas recirculation in primary and secondary air 2-78

2-54 Effect of interstage FGR injection 2-80

2-55 NO_x emissions with interstage on injection 2-81

2-56 Influence of fuel type on NO_x and smoke emissions from liquid fuels (0.59 MW) 2-83

2-57 Effect of nitrogen content upon NO_x emissions from gaseous fuels (0.59 MW) 2-84

LIST OF FIGURES (Continued)

Figure		Page
2-58	Effect of load upon thermal NO_x formation (propane)	2-85
2-59	Effect of fuel nitrogen content upon minimum NO_x emissions (0.59 MW_{th})	2-87
3-1	Small watertube boiler simulator test facility	3-3
3-2	Continuous gas analyzer sample train	3-5
3-3	Commercial watertube boiler burner	3-8
3-4	Atomizer assemblies used in commercial watertube boiler burner	3-10
3-5	Effect of excess oxygen for distillate, residual, and shale derived fuel oils fired in commercial watertube burner (3.1 MW, uninsulated furnace)	3-12
3-6	Effect of excess oxygen for different fuels fired in commercial watertube burner (3.3 MW, insulated furnace) . .	3-14
3-7	Commercial watertube burner--effect of load (No. 2 oil) . .	3-15
3-8	Commercial watertube burner--effect of load (No. 6 oil) . .	3-17
3-9	Commercial watertube burner--effect of load (residual shale oil)	3-18
3-10	Commercial watertube burner--effect of register variations on NO_x vs. smoke emissions (No. 6 oil)	3-19
3-11	2.9 MW distributed mixing burner	3-21
3-12	Effect of burner zone stoichiometry on NO_x emissions with DMB	3-23
3-13	Optimum NO_x emissions from DMB	3-24
3-14	3.5 MW_{th} experimental prototype burner	3-26
3-15	Effect of load and primary air preheat on NO_x emissions . .	3-27
3-16	Effect of load and primary air preheat on smoke emissions	3-28

LIST OF FIGURES (Concluded)

Figure		Page
3-17	Effect of annular air and air distribution	3-30
3-18	Influence of excess air on second-stage NO_x	3-32
3-19	Influence of first-stage stoichiometry on NO_x, CO, and smoke emissions (bench scale and pilot scale, California residual fuel oil)	3-33

LIST OF TABLES

Table		Page
1-1	ANALYSIS OF ALL FUELS EVALUATED IN BENCH SCALE STUDIES . . .	1-5
1-2	DESIGN CRITERIA FOR SCALEUP OF LOW-NO_x CONCEPT	1-18
2-1	NOMINAL PERFORMANCE SPECIFICATIONS FOR FIRETUBE BOILER SIMULATOR	2-5
2-2	CONTINUOUS GAS ANALYZERS	2-7
2-3	SUMMARY OF TEST CONDITIONS FOR BURNER A BASELINE CHARACTERIZATION	2-11
2-4	FUEL ANALYSES	2-12
2-5	DESIGN CRITERIA FOR SCALEUP OF LOW-NO_x CONCEPT	2-46
2-6	FUEL ANALYSIS	2-53
3-1	NORMAL SPECIFICATIONS OF SWS TEST FURNACE	3-4
3-2	CONTINUOUS EMISSIONS ANALYZERS USED FOR FLUE GAS ANALYSIS	3-6
3-3	FUEL PROPERTIES	3-11

1.0 SUMMARY

This report describes results of a research program to develop low-NO_x heavy oil burners for application to industrial package boilers. Bench scale studies (England et al, 1982) have been conducted which define the mechanisms of NO_x formation and control during staged combustion. These studies showed that greater than 80 percent of total NO_x emissions can be due to conversion of fuel-bound nitrogen to NO_x. Conceptual design criteria were established based on these bench scale studies for an optimized two-stage combustion system which minimizes NO_x emissions from both conversion of fuel-bound nitrogen and from molecular nitrogen in the combustion air.

The first phase of this program has been documented in Volume I of this Final Report. The Volume I report documents the bench scale studies which defined optimum conditions for two-stage combustion. This information led to a conceptual two-stage low-NO_x burner design. This second volume contains results from the pilot scale experiments conducted in two separate test facilities with nominal capacities of 0.9 MW_t and 2.9 MW_t. The pilot scale studies included tests of commercial burners for both firetube and watertube boilers. A wide range of petroleum-, coal-, and shale-derived fuels were investigated. Tests were also conducted with prototype advanced low-NO_x burners which demonstrated that NO_x emissions below 100 ppm (corrected to 0 percent O_2) could be achieved almost independent of the bound nitrogen content in the fuel. The conceptual design was successfully scaled from 21 kW_t to 0.9 MW_t to 2.9 MW_t with similar NO_x emissions performance.

1.1 Background

Nitrogen oxides emissions from stationary combustors can be reduced by combustion modification techniques which involve staging the heat release process. However, the application of these techniques to residual fuel oil fired combustors has been only partially successful because of a tradeoff in pollutant emissions. The decrease in NO_x emissions is often accompanied by an increase in particulate emissions. The optimization of combustion modification techniques to control NO_x emissions from liquid fuel fired combustors has also proved difficult because of the limited knowledge of the controlling phenomena.

The conversion of the nitrogen contained in liquid fuels to NO_x can contribute significantly to the total NO_x emissions when such fuels are burned in stationary combustors. The amount of fuel NO (NO produced from fuel nitrogen) increases with increasing fuel nitrogen content. The other contribution to NO_x emissions, thermal NO (produced from molecular nitrogen) is dependent primarily on temperature and oxygen availability and is relatively insensitive to fuel properties. Thus, as fuel nitrogen content increases fuel NO constitutes an increasing fraction of the total emission. The formation of thermal NO is strongly dependent upon temperature; therefore, combustion firing density and heat extraction control the amount of thermal NO produced. Fuel NO formation is strongly affected by fuel/air mixing conditions and is dependent upon burner design.

There have been many studies concerned with the mechanism of fuel nitrogen oxidation which have resulted in the following simplified explanation. Initially the nitrogen in the fuel is released during thermal decomposition. The nitrogen containing hydrocarbons are pyrolized and the dominant nitrogen compound evolved is probably HCN. The fate of this HCN is then almost totally determined by the local reactant stoichiometry:

- Fuel-Lean. When oxygen is present, the formation of NO is favored. For homogeneous premixed conditions, greater than 75 percent of the fuel nitrogen could be converted to NO. The heterogeneous nature of liquid fuel combustion usually limits the conversion to less than 50 percent (unless the fuel nitrogen content is low) and this is dependent upon atomizer and air delivery system design.

- Fuel-Rich. In the absence of oxygen N_2 is favored. Under fuel-rich conditions, nitrogen exists in the gas phase mainly as NO. NH_3 or HCN and their relative concentration is dependent upon stoichiometry and temperature.

For typical fuels and combustion conditions, equilibrium TFN concentrations (the sum of NO, HCN, and NH_3 concentrations) are less than 1.0 ppm for mixtures containing between 60 and 70 percent of the theoretical air requirements. Thus, if a combustor could be operated to achieve these near-equilibrium TFN levels, fuel nitrogen conversion would be minimized.

Staged combustion is the modification of the combustion process to minimize fuel NO formation and, provided heat removal occurs in the second stage, thermal NO formation is also restricted. In staged combustion, fuel is mixed with less than the stoichiometric air requirement. These conditions maximize conversion of fuel nitrogen to N_2 prior to the addition of the remaining air to complete combustion. Staged combustion can be achieved through burner design by reducing the rate of fuel/air mixing producing a fuel-rich zone in the core of the flame, or by physically dividing the total airstream, thus giving a well-defined fuel-rich zone. Under most practical conditions the limit of NO_x control for liquid fuels by staged combustion has traditionally been dictated by the onset of smoke emissions.

The objective at the beginning of this program was to extend the studies conducted under EPA Contract No. 68-02-2624. The specific goals were:

- Document conceptual designs for low-emission heavy fuel oil burners suitable for firetube and watertube package boilers.
- Determine the optimum time/temperature/stoichiometry history during staged liquid fuel combustion in order to minimize NO_x and particulate emissions in advanced low-emission burners and combustors.
- Develop optimum atomizers for advanced low-NO_x combustors.
- Extend the prior fuel effects study to include a wide range of synthetic liquid fuels.

1.2 Bench Scale Studies

Volume I of this final report has documented the bench scale studies conducted in a 21 kW_t down-fired refractory tunnel furnace. The total range of fuels included in the fuel effects studies included 3 distillate petroleum oils, 13 petroleum-derived residual fuel oils, one heavy petroleum crude oil, and 9 coal- and shale-derived liquid fuels. Analyses for each of these fuels are presented in Table 1-1.

Fuel NO_x emission could be determined directly in the tunnel furnace by substitution of combustion air with a nitrogen-free oxidant consisting of argon, oxygen, and carbon dioxide (the furnace is dubbed the "Argon" furnace for this reason). Figure 1-1 presents total and fuel NO_x emissions for all of the fuels tested under excess air conditions. These data were taken at 5 percent excess O_2, 132°C air preheat and 0.53 cc/sec firing rate. An ultrasonic fuel atomizer was used with an air atomization pressure of 103 kPa (gauge). Fuel viscosity was maintained at 12 centistokes by appropriate selection of fuel temperature. Total NO_x refers to emissions produced with air as the oxidant. Fuel NO_x is defined as the emissions measured when burning the fuel in the argon/oxygen/carbon dioxide mixture. Both total and fuel NO_x emissions increase with increasing fuel nitrogen content. The difference between total and fuel NO_x is defined to be thermal NO_x which is approximately constant for all of the heavy residual oils. In general, alternative fuels have higher nitrogen contents than petroleum-derived fuels and therefore produce higher fuel NO_x emissions. With few exceptions, fuel NO_x emissions from both alternative and petroleum-derived fuels appear to correlate well on the basis of fuel-nitrogen content. The total NO_x emissions from alternative fuels (dashed line) are higher than from pure petroleum-derived fuels which suggests a greater production of thermal NO_x. Distillation results indicate that both total mass and nitrogen are evolved for these alternative fuels at significantly lower temperatures than for the petroleum-derived residual fuel oils. Thermal NO formation may be increased for these fuels because of higher peak flame temperatures in the early portion of the flame since more fuel is burned prior to vitiation of the

TABLE 1-1. ANALYSIS OF ALL FUELS EVALUATED IN BENCH SCALE STUDIES

	D1	D2	D3	R1	R2	R3	R4	R5	R6	R7	R8	R9	R10
	Alaskan Diesel	W. Texas Diesel	California No. 2 Oil	East Coast	Middle East	Low Sulfur No. 6 Oil	Indo/Malaysian	Venezuelan Desulfurized	Pennsylvania (Amarada Hess)	Gulf Coast	Venezuelan	Alaskan	California
Symbol	◆	▲	◑	⬡	◺	✙	△	∩	◺	◇	∩	□	▽
Ultimate Analysis:													
Carbon, %	86.99	88.09	86.8	86.54	86.78	86.57	86.53	85.92	84.82	84.62	85.24	86.04	85.75
Hydrogen, %	12.07	9.76	12.52	12.31	11.95	12.52	11.93	12.05	11.21	10.77	10.98	11.18	11.83
Nitrogen, %	0.008	0.026	0.053	0.16	0.18	0.22	0.24	0.24	0.34	0.36	0.40	0.51	0.62
Sulfur, %	0.31	1.88	0.27	0.36	0.67	0.21	0.22	0.93	2.26	2.44	2.22	1.63	1.05
Ash, %	<.001	<.001	<.001	0.023	0.012	0.02	0.036	0.033	0.067	0.027	0.081	0.034	0.038
Oxygen, %	0.62	0.24	0.36	0.61	0.41	0.46	1.04	0.83	1.3	1.78	1.10	0.61	0.71
Conradson Carbon Residue, % *				2.1	6.0	4.4	3.98	5.1	12.4	14.8	6.8	12.9	
Asphaltene, %				0.34	3.24	0.94	0.74	2.59	4.04	7.02	8.4	5.6	
Flash Point, °F				205	350	325	210	176	275	155	210	215	
Pour Point, °F				50	45	105	61	48	66	40	58	38	
API Gravity at 60°F	33.1	18.3	32.6	24.9	19.8	25.1	21.8	23.3	15.4	13.2	14.1	15.6	19.5
Viscosity, SSU, at 140°F	33.0	32.0	30.8	131.2	490	222.4	100	113.2	1049	835	742	1,071	246.1
at 210°F	29.5	28.8	29.5	45	131.8	69.6	65	50.5	240	181	196.7	194	70.00
Heat of Combustion:													
Gross Btu/lb			19,330	19,260	19,070	19,110	19,070	18,400	18,520	18,240	18,240	18,470	
Net Btu/lb				18,140	17,980	17,970	17,980	17,300	17,500	17,260	17,400	17,580	
Calcium, ppm				7.1	1.2	9.52	14	8.7	9.2	4.4	9.1	6.9	
Iron, ppm				16	2.6	123.6	16	6.5	13.2	19	11	24	
Maganese, ppm				0.09	0.02	0.46	0.13	0.09	0.10	0.13	0.09	0.08	
Magnesium, ppm				3.7	0.08	2.23	3.6	3.6	3.3	0.4	3.8	1.4	
Nickel, ppm				6.7	13	14.10	19		32.7	29	52	50	
Sodium, ppm				37	0.98	3.74	15		64.5	3.6	32	37	
Vanadium, ppm				14	25	3.11	101		81.5	45	226	67	

* ASTM D-189

TABLE 1-1. ANALYSIS OF ALL FUELS EVALUATED IN BENCH SCALE STUDIES (Concluded)

	R11	R12	R13	R14	A1	A2	A3	A4	A5	A6	A7	A8	A9
	California	California	California	California (Kern County)	Shale-Derived DFM	Synthoil	Crude Shale	SRC II Blend	Shale Residual	SRC II	Shale Fraction (520–850°F)	Shale Fraction (+850°F)	SRC II Heavy Distillate
	○	◇	✣	⬯	◥	■	●	▲	◣	◆	◗	◓	▲
Ultimate Analysis:													
Carbon, %	85.4	85.33	86.68	86.61	86.18	86.30	84.6	89.91	86.71	85.91	85.39	85.92	88.98
Hydrogen, %	11.44	11.23	10.44	10.93	13.00	7.44	11.3	9.27	12.76	8.74	11.53	10.61	7.64
Nitrogen, %	0.77	0.79	0.86	0.83	0.24	1.36	2.08	0.45	0.46	0.96	1.92	2.49	1.03
Sulfur, %	1.63	1.60	0.99	1.16	0.51	0.80	0.63	0.065	0.28	0.30	0.72	0.63	0.39
Ash, %	0.043	0.032	0.20	0.030	0.003	1.56	.026	0.004	0.009	0.04	0.002	0.24	0.058
Oxygen, %	0.71	1.02	0.85	0.44	1.07	2.54	1.36	0.30	0.03	4.08	0.44	0.11	1.90
Conradson Carbon Residue, % *	8.72	9.22	15.2	8.3	4.1	23.9	2.9	6.18	0.19	0.51	0.07	9.3	
Asphaltene, %	5.18	5.18	8.62	3.92	0.036	16.55	1.33	4.10	0.083		0.12	4.24	
Flash Point, °F		150	180	225	182	210	250	70	235	173	255	370	265
Pour Point, °F	38	30	42	65	40	80	80	<−72	90	−55	70	95	8
API Gravity at 60°F	15.4	15.1	12.6	12.3	33.1	S=1.14	20.3	10.0	29.0		22.3	12.0	1.3
Viscosity, SSU, at 140°F	854	748.0	720	4630	36.1	10,880	97	40.6	54.3	39	62.9	3050	67.2
at 210°F	129	131.6	200	352	30.7	575	44.1	32.5	37.3		41.8	490	41.3
Heat of Combustion:													
Gross Btu/lb	18,470	18,460	18,230	18,430	19,430	16,480	18,290	17,980	19,350	17,100	18,520	18,000	17,120
Net Btu/lb	17,430	17,440	17,280	17,430	18,240	15,800	17,260	17,130	18,190		17,470	17,030	16,240
Calcium, ppm	21	14	90.6	4.4	0.13	1,670	1.5	0.33	4.20		<0.5	238	
Iron, ppm	73	53	77.2	15	6.3	109	47.9	3.9	<0.5		2.9	86	
Manganese, ppm	0.8	0.1	0.87	0.15	0.06	6.2	0.17	<0.5	<0.5		0.033	1.3	
Magnesium, ppm	5.1	3.8	31.4	1.1		170	5.40	0.17	0.15		0.021	51	
Nickel, ppm	65	82	88.0	68	0.43	2.6	5.00	<0.5	<0.5		<0.5	7.4	
Sodium, ppm	21	2.6	22.3	3.4	0.09	148	11.71	0.31	2.51		<0.1	11	
Vanadium, ppm	44	53	66.2	39	<.1	6.5	<.3	<1.0	<1.0		<0.2	1.1	

* ASTM D-189

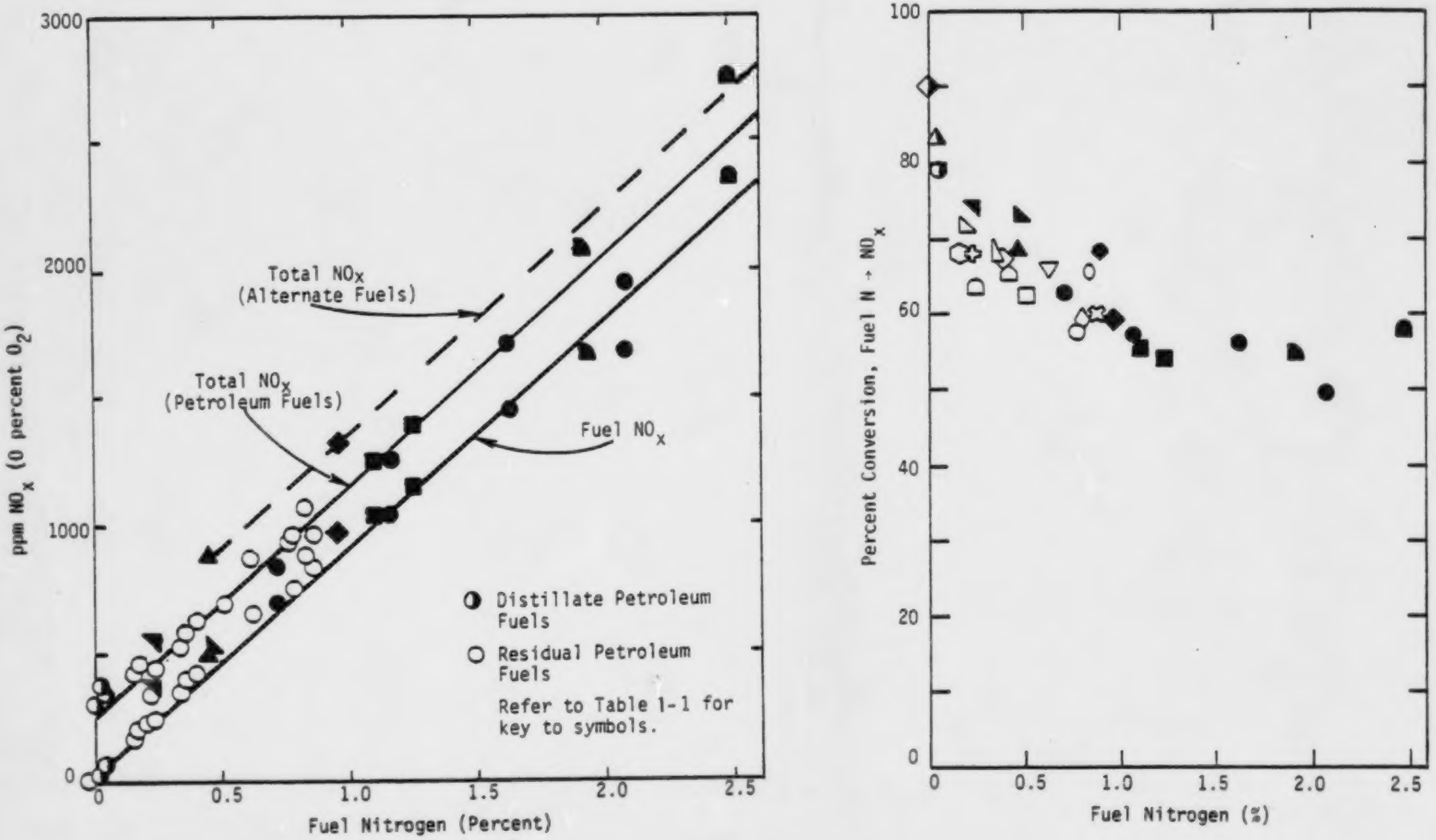

Figure 1-1. NO_x emissions and fuel N conversion under unstaged conditions (bench scale).

combustor air with recirculated combustion products, or because the relatively high vaporization rates produce higher local combustion intensities.

Figure 1-2 shows the TFN level measured at the exit of the fuel-rich first zone as a function of first-stage stoichiometric ratio (SR_1) for the Alaskan diesel oil, three petroleum-derived liquid fuels, three alternate liquid fuels, and methane doped with 0.79 percent nitrogen (by weight) as ammonia. All fuels investigated showed similar trends. TFN concentration decreased with decreasing SR_1 and minimized at approximately $SR_1 = 0.8$. TFN increased significantly as the primary zone stoichiometry was further reduced. TFN for both the ammonia-doped methane and the fuel oil with similar nitrogen content (R-14) showed similar characteristics under fuel-lean conditions. However, below $SR_1 = 0.7$ the heavy oil produced significantly less TFN than the gaseous fuel. These results suggest that although the impact of fuel composition is reduced under staged conditions there can still be a significant impact on NO_x emissions.

The ultimate level of exhaust NO_x produced during staged combustion results from conversion of TFN exiting the first stage and any thermal NO_x production which occurs during burnout. Second-stage thermal NO_x production was not considered to be significant in this study because changes in heat extraction during burnout had almost no effect on final emissions. Figure 1-3 shows minimum exhaust NO_x and TFN level at the exit of the first stage as a function of total fuel-nitrogen content for seven liquid fuels and the methane-ammonia mixture. In general, the minimum exhaust NO_x concentration occurred at $SR_1 = 0.78 \pm 0.02$. NO_x emissions (and TFN) under staged conditions correlate well with total fuel-nitrogen content, but the slope is significantly less than under excess air conditions. Only the SRC-II heavy distillate exhibited unusually high emissions, and this was the direct result of the high TFN yield. NO, NH_3 and HCN were also substantially higher at the optimum stoichiometry for this fuel than with fuels with comparable nitrogen content. The increased TFN may be the result of basic chemical bonding differences between the parent coal from which the SRC-II was derived, and petroleum liquids. Since this fuel was not tested at pilot scale, this

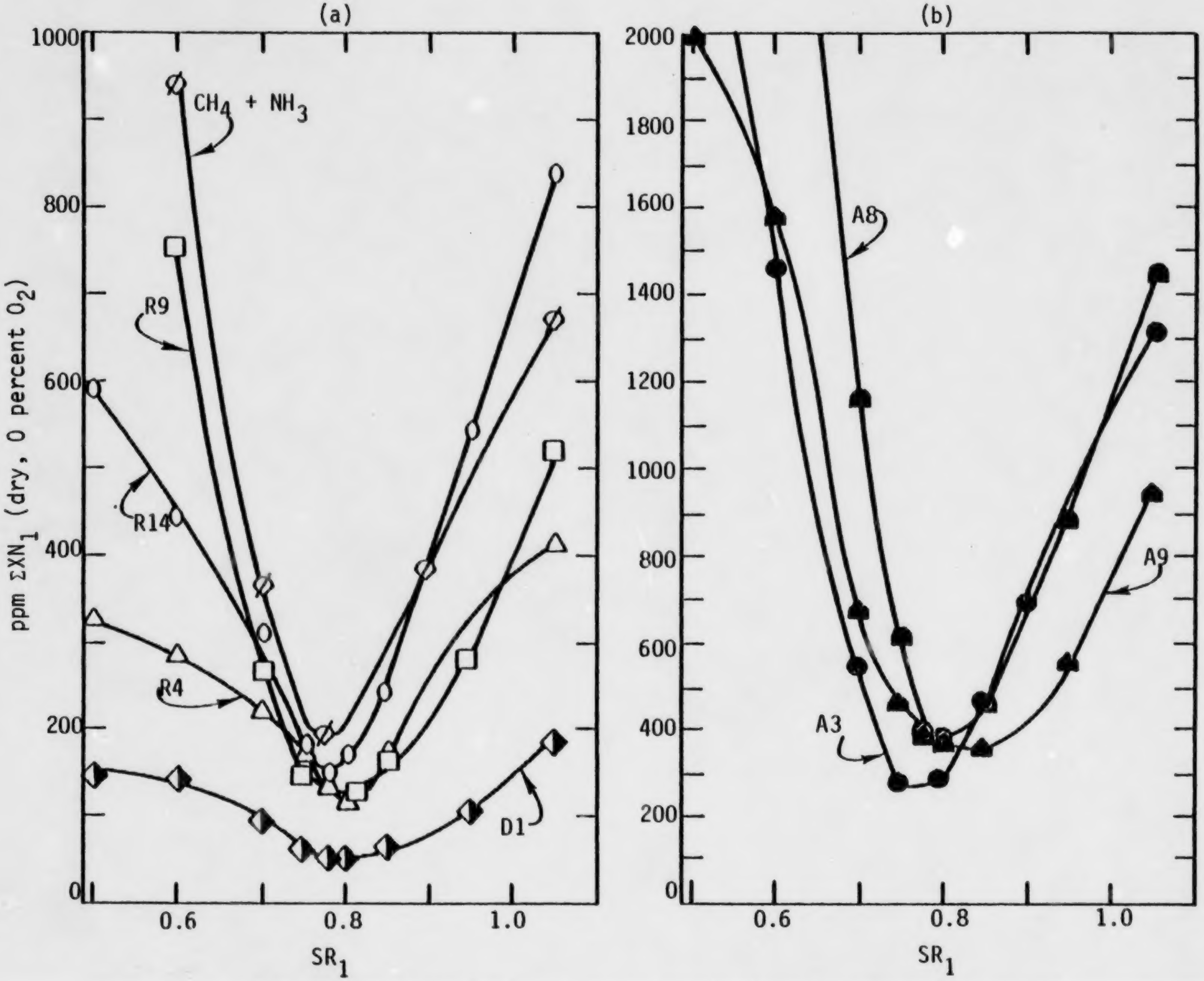

Figure 1-2. The effect of fuel type and stoichiometry on the production of TFN (ΣXN) for (a) petroleum oils and (b) alternate fuels.

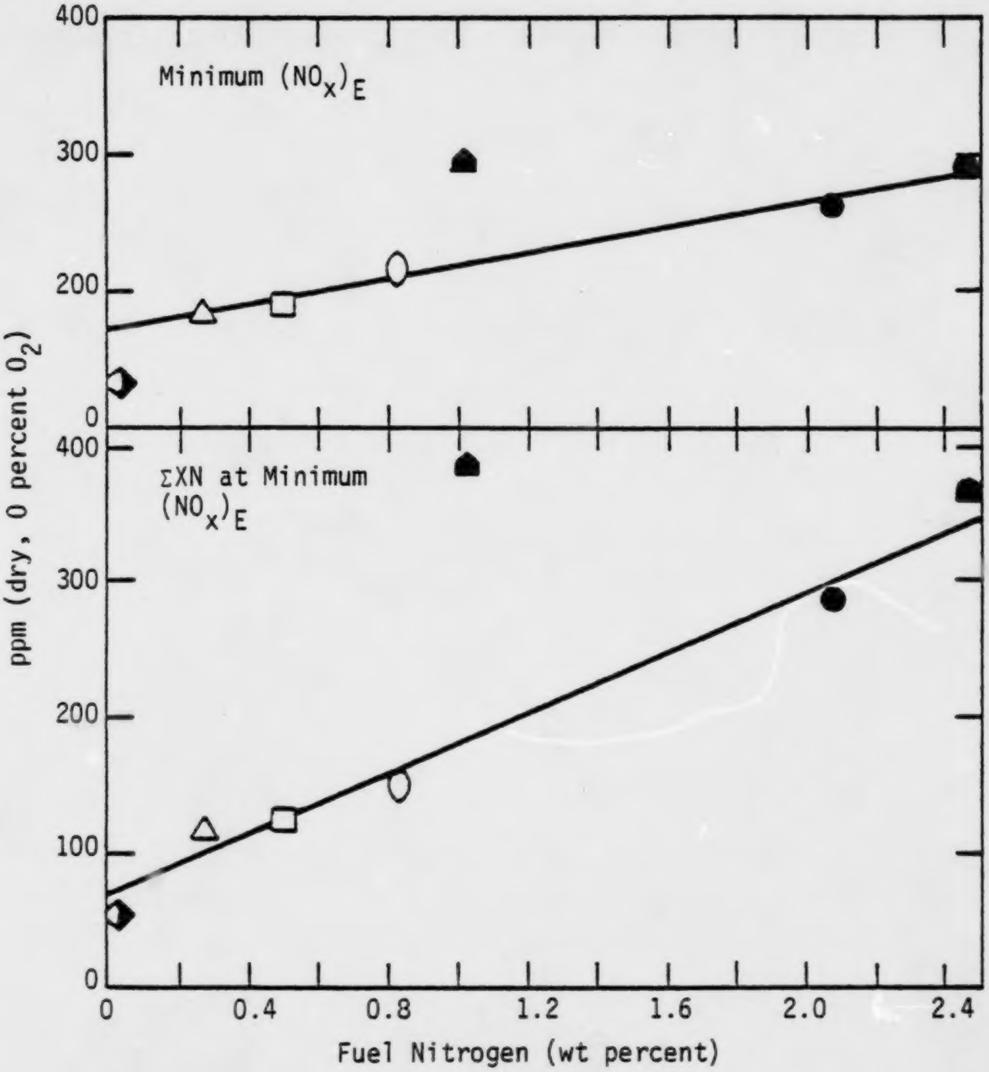

Figure 1-3. The effect of fuel bound nitrogen content on exhaust NO_x and TFN (ΣXN) in the primary zone at $SR_1 = 0.7$ (3 percent overall excess O_2).

anomalous behavior could not be confirmed; however it is well outside the limits of normal experimental errors. The results do indicate that high exhaust NO_x levels can be directly associated with high first-stage TFN levels.

The TFN concentrations shown in Figure 1-3 are in excess of equilibrium levels. Sarofim et al (1976) have suggested that increasing the temperature of the primary zone would prove beneficial. The impact of first-stage heat extraction was investigated in the bench scale tunnel furnace by inserting or removing cooling coils to extract heat along the walls of the furnace, and by inserting or removing choke sections in the furnace which reduce radiative heat loss. The results presented in Figures 1-4 and 1-5 were obtained with the crude shale oil (A3) and demonstrate the impact of first-stage heat loss on the fate of fuel nitrogen. The hot conditions refer to the furnace without primary zone cooling and with a choke section installed at the exit of the first stage to minimize radiative heat loss from the first stage. Cooling coils were added in the first stage and the radiation choke was removed for the cool furnace conditions. Figure 1-4 shows exhaust NO_x and primary zone gas temperature as a function of stoichiometric ratio for these two furnace conditions. Minimum NO_x emissions were reduced for the hot furnace case, and the optimum stoichiometry was shifted towards more fuel-rich conditions.

The axial profiles presented in Figure 1-5 provide an explanation for this shift in the minimum emission levels. As shown in the figure, heat extraction from the first stage impacts the rate of decay of TFN species. Under cold conditions both NO and HCN essentially freeze, whereas without heat extraction the initial rate of decay for all three species is much faster, leading to low TFN concentrations at the exit of the fuel-rich first stage. Heat extraction also affects the rate of CO oxidation.

The bench scale results demonstrated that a two-stage combustion system can be driven toward equilibrium levels by increasing the temperature in the fuel-rich first stage. Since the ultimate level of TFN at the exit of the first stage is kinetically limited, the minimum NO_x level is controlled by a

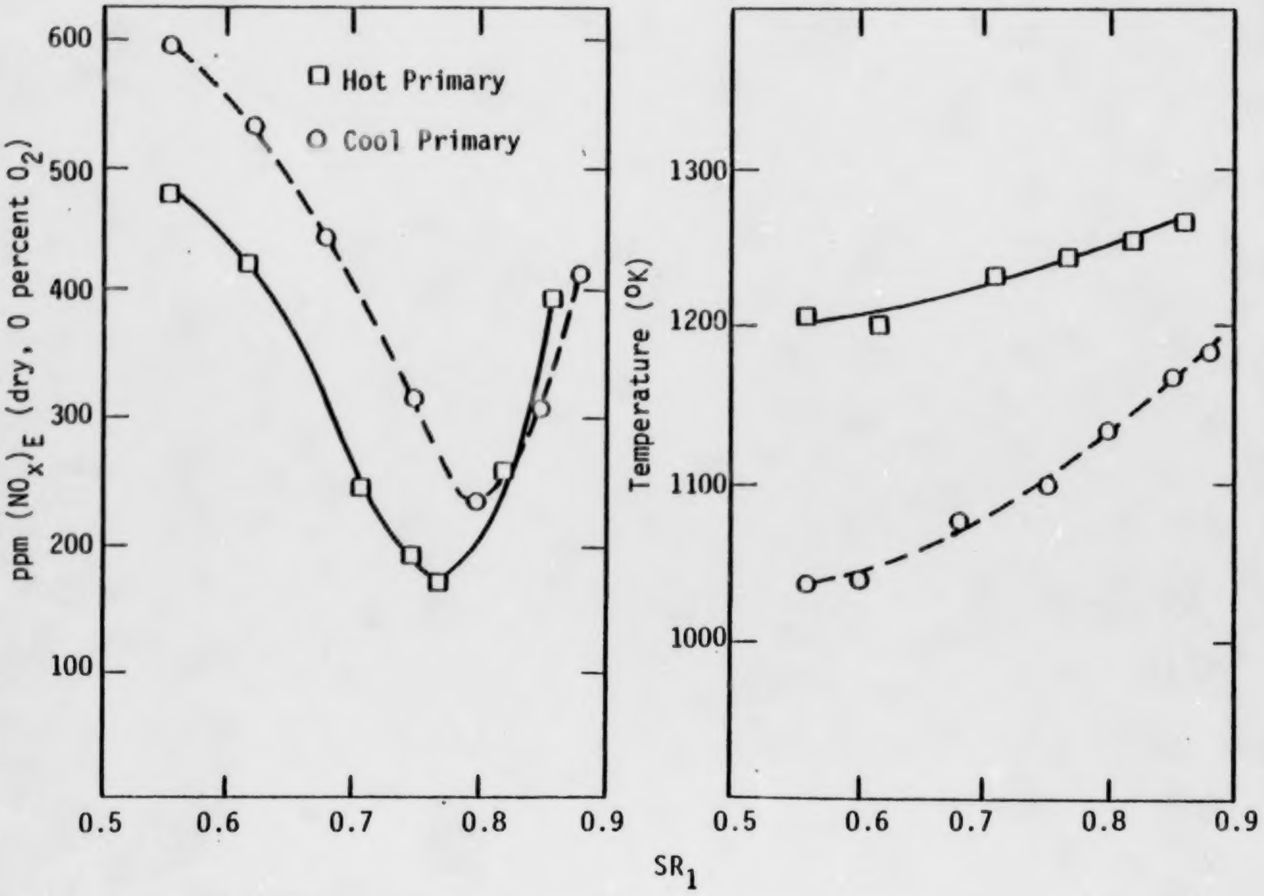

Figure 1-4. The influence of fuel-rich holdup zone temperature profile on exhaust NO_x.

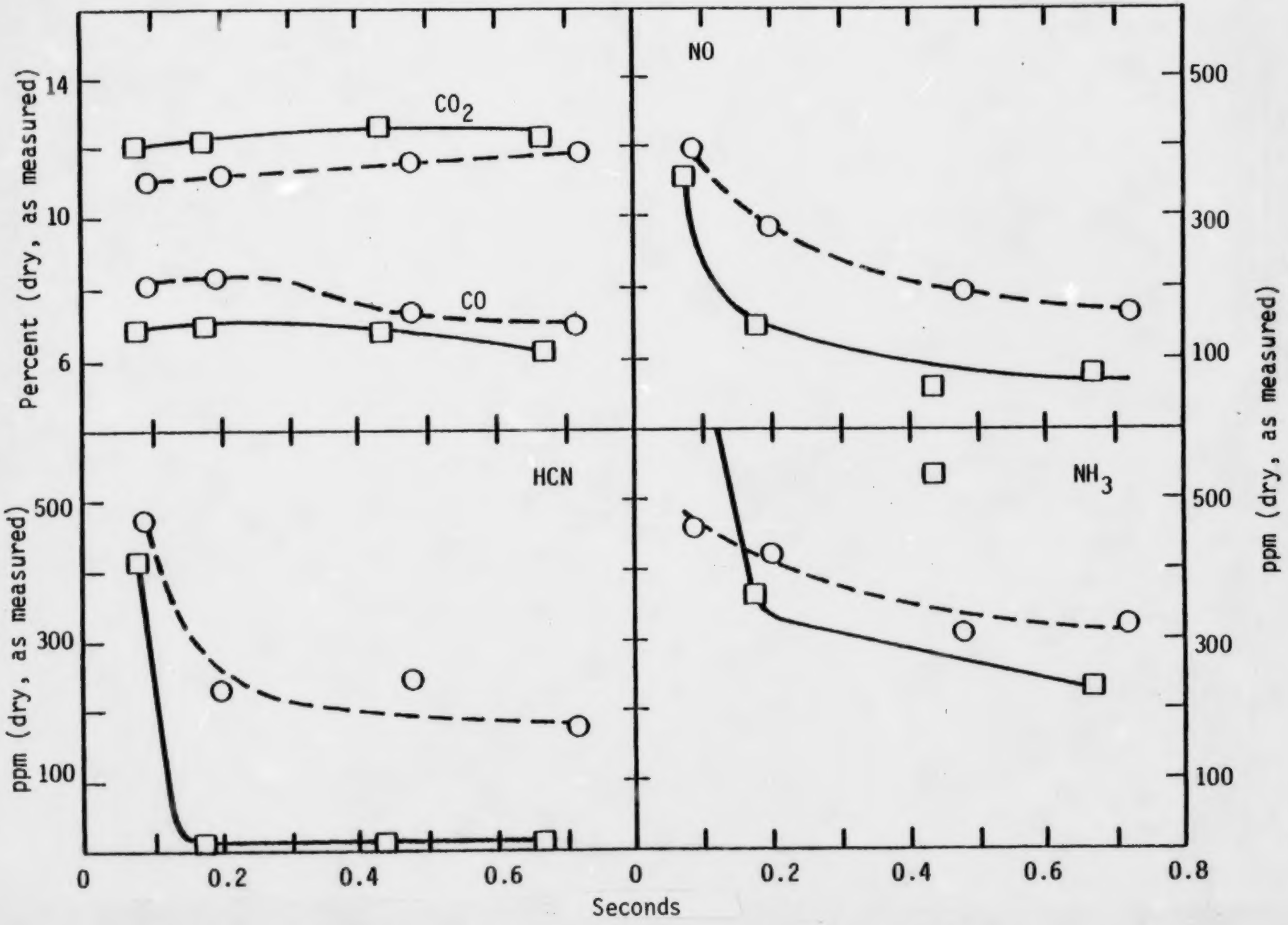

Figure 1-5. CO oxidation and decay of XN species for hot and cool primary zone temperature profiles.

tradeoff between temperature in the rich stage and the time required for TFN decay at that temperature. This suggests that an optimum staged combustion system should minimize heat loss from the first stage to maintain gas temperatures as close to adiabatic as possible. Conditions in the second stage should also be optimized. The oxidation of TFN to NO is much lower in diffusion flames than in premixed flames; therefore, mixing should be controlled to provide an attached diffusion flame in the second stage. This suggests that relatively slow mixing should take place between second-stage air and first-stage combustion products. Mixing should also be controlled to minimize peak second-stage flame temperatures, thereby minimizing thermal NO_x formation. Studies undertaken in the tunnel furnace under EPA contract 68-02-2624 showed that two methods of secondary air injection (radial versus axial injection) providing different mixing rates in the second stage produced similar NO_x emissions, suggesting that NO_x emissions were insensitive to second-stage mixing in that experiment. The scale of the bench scale tunnel furnace is so small that mixing was probably rapid in both cases. However, results obtained at pilot scale showed that mixing can have a significant effect on NO_x emissions (England et. al., 1982). Since mixing is a scale-dependent phenomenon, its significance can be expected to increase as scale increases. Second-stage mixing effects were investigated in this study in the pilot scale experiments.

In practice there are many possible approaches to controlling mixing including variation in air injection velocity, injection angle, number of injectors, and swirl intensity. The approach taken for a specific application must provide mixing which most closely achieves the mixing goals of the conceptual design while maintaining a flame shape which is commensurate with furnace geometry.

1.3 Pilot Scale Studies

The pilot scale studies were directed towards identifying the impact of fuel type and operating conditions on NO_x emissions using conventional package boiler burner equipment, and developing advanced low-NO_x burner concepts based on the optimization of two-stage combustion. Experiments were conducted in two test facilities: a 1.0 MW test furnace which simulates the thermal environment and geometry of a firetube package boiler furnace (Firetube Simulator) and a 3.0 MW test furnace which simulates the thermal environment of a package watertube boiler (Small Watertube Simulator--SWS).

The control of NO_x emissions from practical boiler/burner systems is usually limited by a tradeoff between decreased NO_x emissions and increased smoke emissions. Figure 1-6 shows NO_x vs. smoke emissions produced in the SWS firing a California No. 6 oil with two distinctly different burners. The results in Figure 1-6a were obtained with a commercially available burner which is widely applied on packaged watertube boilers. The combustion air is divided into two coaxial streams with variable swirl and flow through each passage. Air and fuel are mixed in the refractory throat of the burner and the flame is stabilized by recirculation of hot partial products of combustion. The data show that as the minimum NO_x level decreases through adjustments to the burner and excess O_2 level, smoke emissions increase. The tests indicate that minimum NO_x emissions are similar for similar smoke levels regardless of burner settings. The figure also shows data with increased furnace insulation to raise gas temperature at the exit of the furnace. This resulted in slightly lower achievable minimum NO_x levels for equivalent smoke emissions, suggesting that the burnout of soot which is formed in the flame is enhanced by the increased furnace temperature.

The data in Figure 1-6b were obtained with a distributed mixing coal burner designed under EPA Contract No. 68-02-2667, which was modified for oil firing. The burner is similar to the commercial burner except for two major differences: (1) throat diameter is larger to decrease air velocity at the throat; (2) a portion of the combustion air is added through four ports surrounding the burner throat. This permits the burner to be operated with less than the stoichiometric air requirements at the burner throat. The result is the creation of a fuel-rich zone within the core of the flame with progressive air addition further downstream. It can be seen in the figure that minimum NO_x was again limited by the onset of smoke emissions regardless of burner settings. Comparison of results obtained with the two burners shows that approximately the same minimum level of NO_x emissions (150 ppm)

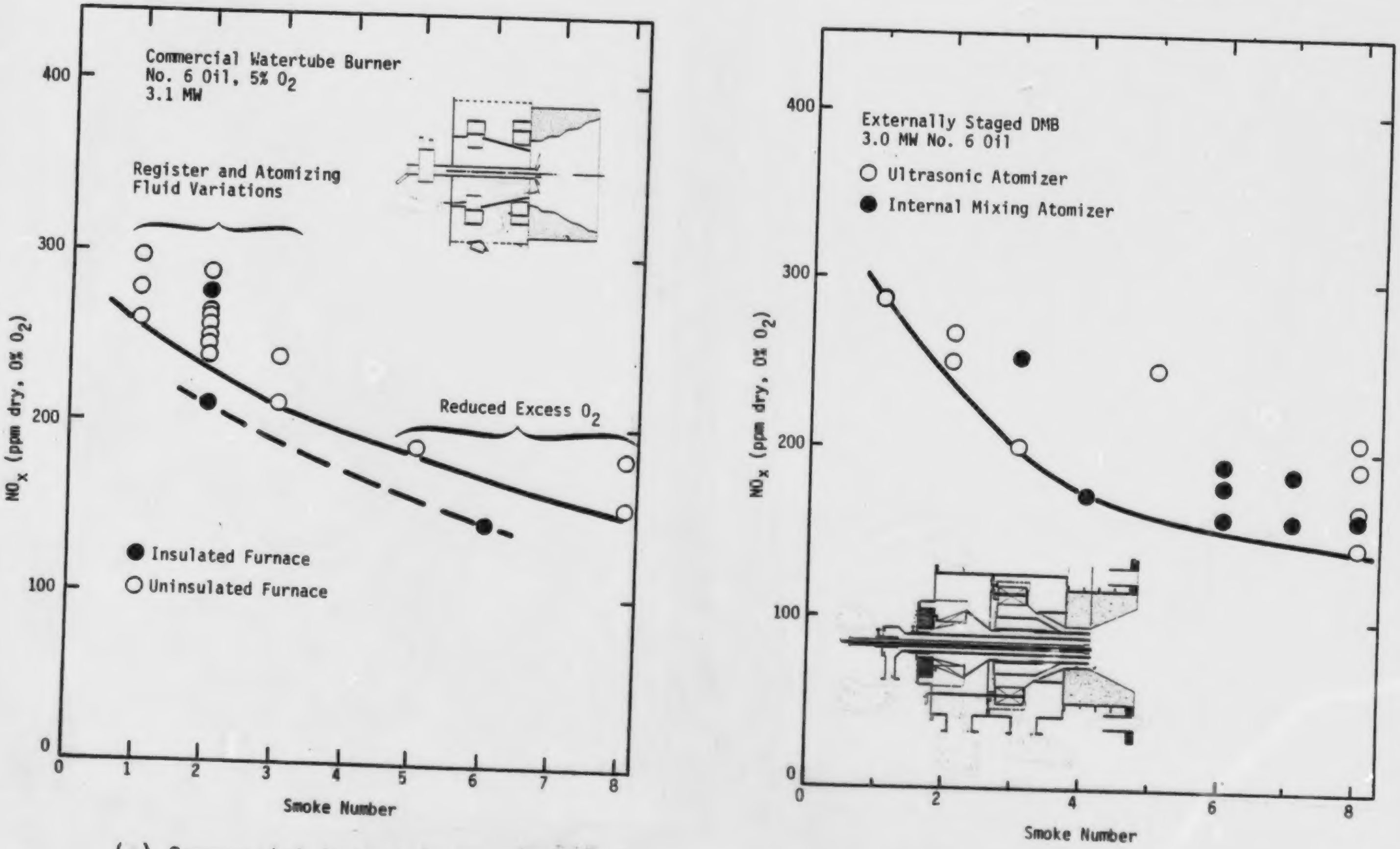

(a) Commercial Watertube Burner

(b) Distributed Mixing Burner

Figure 1-6. NO_x versus smoke emissions for (a) commercial watertube burner and (b) distributed mixing burner (3 MW_t).

was achieved at a Bacharach smoke number of 6 in spite of the substantial difference in fuel/air mixing. This suggests that there is a limit to the level of NO_x reduction possible with conventional burner systems.

The bench scale studies indicated that staged combustion can be further optimized by providing a physically separate first stage. This permits the optimization of conditions in the first stage without affecting the second stage, or vice versa. The bench scale studies suggested that an optimum two-stage combustion system should be designed according to the criteria shown in Table 1-2. The combustion process is divided into three zones:

- A fuel injection zone
- A fuel-rich holdup zone
- A second-stage burnout zone

The table shows the desired optimum conditions for each zone. Fuel injection should provide rapid mixing of small fuel droplets with the primary air and minimum heat extraction in order to drive the liquid fuel into the gas phase as quickly as possible. The fuel-rich holdup zone should provide a plug flow residence time of >200 ms with minimum heat extraction in order to maximize TFN decay. Conditions in the second-stage burnout zone should provide slow mixing of the second-stage air with the primary combustion products in order to minimize oxidation of TFN to NO_x and peak flame temperatures should not exceed 1500°C in order to minimize thermal NO_x formation.

Two prototype low-NO_x burners, shown in Figure 1-7, were constructed with nominal design firing rates of 0.6 MW and 2.9 MW. The first stage was constructed from high-temperature refractories and insulation to minimize heat loss through the walls of the first stage, permitting near-adiabatic temperatures to be achieved. Fuel and primary air were injected at the entry of a divergent quarl which forms the initial section of the fuel-rich holdup zone. Calculated plug flow residence time in the fuel-rich zone for a first-stage stoichiometric ratio of 0.7 was approximately 0.56 sec for the small prototype burner, and 0.43 sec for the intermediate prototype burner. The

TABLE 1-2. DESIGN CRITERIA FOR SCALEUP OF LOW-NO_x CONCEPT

Parameter	Optimum Range Defined by Small Scale
A. Fuel Vaporization Zone	
1) Fuel/Air Mixing	Rapid mixing of fuel and air for maximum utilization of residence time.
2) Fuel Injection	Finely atomized droplets to allow rapid vaporization of fuel. 98% of droplets <50 μm.
3) Heat Extraction	Minimum heat loss to maximize droplet vaporization.
4) Geometry	Not defined.
B. Fuel Rich Holdup Zone	
1) Residence Time	Mean residence time >200 msec at high temperature.
2) Heat Extraction	Minimize heat extraction to maximize rate of decay of XN species to N_2. Preferably exit temperatures >1400K.
3) Geometry	Designed to maximize true residence time/volume ratio.
4) Stoichiometry	Variable from 0.4 to 1.16. Optimum at 0.65-0.85.
C. Second Stage Burnout	
1) Secondary fuel/air mixing	Slow to minimize peak flame temperature, thus minimizing second stage thermal NO_x formation.
2) Heat Extraction	Optimize to limit peak flame temperature <2800F

primary combustion products were directed through a convergent section which serves to minimize radiative heat loss, ensure complete mixing of the primary products, and minimize back-mixing of the secondary air into the primary zone. Secondary air was injected parallel to the burner axis annularly around the primary exit. Two different commercial atomizers were used, an ultrasonic air-assist atomizer and an internal mixing steam-assist atomizer.

Also shown in Figure 1-7 are the Firetube Simulator and Small Watertube Simulator furnaces. The combustion chamber of the Firetube Simulator is 3.2 meters long with an internal diameter of 0.6 meters. The furnace is comprised of calorimetric sections cooled by heat transfer fluid and the wall temperature is nominally 230°C. The furnace of the Small Watertube Simulator is 5.2 meters in length and 1.8 meters inside diameter. The furnace is externally spray-cooled and has a partial refractory lining to control total heat extraction.

Figure 1-8 shows the influence of first-stage stoichiometric ratio (SR_1) on exhaust emissions from the bench scale studies carried out in the tunnel furnace and from the prototype tests with residual oils containing approximately 0.6 percent nitrogen. The dependence of NO_x emissions on SR_1 was similar in all three experiments. Smoke and CO emissions from the small prototype burner were low for $SR_1 >0.7$, but increased sharply as SR_1 was decreased further. CO emissions were <100 ppm and smoke number was generally <5 at the point where the minimum NO_x level occurred. CO and smoke emissions performance for the intermediate prototype was similar. The minimum NO_x level ranged from approximately 89 ppm in the tunnel furnace to 84 ppm in the small prototype burner and 74 ppm in the intermediate prototype burner. The optimum SR_1 appears to shift downward as scale increases, going from 0.8 for the tunnel furnace to 0.7 in the small prototype burner, and 0.56 in the intermediate prototype burner. This shift in the optimum SR_1 and minimum NO_x level is most likely due to reduced first-stage heat loss associated with the increase in scale which leads to higher temperatures in the first stage. Equilibrium calculations (free energy minimization) confirmed that the optimum SR_1 should move more fuel-rich with increased temperature; however, the TFN concentrations which were measured in the tunnel furnace and small

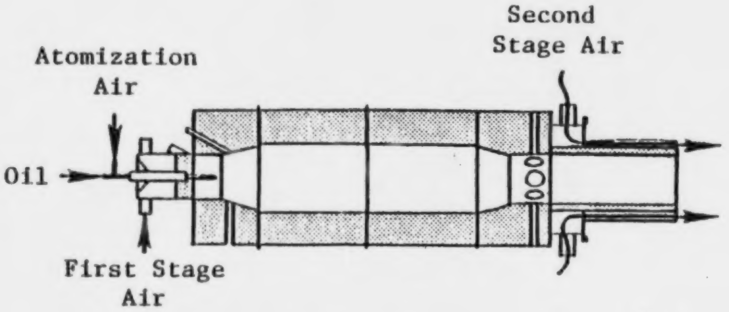
Atomization
Air
Second
Stage Air
Oil
First Stage
Air

(a) Small Prototype Burner (2 x 10^6 Btu/hr)

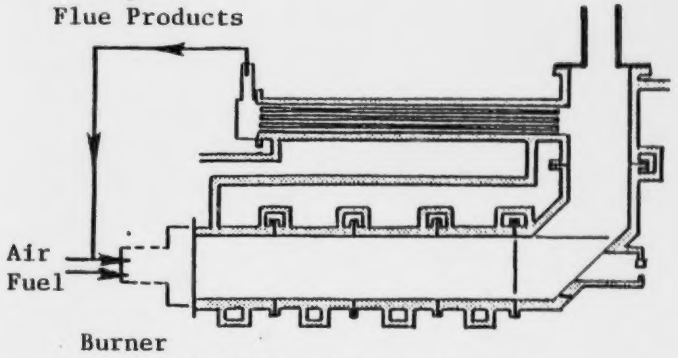
Recycled
Flue Products
Air
Fuel
Burner

(b) Firetube Simulator

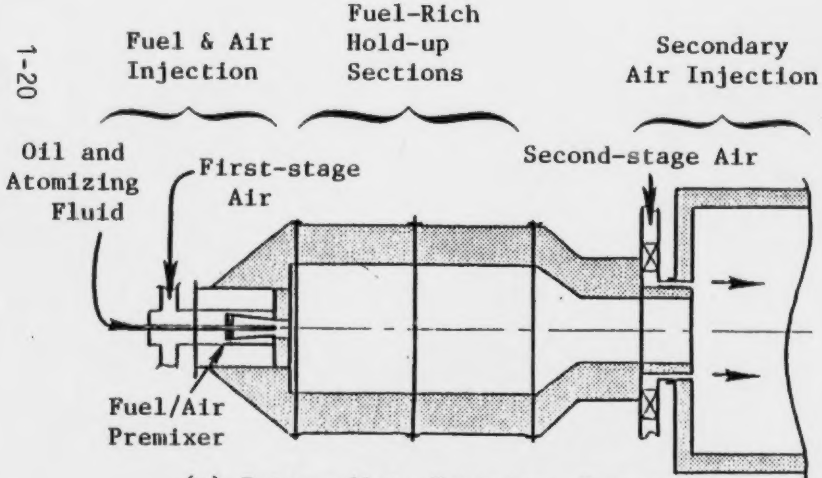
Fuel & Air
Injection
Fuel-Rich
Hold-up
Sections
Secondary
Air Injection
Oil and
Atomizing
Fluid
First-stage
Air
Second-stage Air
Fuel/Air
Premixer

(c) Intermediate Prototype Burner (10 x 10^6 Btu/hr)

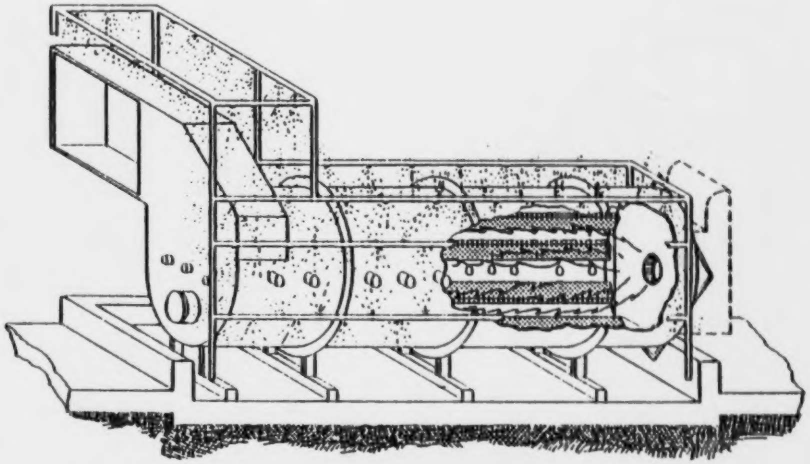

(d) Small Watertube Simulator

Figure 1-7. Prototype burners and experimental test furnaces.

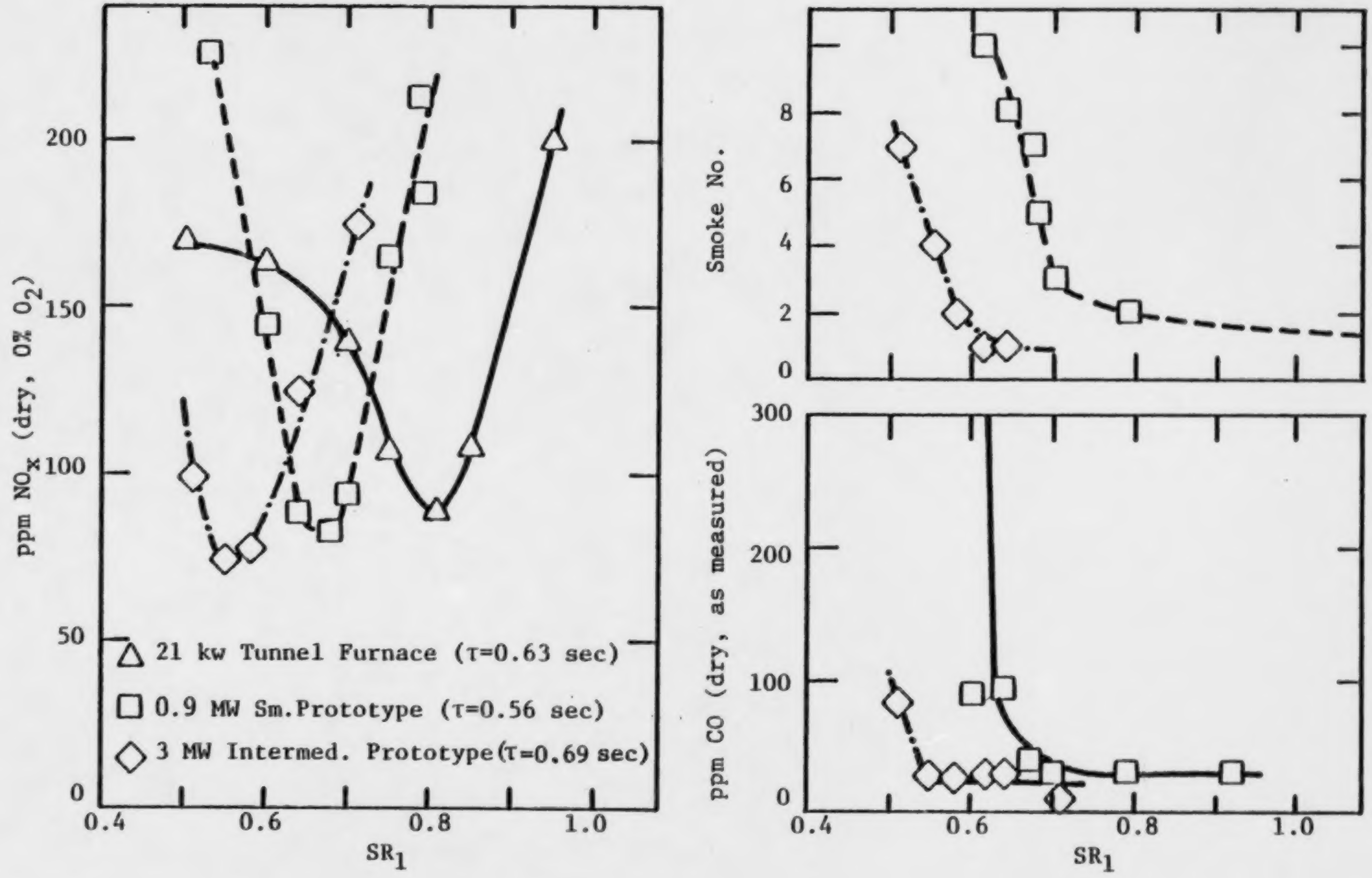

Figure 1-8. Influence of first-stage stoichiometry on NO_x, CO, and smoke emissions (bench scale and pilot scale, California residual fuel oil).

prototype burner are greatly (approximately 2 orders of magnitude) in excess of equilibrium values. Hence, even with first-stage exit temperatures of 1600°C at SR_1 = 0.7 and a first-stage residence time of 500 ms, kinetic limitations are significant. Decreasing SR_1 reduced first-stage NO but below approximately SR_1 = 0.8, significant amounts of NH_3 and HCN were formed. Thus, as in the bench scale studies, there exists a minimum in the exhaust NO_x because of a competition between decreased first-stage NO and increased oxidizable nitrogen species. Other than shifting the optimum SR_1, concept scale-up did little to alter this competition or the TFN species distribution. The residence time in the fuel-rich zone to achieve the desired TFN concentration is an important practical design parameter since it largely determines the size of the precombustor. Figure 1-9 summarizes minimum exhaust NO_x and TFN data for the tunnel furnace and for the two prototype burners firing in both the Firetube Simulator and the Small Watertube Simulator. In both the bench scale and pilot scale studies, increasing the first-stage residence time significantly decreased exhaust NO_x and TFN concentration. The TFN concentration in the prototype burners was lower than in the tunnel furnace because of the increased rich-zone temperature associated with the increase in scale.

Mean first-stage residence time was varied in the small prototype burner/firetube simulator tests by altering the firing rate and in the small prototype burner/watertube simulator tests by changing the length of the first-stage chamber. A strong correlation between the two sets of experiments suggests that the controlling processes are dominated by the kinetics (time and temperature) and not by aerodynamics, and that the principal influence of firing rate is on residence time. Clearly, increasing firing rate also increased first-stage temperature, but this effect is small because even at 0.6 MW the prototype heat losses were low. Gas temperatures at the exit of the first stage was approximately 1600°C at SR_1 = 0.7 compared with an adiabatic flame temperature of approximately 1750°C.

Since the time/temperature history of the fuel-rich zone was found to be the primary scaling parameter, one-dimensional kinetic calculations (Kramlich et al, 1981) were conducted to quantify this influence. The model assumed a

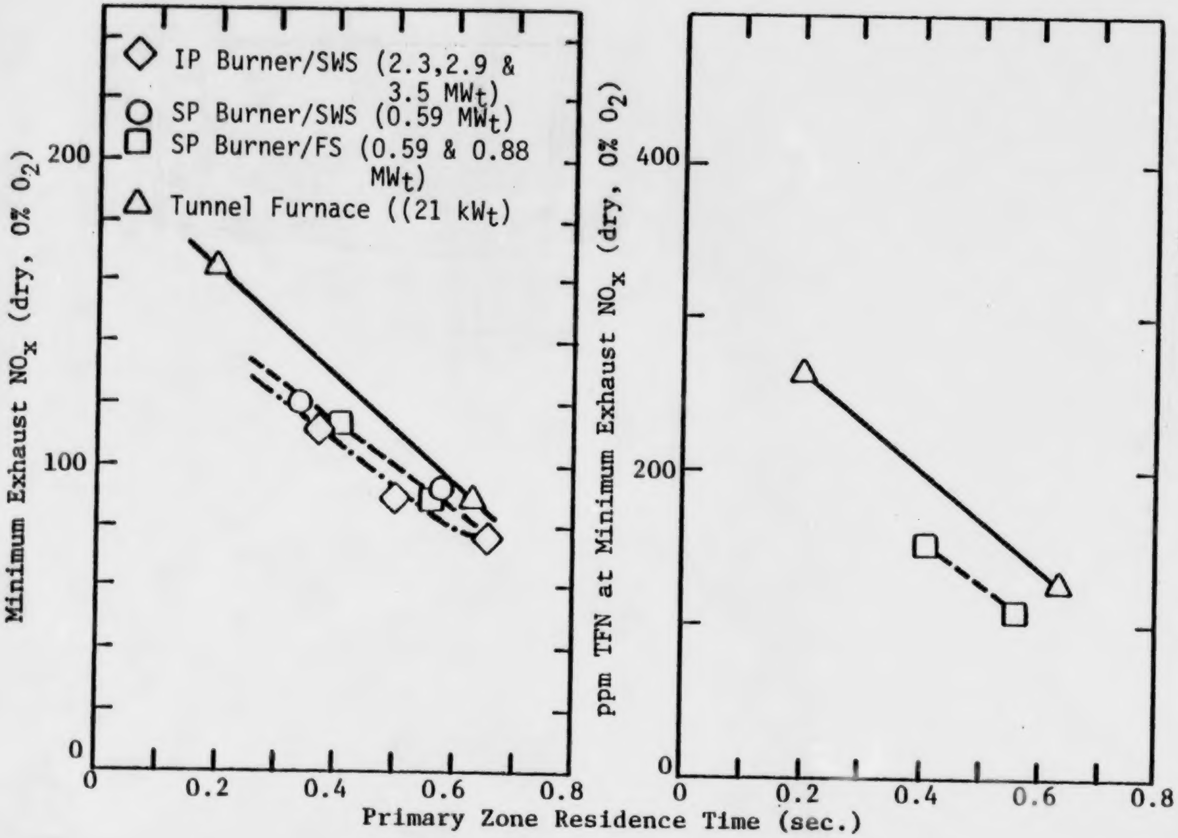

Figure 1-9. Effect of first-stage residence time on exhaust NO_x emissions and TFN decay for bench scale, small pilot scale (SP), and intermediate pilot scale (IP) staged combustors.

2 ms well-stirred reaction ignition zone followed by a variable length plug flow reactor and the fuel was methane containing 1 percent nitrogen as HCN. Preliminary runs showed that the initial speciation at the inlet to the first stage had little effect on the ultimate TFN level. The model showed that TFN decay is rapid at high temperature, but that the decay slows dramatically below 1425°C. Thus, increasing first-stage residence time is only beneficial if the heat extraction rate is low enough to keep the local gas temperature above 1425°C. Further, the rate of NO decay decreases significantly when the NH_3 concentration falls to zero, indicating that TFN speciation is important in first-stage processing. These calculations support the concept that reactions in the form: $NO + HN_i \longrightarrow N_2$ are controlling the fuel-rich TFN reduction and that it is essential to have both high temperatures (above 1425°C) and a proper TFN species distribution in order to achieve very low exhaust NO_x levels. The calculations also indicate the need for a long residence time in the primary zone, but that the required time to achieve a given level of TFN decreases with increasing first-stage temperatures.

Figure 1-10 summarizes NO_x from each of the pilot scale and bench scale experiments as a function of fuel nitrogen content. Figure 1-10a shows NO_x from the commercial burners tested in the Firetube Simulator and the Small Watertube Simulator, the 3 MW distributed mixing burner, the bench scale tunnel furnace and the two pilot scale prototype burners. Data from the tunnel furnace showed that NO_x emissions were >1000 ppm for fuels with nitrogen content over 0.6 percent. However, the application and optimization of staged combustion dramatically reduced NO_x emissions to 190 ppm at this same level of fuel-bound nitrogen. NO_x emissions from the Firetube Simulator with commercial burner A were also high, reaching 1060 ppm when burning the high nitrogen (2.08 wt-% nitrogen) crude Paraho shale oil. In contrast, NO_x from commercial burner B in the same furnace was only 550 ppm when firing the same fuel. This illustrates the strong dependence of NO_x emissions on burner design for conventional burner systems. The application of staged combustion to commercial burner A further decreased NO_x emissions to 490 ppm when burning the shale oil, but at the expense of increased smoke emissions.

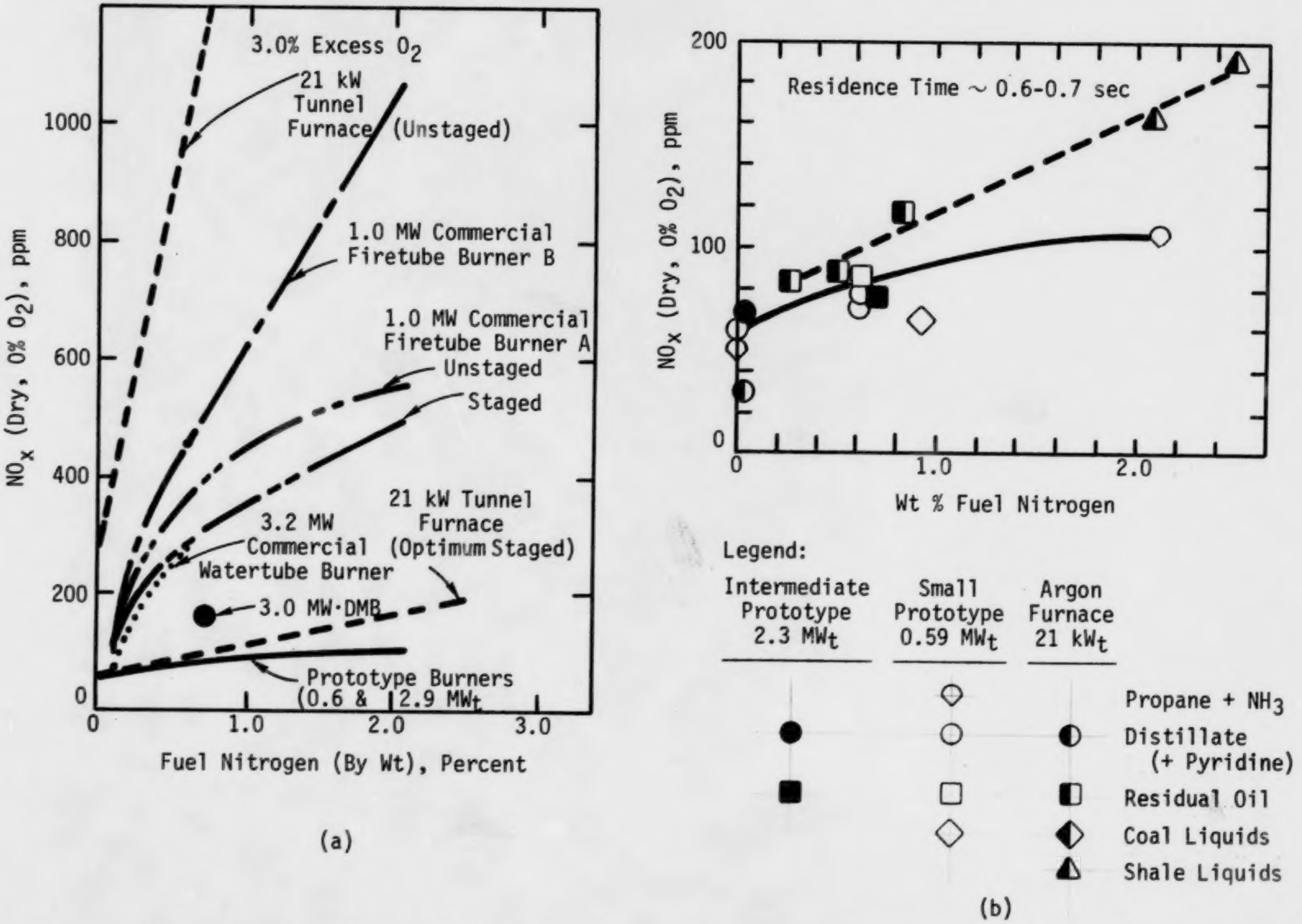

Figure 1-10. Effect of fuel nitrogen content on NO_x emissions from (a) all bench scale and pilot scale burners tested and (b) low-NO_x prototype burners.

NO_x emissions from a 3 MW commercial watertube burner in the Small Watertube Simulator were much lower than either of the commercial firetube burners for fuels with equivalent bound nitrogen content. NO_x emissions were very strongly dependent on fuel nitrogen content with all of the conventional burner systems which were tested. It can be seen that the NO_x emissions from the optimized tunnel furnace and the prototype pilot scale burners were influenced by fuel nitrogen to a much lesser extent and were only a fraction of the emission level from the commercial burners.

Figure 1-10b shows the fuel nitrogen dependence more closely for the tunnel furnace and for the pilot scale prototype burners. Data are shown for various fuels including a distillate oil (with and without pyridine added), residual oils, a coal-derived liquid and a propane/NH_3 mixture. The data indicate that NO_x is only weakly dependent on nitrogen content with the small and intermediate prototype burners. Comparison of results obtained with the NH_3-doped gas, pyridine-doped distillate oil and actual residual oils shows that differences in NO_x due to fuel volatility are small in absolute terms but may become significant in relative terms, especially for systems with short residence time in the first stage where the characteristic time for the vaporization of fuel approaches the time available for TFN decay. Scale-up of the concept reduced the dependence of NO_x emissions on fuel nitrogen level. This is probably due to the increased temperature in the fuel-rich zone because of the increase in scale.

In conclusion, these results indicate that it should be possible to apply the low-NO_x burner concept developed in this program to systems of different scale in order to achieve NO_x emissions below 100 ppm even when firing high-nitrogen fuels. Successful scaling criteria for advanced low-NO_x burners were developed and verified over a range in scale of 750 to 1.

2.0 FIRETUBE BURNER STUDIES

These studies were conducted to extend and verify the small-scale furnace results for flames more representative of those found in small industrial boilers. Experiments were conducted in a 1 MW cold-wall test furnace, firing a wide range of conventional and alternative liquid fuels. The experimental combustor is designed to simulate the furnace of a small firetube boiler by matching geometry and flame zone heat extraction. Two commercial burners and an experimental prototype low-NO_x burner were extensively evaluated.

Data from the commercial burners was used to generate an emissions baseline for typical commercial burners firing a wide range of fuels against which emissions from the experimental burner could be compared. This provides the necessary link to allow the experimental burner for extension of these results to actual package boilers. The effect of staging combustion air with the unmodified burners was also investigated.

The experimental prototype burner was designed based upon criteria developed from the small-scale tunnel furnace results described in Volume I. These results provided insight into the fundamental mechanisms of NO_x formation and control. The burner concept is based on optimization of two-stage combustion. The burner was extensively tested to determine the effects of fuel type, mixing, temperature, residence time, and confinement. These results were than used to establish generalized design criteria for two-stage low-NO_x burners. These criteria have been validated in tests at 3 MW scale, described in section 3 of this report volume.

2.1 Firetube Boiler Simulator Facility

The highlights of the Firetube Boiler Simulator Facility are illustrated in Figure 2-1. The facility is equipped with feed and metering systems for propane gas, light oil, and residual oil. The combustion air is supplied by a blower and is split into four separately metered streams. Flue gases are normally vented directly to atmosphere but can also be cooled and recycled

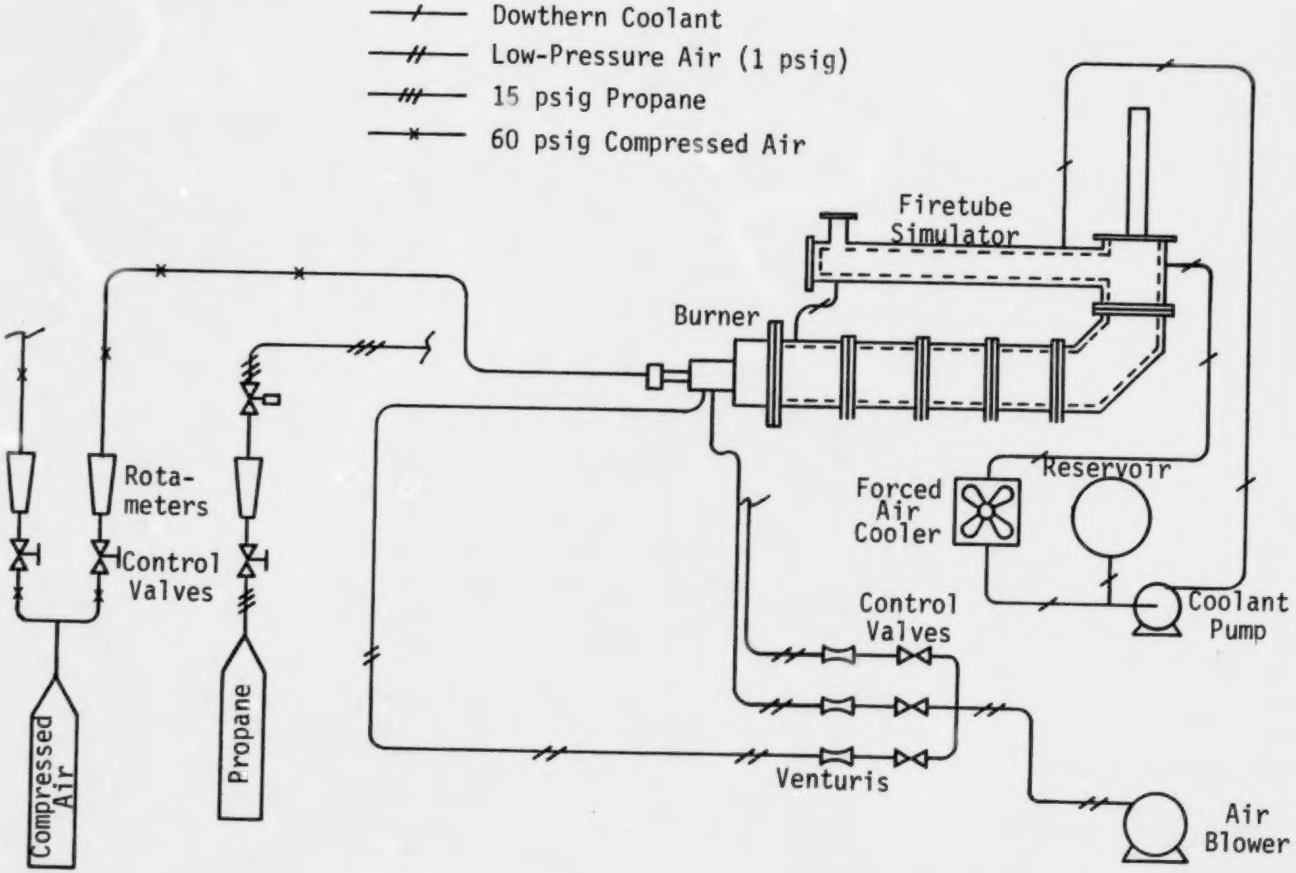
Dowthern Coolant
Low-Pressure Air (1 psig)
15 psig Propane
60 psig Compressed Air
Firetube Simulator
Burner
Rota-meters
Control Valves
Reservoir
Forced Air Cooler
Coolant Pump
Control Valves
Venturis
Air Blower
Compressed Air
Propane

Figure 2-1. Firetube boiler simulator facility.

into the burner or furnace. A closed coolant system uses Dowtherm G as the heat transfer fluid. Coolant is circulated sequentially through the combustor walls to a forced-air heat exchanger.

The combustor furnace is illustrated in Figure 2-2. The furnace is 59 cm inside diameter by 305 cm horizontal length. Coolant is circulated through a double-shell jacket which allows axial heat transfer profiles to be determined. The cooling jacket extends through the elbow section to the beginning of the stack. Observation and sampling ports are located in the walls and at the rear of the furnace. Table 2-1 lists the nominal performance characteristics of the furnace. Further details of the furnace design can be found elsewhere (Muzio and Wilson, 1973; Heap et al, 1976).

Exhaust gases are sampled using a 316 stainless steel water-jacketed probe. Water vapor is removed from the sample using a cyclone submerged in an ice bath (Figure 2-3). The sample delivery system uses all Teflon/316 stainless steel materials.

Continuous gas analyzers are used to measure concentrations of O_2, CO, CO_2, and NO/NO_x. Smoke numbers are measured using a Bacharach smoke pump. Table 2-2 lists the type and model of the analyzers used. Particulate loading and size distribution was determined for selected conditions using the EPA high-volume Source Assessment Sampling System (SASS).

2.2 Evaluation of Commercial Burner A

Burner A is illustrated in Figure 2-4. The nominal firing rate is 1.0 MW (3.4×10^6 Btu/hr) on No. 6 fuel oil. The burner possesses an integral blower and air damper, fuel-oil heater and bypass control valve, gas pilot, twin-fluid atomizer, and full flame safeguard and automatic operating controls. Burner construction is largely of sheet metal. A separate air compressor was supplied by the manufacturer.

The burner throat is 22.8cm in diameter and a stamped sheet metal diffuser is used to stabilize the flame. The diffuser imparts an unknown degree

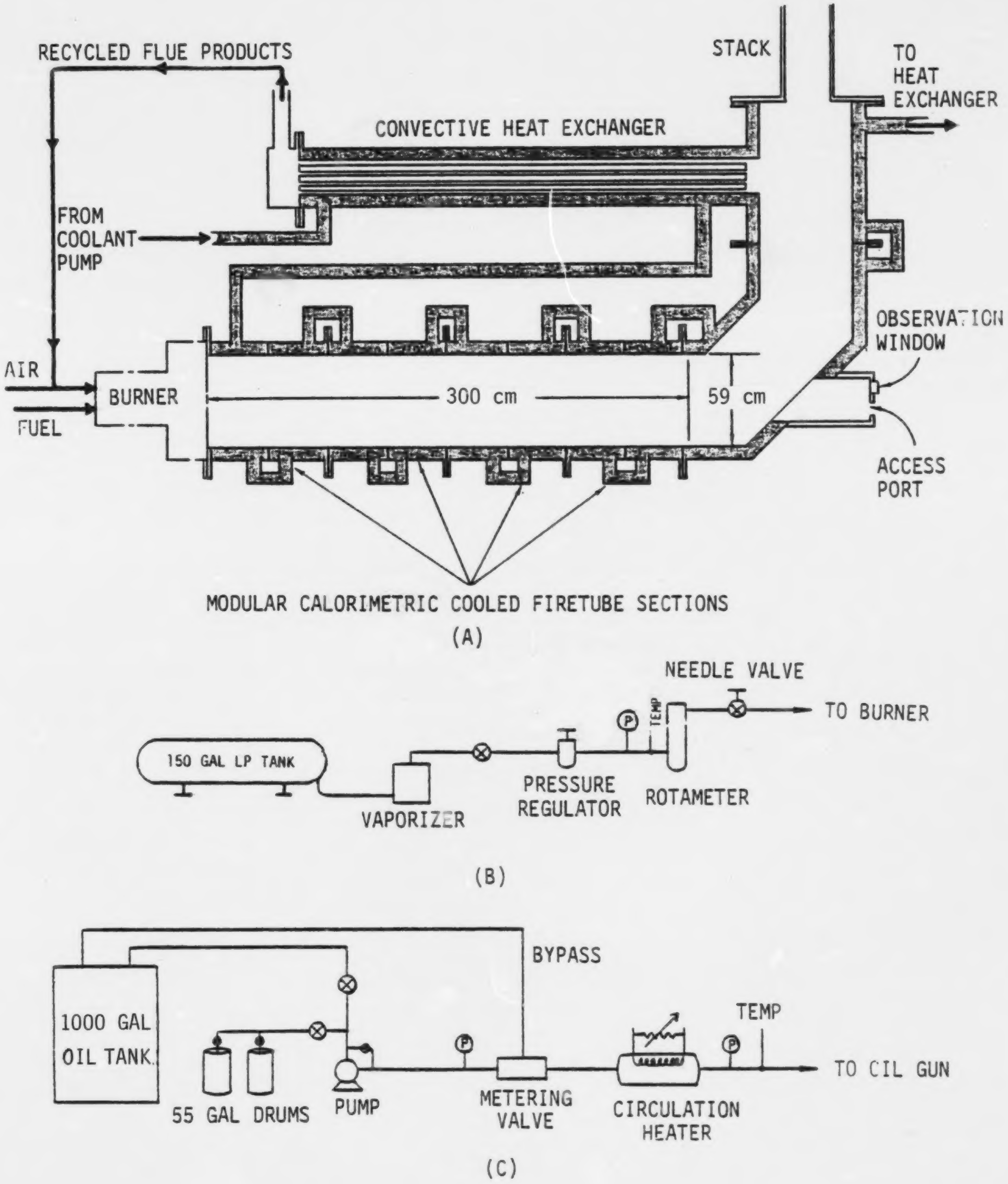
RECYCLED FLUE PRODUCTS
STACK
TO HEAT EXCHANGER
CONVECTIVE HEAT EXCHANGER
FROM COOLANT PUMP
OBSERVATION WINDOW
AIR
FUEL
BURNER
300 cm
59 cm
ACCESS PORT
MODULAR CALORIMETRIC COOLED FIRETUBE SECTIONS
(A)
NEEDLE VALVE
TO BURNER
150 GAL LP TANK
P
TEMP
VAPORIZER
PRESSURE REGULATOR
ROTAMETER
(B)
BYPASS
1000 GAL OIL TANK
TEMP
P
P
55 GAL DRUMS
PUMP
METERING VALVE
CIRCULATION HEATER
TO OIL GUN
(C)

Figure 2-2. (A) Firetube Boiler Simulator, (B) Gas Fuel System (C) Liquid Fuel System.

TABLE 2-1. NOMINAL PERFORMANCE SPECIFICATIONS FOR FIRETUBE BOILER SIMULATOR

Parameter	Value
Dimensions	
Shape	Horizontal Cylinder
Inside Diameter	59 cm (23.25 inches)
Length	305 cm (10 ft)
Volume (Horizontal)	0.835 m^3 (29.5 ft^3)
Internal Surface Area	5.7 m^2 (61 ft^2)
Thermal	
Firing Rate (Nominal)	0.9 MW (3 x 10^6 Btu/hr)
Wall Temperature (Approx)	230°C (450°F)
Heat Release/Volume	1.05 MW/m^3 (102,000 Btu/ft^3)
Flue Gas Exit Temperature	800-1100°C (1500-2000°F)

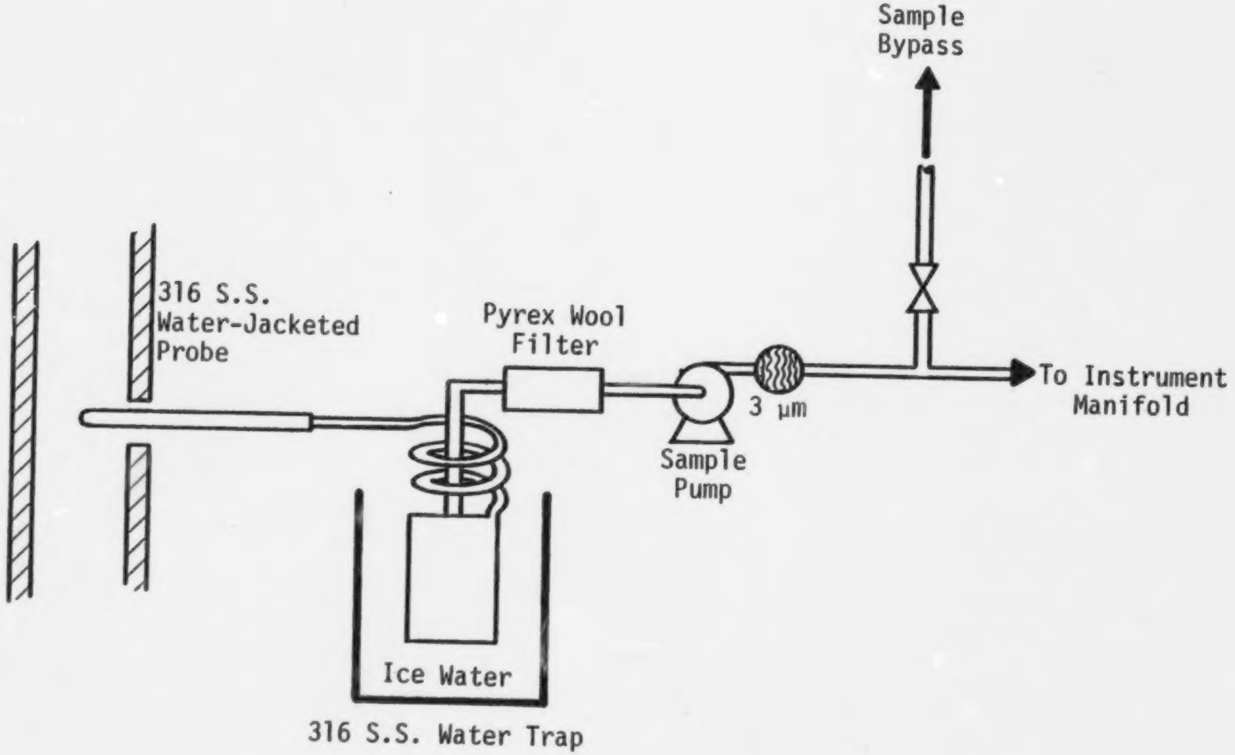
Sample
Bypass
316 S.S.
Water-Jacketed
Probe
Pyrex Wool
Filter
To Instrument
Manifold
3 µm
Sample
Pump
Ice Water
316 S.S. Water Trap

Figure 2-3. Exhaust sampling system used on firetube boiler simulator.

TABLE 2-2. CONTINUOUS GAS ANALYZERS

Species	Make/Model	Principle
O_2	Taylor Servomex/OA-250	Paramagnetic
CO_2	ANARAD/AR-600	Infrared
CO (%)	ANARAD/AR-500	Infrared
CO (PPM)	ANARAD/AR-500	Infrared
NO/NO_x	TECO/IOAR	Chemiluminescence (Low Pressure)
Smoke	Baccarach	Smoke Spot Comparison

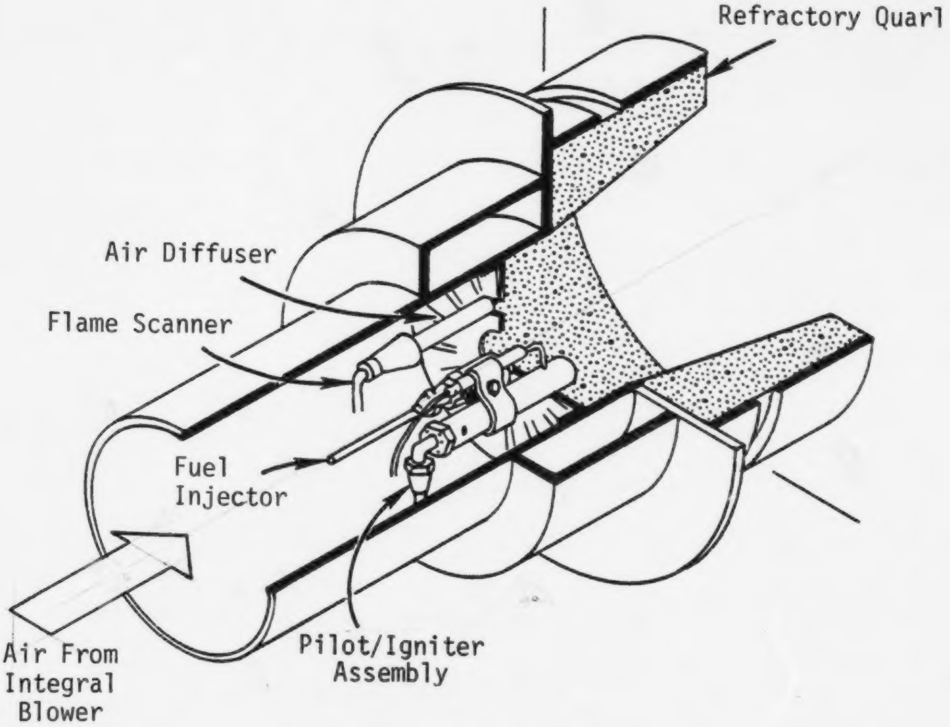
Refractory Quarl
Air Diffuser
Flame Scanner
Fuel Injector
Pilot/Igniter Assembly
Air From Integral Blower

Figure 2-4. Commercial Burner A.

of swirl to the combustion air. The atomizer is located in the center of the plate which is cut to allow flow of unswirled air around the atomizer (presumably to prevent coking due to recirculated raw fuel). The pilot and flame detector are located in the diffuser plate.

The twin-fluid atomizer is illustrated in Figure 2-5. The atomizer is an internal mixing type and uses air as the atomizing fluid. High-velocity air passes through an annular passage and impinges on radial oil jets. The resulting air/oil mixture is forced through swirl slots and then through a single orifice in the atomizer cap. The entire unit disassembles for cleaning.

Table 2-3 summarizes the range of test conditions investigated to establish baseline emission performance for Burner A. A series of tests were conducted firing the Indo/Malaysian residual oil (fuel-bound nitrogen = 0.24 percent) to determine the impact of burner operating variables such as excess air, load, and atomization parameters. After determining the sensitivity of emissions to burner adjustments, two additional petroleum-derived fuels were evaluated, ranging in nitrogen content from 0.05 percent (D3-California No. 2 oil) to 0.77 percent (R11-California No. 6 oil). Three high-nitrogen alternative liquid fuels were also tested, including two shale-derived oils and one coal-derived oil. Nitrogen content of the alternative liquids ranged from 0.45 percent to 2.08 percent. Analysis of these fuels is presented in Table 2-4.

The following sections present the results of these tests. NO_x emissions are corrected to 0% O_2 (for comparison on a mass basis) using the following relationship:

$$(NO_x)_{meas} \times \frac{21}{21 - (O_2)_{meas}} = (NO_x)_{0\%\ O_2}$$

2.2.1 Baseline Characterization

NO_x emissions versus excess oxygen are shown in Figure 2-6 as a function of burner firing rate. At full load, NO_x increased from approximately

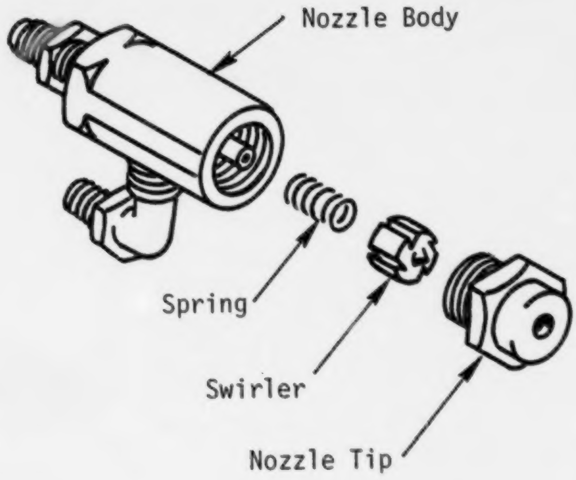
Nozzle Body
Spring
Swirler
Nozzle Tip

Figure 2-5. Oil nozzle assembly--Commercial Burner A.

TABLE 2-3. SUMMARY OF TEST CONDITIONS FOR BURNER A BASELINE CHARACTERIZATION

Fuel	Firing Rate MW (10^6 Btu/hr)	Atomizing Fluid	Atomizing Pressure kPa (psig)	Oil Temperature (°C)	Excess Oxygen (%, dry basis)
Indo/Malaysian Residual Oil (R4)	1.0 (3.4)	Air	110 (16)	86-87	1.0-6.1 *
	0.8 (2.7)	Air	97 (14)	87-89	0.9-6.2 *
	0.6 (2.0)	Air	97 (14)	88-93	0.8-6.2 *
	1.0 (3.4)	Air	38-207 *	85-93	2.8-3.1
	1.0 (3.4)	Air	111-124 *	69-103*	2.2-2.4 *
	1.0 (3.4)	Steam	42-360 *	86-89 *	2.8-3.0
California No. 2 Oil (D3)	1.0 (3.4)	Air	117 (17)	42	1.9-6.3 *
California No. 6 Oil (R11)	1.0 (3.4)	Air	124 (18)	96	1.7-5.9 *
Crude Paraho Shale Oil (A3)	1.0 (3.4)	Air	117 (17)	78	1.8-5.9 *
Residual Paraho Shale Oil (A5)	1.0	Air	110 (16)	58	1.9-6.3 *
SRC-II Blend (A6)	1.0	Air	110 (16)	38	1.6-6.0 *

*Indicates test variable.

TABLE 2-4. FUEL ANALYSES

	D3	R2	R4	R11	A3	A5	A6
	California No. 2 Oil	Middle East	Indo/ Malaysian	California	Crude Shale (Paraho)	Residual Shale	SRC II
Ultimate Analysis:							
Carbon (%)	86.8	86.78	86.53	85.4	84.6	86.71	85.91
Hydrogen (%)	12.52	11.95	11.93	11.44	11.3	12.76	8.74
Nitrogen (%)	0.053	0.18	0.24	0.77	2.08	0.46	0.96
Sulfur (%)	0.27	0.67	0.22	1.63	0.63	0.28	0.30
Ash (%)	<0.001	0.012	0.036	0.043	0.026	0.009	0.04
Oxygen (%)	0.36	0.41	1.04	0.71	1.36	0.03	4.08
Conradson Carbon Residue (%)		6.0	3.98	8.74	2.9	0.19	0.51
Asphaltene (%)		3.24	0.74	5.18	1.33	0.083	
Flash Point, °F		350	210		250	235	173
Pour Point, °F		48	61	38	80	90	-55
API Gravity at 60°F	32.6	19.8	21.8	15.4	20.3	29.0	
Viscosity, SSU, at 140°F	30.8	490	199	854	97	54.3	39
at 210°F	29.5	131.8	65	129	44.1	37.3	
Heat of Combustion:							
Gross Btu/lb	19,330	19,070	19,070	18,470	18,290	19,350	17,100
Net Btu/lb		17,980	17,980	17,430	17,260	18,190	
Calcium, ppm		1.2	14	21	1.5	4.20	
Iron, ppm		2.6	16	73	47.9	<0.5	
Maganese, ppm		0.02	0.13	0.8	0.17	<0.5	
Magnesium, ppm		0.08	3.6	5.1	5.40	0.15	
Nickel, ppm		13	19	65	5.00	<0.5	
Sodium, ppm		0.98	15	21	11.71	2.51	
Vanadium, ppm		25	101	44	<0.3	<1.0	

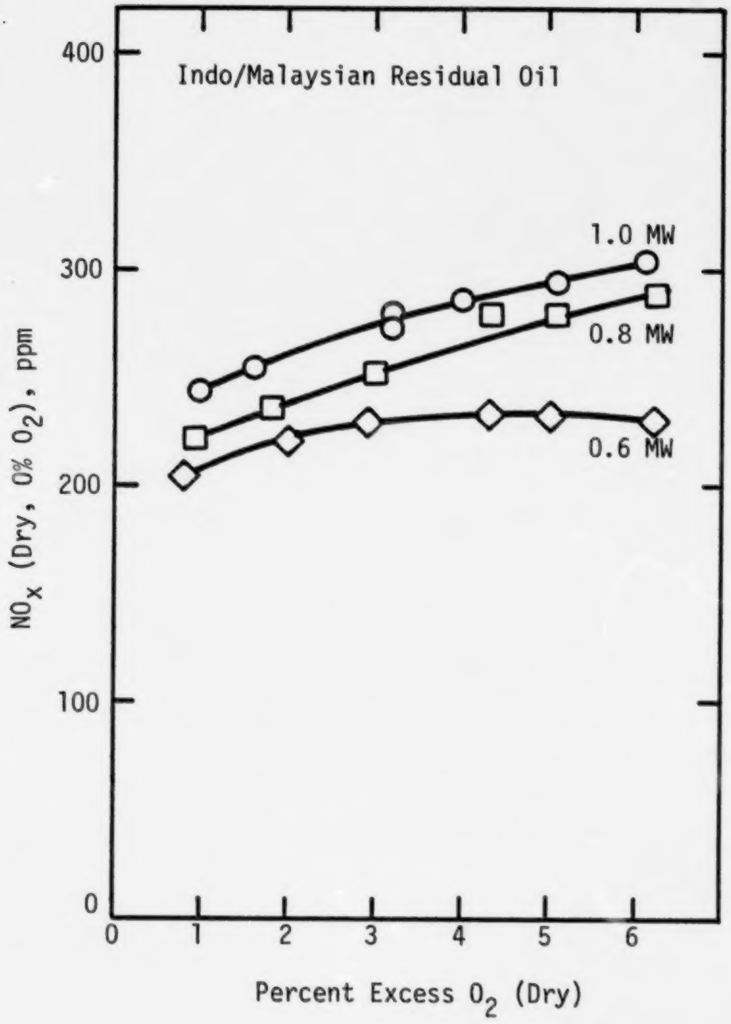

Figure 2-6. NO_x emissions from Commercial Burner A--effect of excess air and load.

250 ppm to 300 ppm as excess oxygen was increased from 1 to 6 percent. A similar increase was observed at lower loads, although for constant excess oxygen, NO_x emissions decreased slightly as load decreased.

Smoke emissions are shown in Figure 2-7. Smoke generally decreased with increasing excess oxygen and increased with decreasing load. At 0.6 MW, smoke emissions proved very sensitive to excess oxygen level. This increase is generally attributed to slower fuel-air mixing at low load caused by decreased air velocity in the burner throat.

The trends observed in Figure 2-6 and 2-7 are typical for state-of-the art commercial burners not designed for low-NO_x emissions; however, burner turndown performance varies among burners built by different manufacturers, as throat and nozzle design vary significantly. Burners of this size frequently operate in an on/off mode as boiler demand varies and hence are not required to operate at any appreciable turndown. Where burner load is modulated to follow steam demand, the burner must be adjusted to increase excess oxygen as turndown increases (load decreases) in order to maintain acceptable smoke and CO emissions. Figure 2-8 shows NO_x emissions at constant smoke number as a function of burner load. Excess air was increased as load decreases in order to maintain smoke number constant. NO_x concentration decreased slightly as load decreased.

Atomizer design is another important factor which determines burner performance. It is often necessary to perform regular maintenance on the atomizer to maintain optimum performance. If the atomization conditions drift from the recommended operating point, burner performance can deteriorate. NO_x and smoke emissions were found to be only slightly sensitive to atomizing air pressure (Figure 2-9 and 2-10). NO_x emissions varied from approximately 295 to 250 ppm as atomizing pressure was varied from 48 to 200 kPa (7 to 29 psig). Smoke emissions remained essentially constant. Increasing oil temperature from 70 to 100°C decreased NO_x from 290 to 240 ppm (Figure 2-11). Smoke number was not affected. This temperature variation produced a variation in oil viscosity from approximately 44 to 13

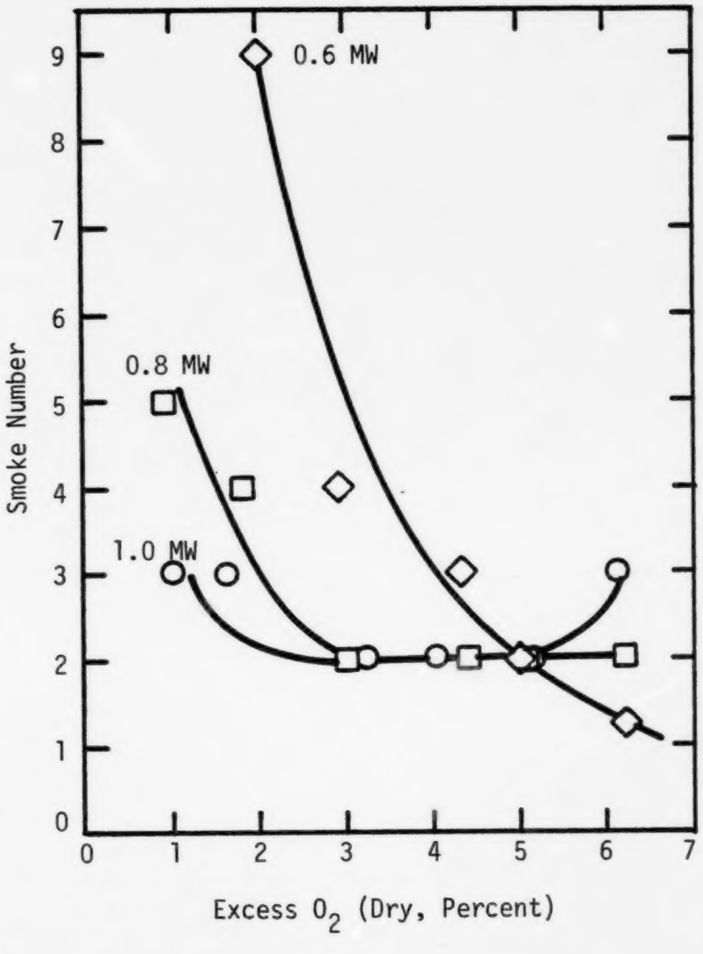

Figure 2-7. Smoke emission from Commercial Burner A--effect of turndown.

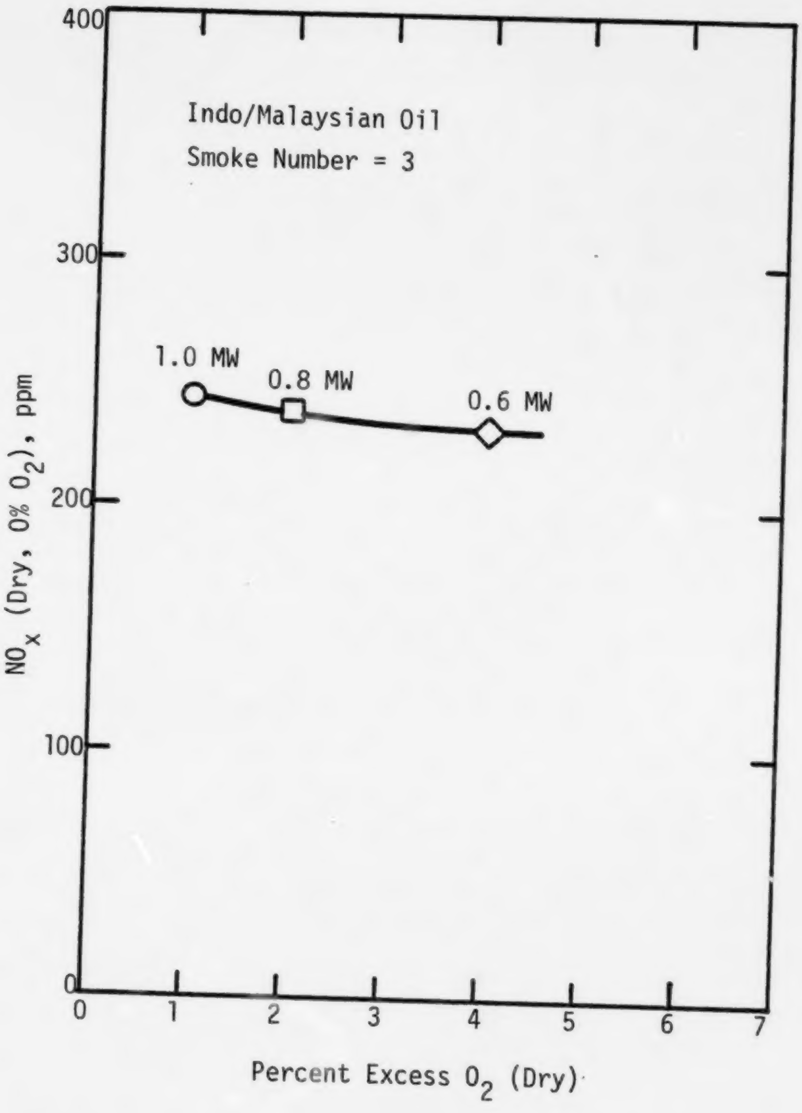

Figure 2-8. Approximate turndown performance for Burner A.

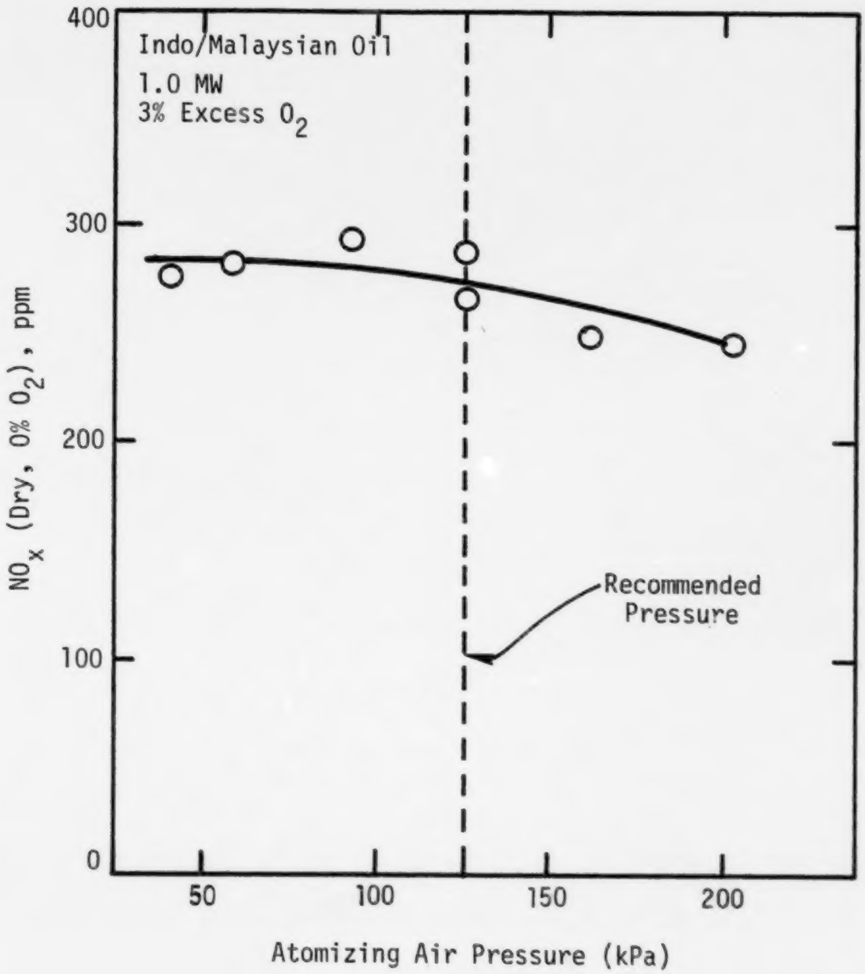

Figure 2-9. NO_x emissions from Commercial Burner A--effect of atomizing air pressure.

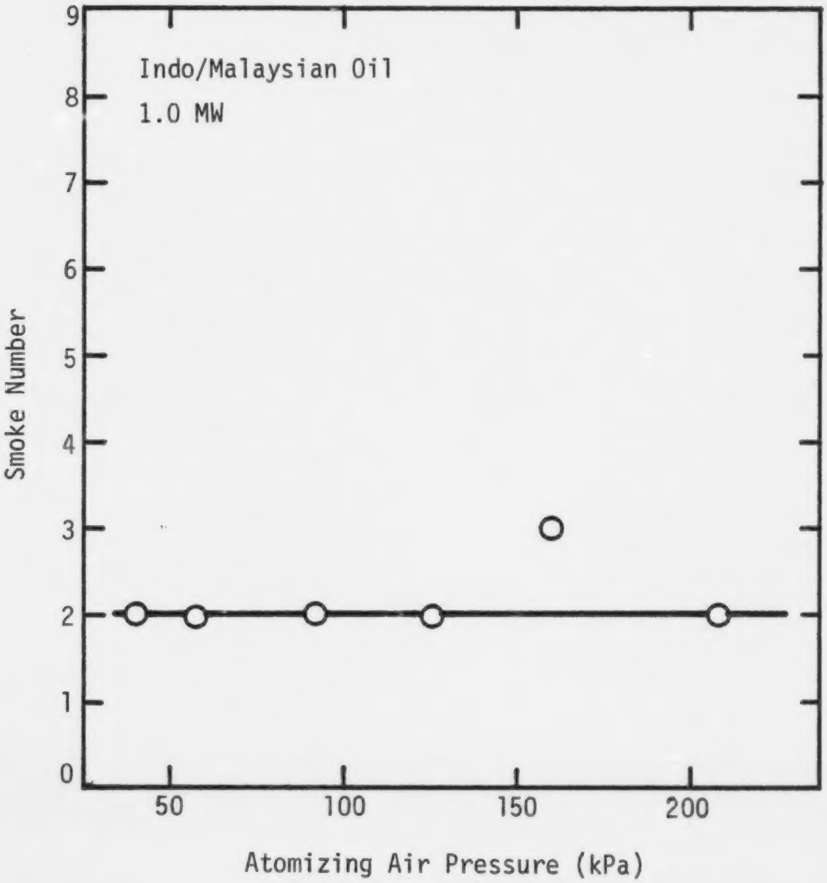

Figure 2-10. Smoke emissions from Commercial Burner A--effect of atomizing air pressure.

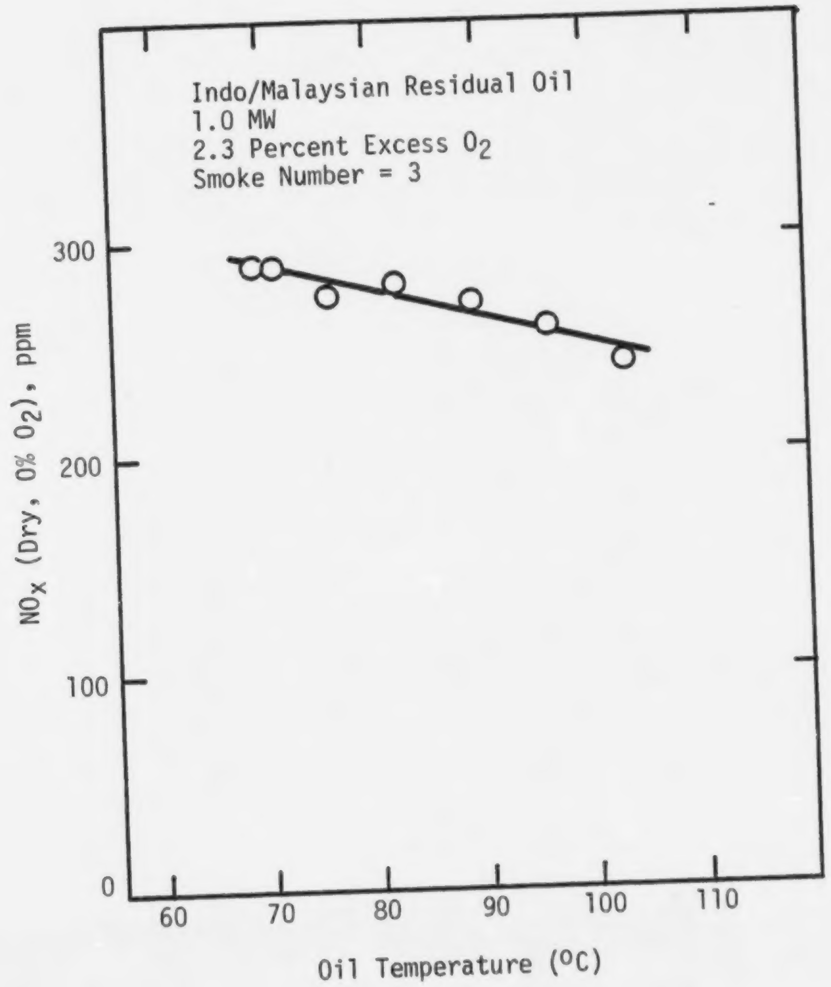

Figure 2-11. Effect of oil temperature on NO_x emissions from Burner A.

centistokes (200 to 60 SSU). Therefore it can be seen that atomization conditions can have significant impact on NO_x and smoke.

During normal operation, atomizing air and oil pressure increased slightly with load (Figure 2-12). Figure 2-13 shows atomizing air consumption, expressed as the ratio of air mass to oil mass, versus atomizing pressure for two loads. At full load, normal atomizing fluid consumption was approximately 15 percent of the fuel mass flow. At a turndown ratio of 1.25 (corresponding to 0.8 MW), atomizing air consumption was 22 percent of the fuel flow by weight.

Figures 2-14 and 2-15 show NO_x and smoke emissions using steam as the atomizing medium. NO_x initially decreased and then increased as steam pressure increased, suggesting an optimum atomizing pressure of approximately 172 kPa (25 psig) which produces a minimum NO_x level of 225 ppm. Smoke number was generally insensitive to atomizing steam pressure.

Particulate emissions from Burner A were measured using the EPA Source Assessment Sampling System (SASS). Figure 2-16 shows the results of two runs under similar conditions firing the Indo/Malaysian No. 6 oil (R4) under normal operating conditions. Results of the two runs were in fair agreement. Total particulate loading was approximately 0.041 pounds per million Btu and mean particle size was approximately 1.2 microns. The fairly large amount of particulate in the 10 μm and 3 μm cyclones suggests much of the total particulate emission is due to cenosphere formation. This was confirmed by examination of the particulate under electron microscope. Figure 2-17 shows scanning electron micrographs of particulate collected in the 10 μm and 3 μm cyclones. The material consists almost entirely of hollow porous spheres with the exception of a few smaller, rounded solid spheres which are probably ash particles. The hollow porous cenospheres are actually remnants of oil droplets which escaped complete combustion.

The particulate matter in the smaller size fraction consists predominantly of fluffy material which is probably soot. Figure 2-18 shows SEM's of the particulate retained on the 1 μm cyclone and filter paper. The

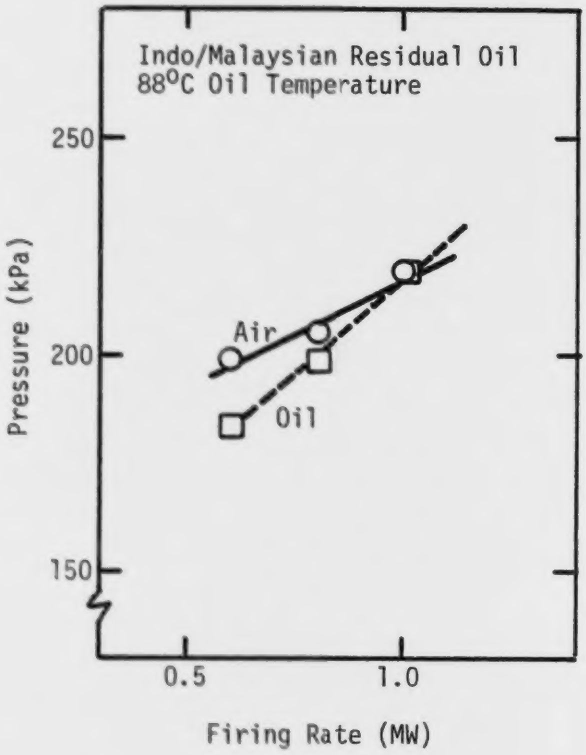

Figure 2-12. Pressure characteristics of Burner A atomizer.

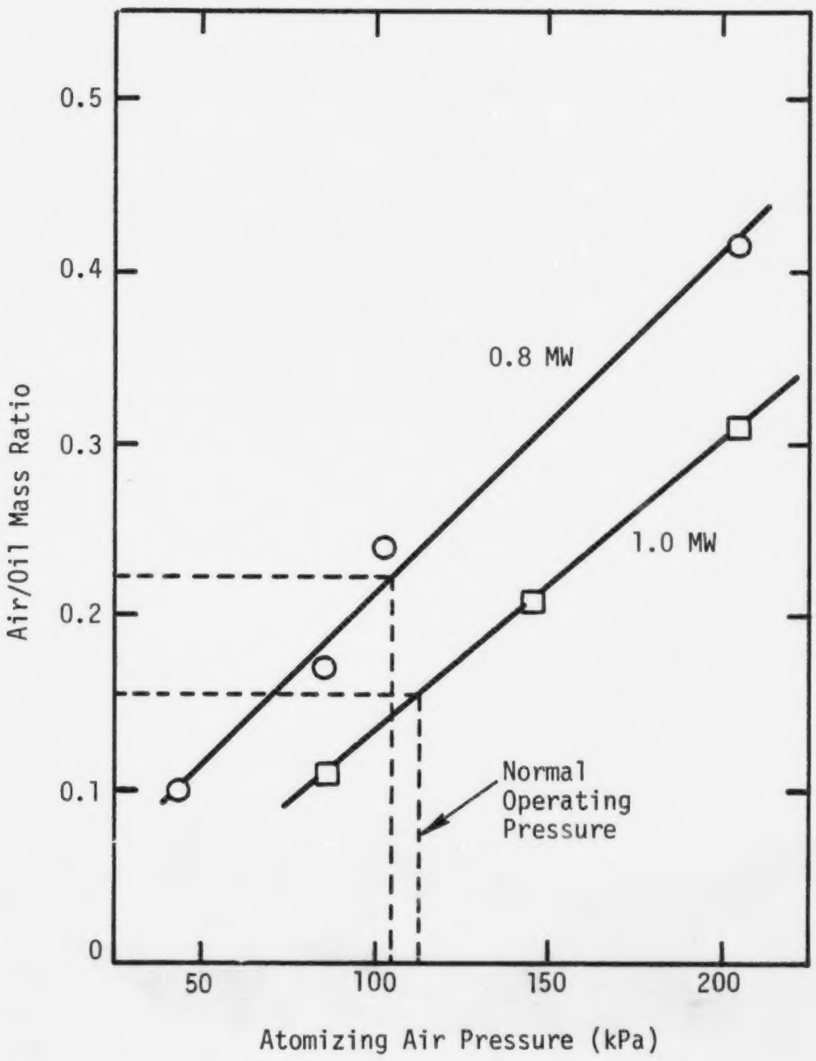

Figure 2-13. Atomizing fluid consumption for Commercial Burner A.

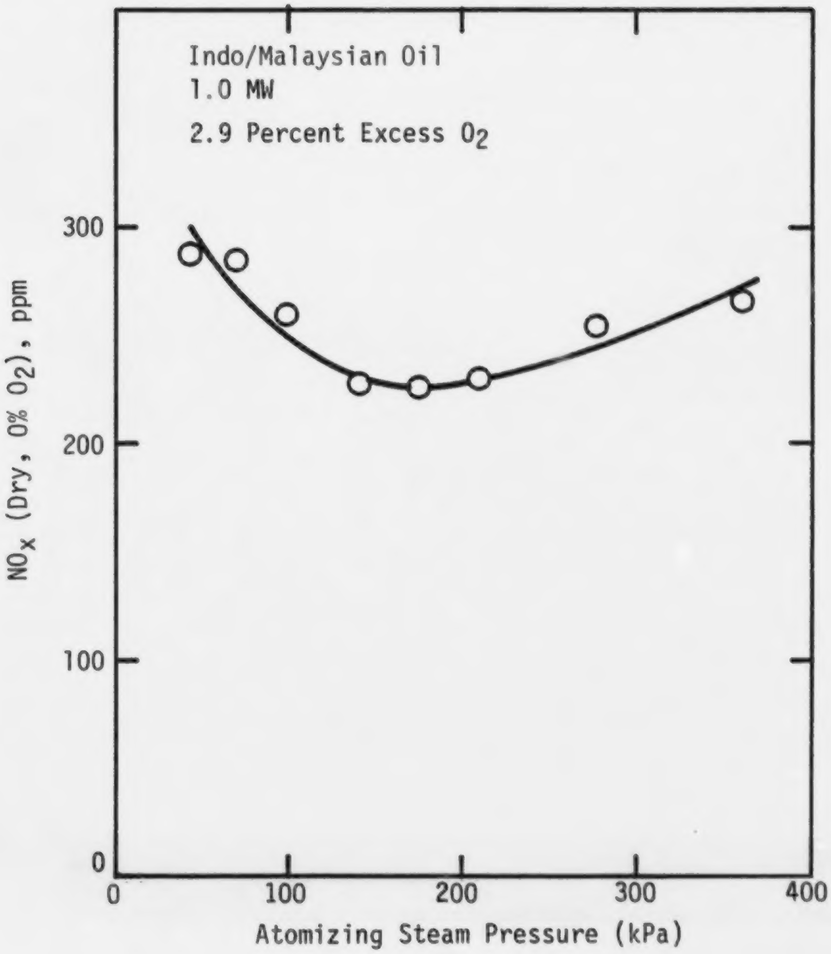

Figure 2-14. NO_x emissions from Burner A using steam as the atomizing medium.

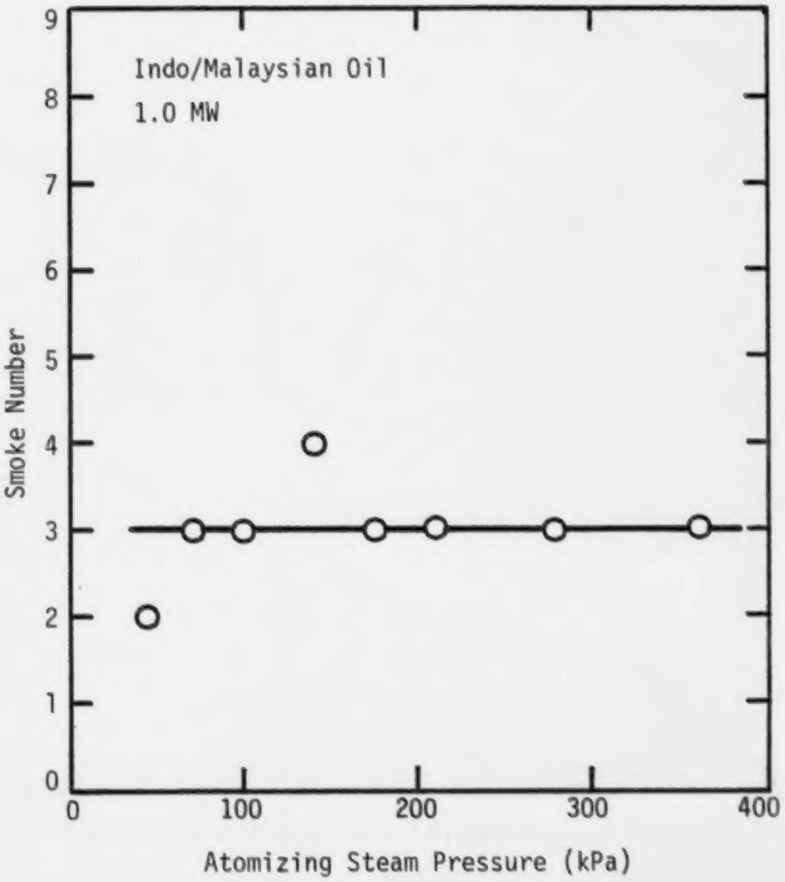

Figure 2-15. Smoke emissions from Burner A using steam as the atomizing medium.

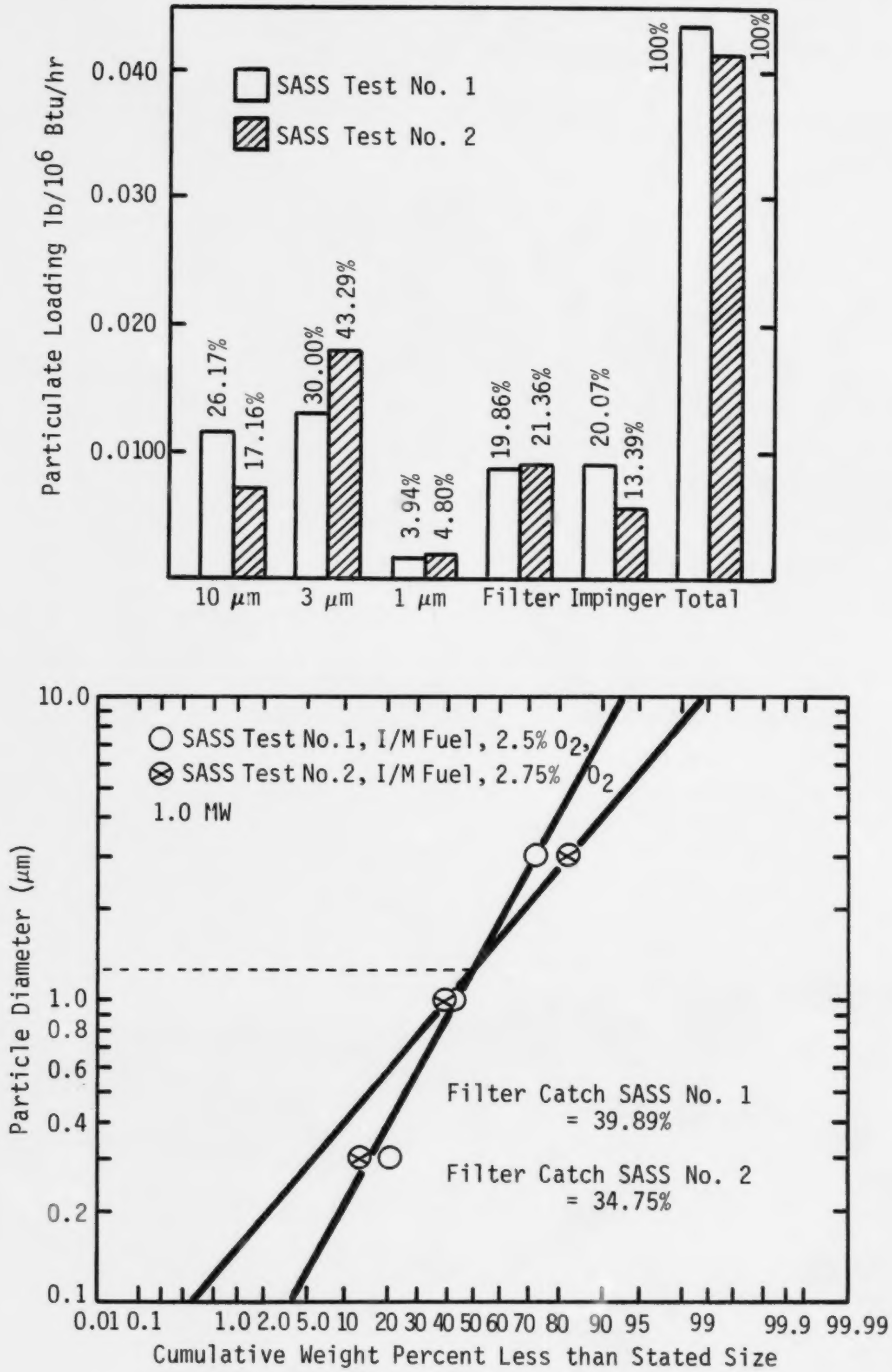

Figure 2-16. Particulate emissions and size distribution from Burner A.

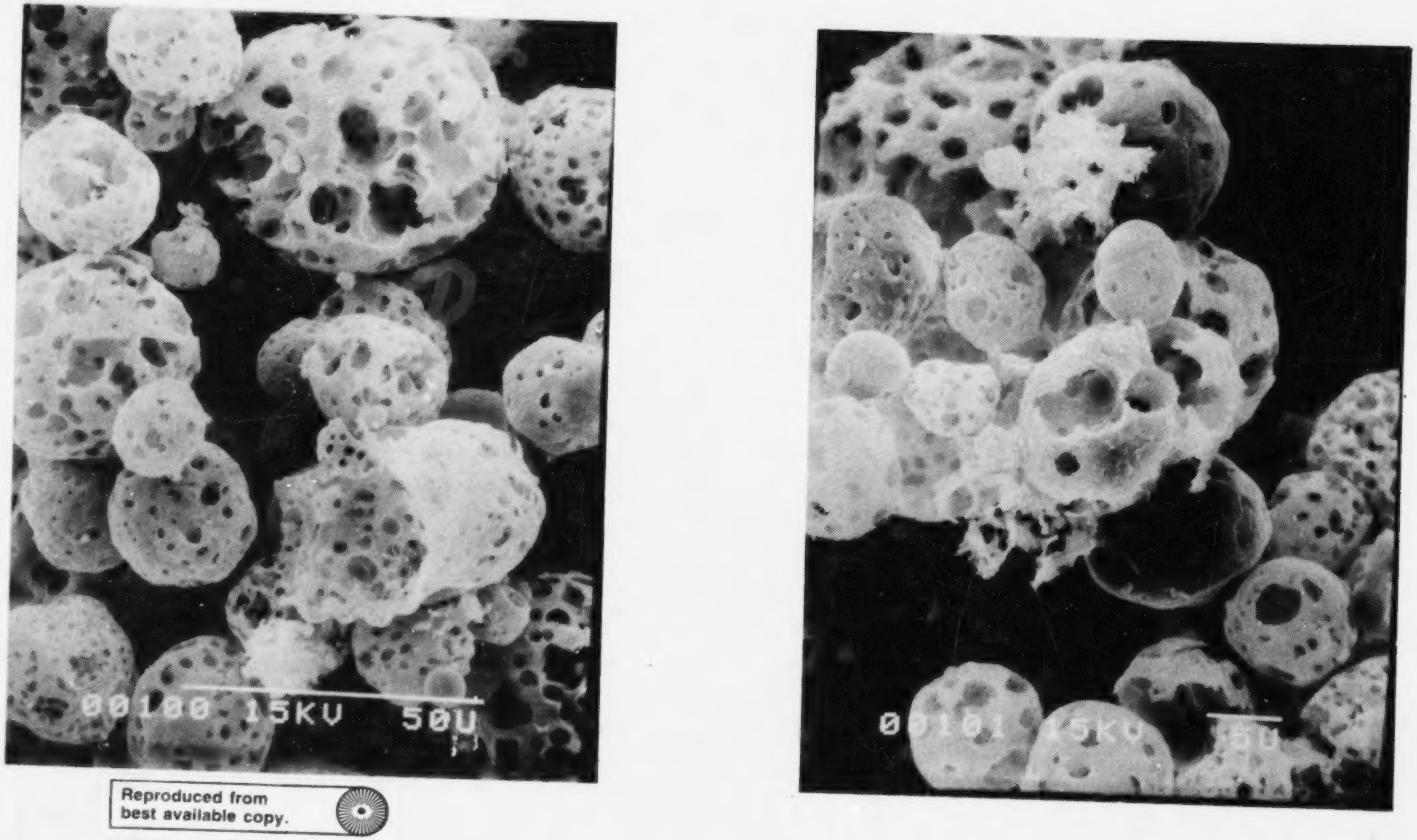
00100 15KV 50U
00101 15KV 50U

Reproduced from best available copy.

a) 10 μm Cyclone

b) 3 μm Cyclone

Figure 2-17. Scanning electron micrographs of coarse particulate collected during SASS runs.

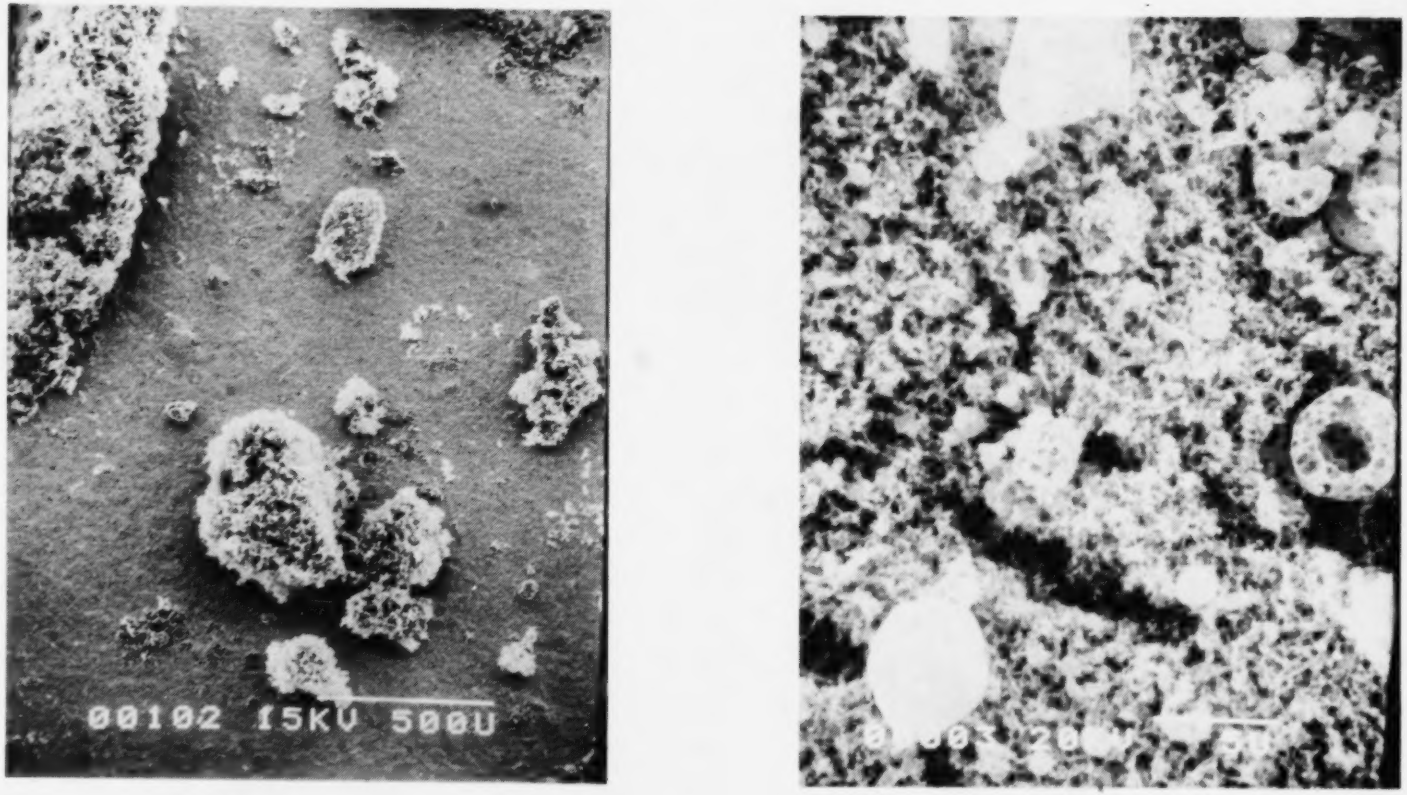
00102 15KV 500U

a) 1 μm Cyclone

b) Filter Paper

Figure 2-18. Scanning electron micrographs of fine particulate collected in SASS runs.

material in the 1 μm cyclone appeared to be large agglomerates of fine, fluffy material. The size of these agglomerates (too large for 1 μm cyclone) suggests that most of the material was originally much smaller and agglomerated after collection in the cyclone trap. The material on the filter was primarily fine soot-like material with fragments of cenospheres. A few small, smooth spheres are also present which are probably ash particles.

2.2.2 Fuel Effects

The results of firing different fuel oils on NO_x and smoke emissions is shown in Figures 2-19 and 2-20. Fuel temperature was adjusted for each fuel to maintain oil viscosity at or below approximately 21 centistokes (100 SSU). Lowest NO_x emissions were achieved with the distillate fuel oil (D3 California No. 2 oil) and the highest emissions were achieved with the crude Paraho shale oil (A3). NO_x emissions increased with increasing fuel nitrogen content, as shown in Figure 2-21.

Smoke emissions were also sensitive to fuel type and appeared to be lowest for the Indo/Malaysian residual oil (R4) and the residual shale oil (A5). The highest smoke emissions were produced with the SRC-II 5.75:1 Middle/Heavy blend (A6).

2.2.3 Staged Combustion

Tests were conducted to determine the effectiveness of reducing NO_x emissions by staging a conventional burner. This was achieved by injecting a portion of the combustion air through a water-cooled boom which was positioned on the centerline of the firetube from the aft viewport. The staging or secondary air was injected radially outward from the boom. Figure 2-22 shows NO_x emissions versus the stoichiometric ratio supplied through the burner for two axial injection locations. The residence time between the burner and the staging air and injection location was estimated to be approximately 0.3 and 0.5 seconds for the two cases.

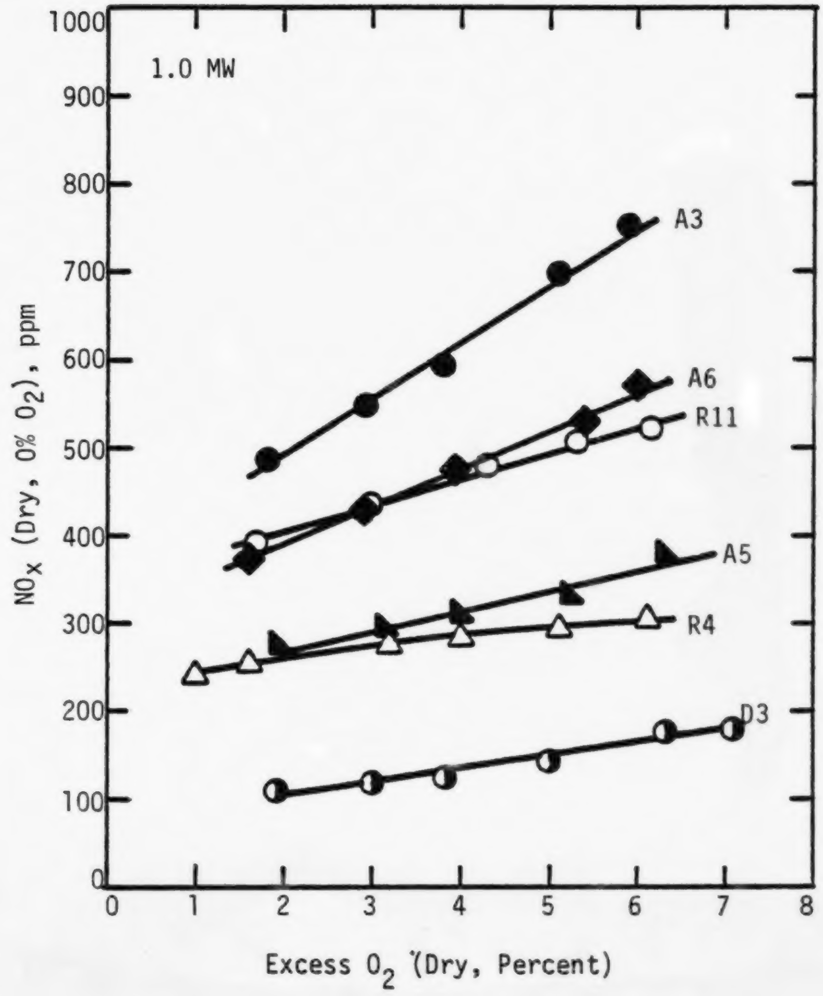

D3	California No. 2 Oil (0.053% N)
R4	Indo/Malaysian Residual Oil (0.24% N)
R11	California No. 6 Oil (0.77% N)
A3	Crude Paraho Shale Oil (2.08% N)
A5	Residual Paraho Shale Oil (0.46% N)
A6	SRC-II 5.75:1 Middle/Heavy Blend (0.96% N)

Figure 2-19. NO_x emissions for various fuels tested with commercial burner A.

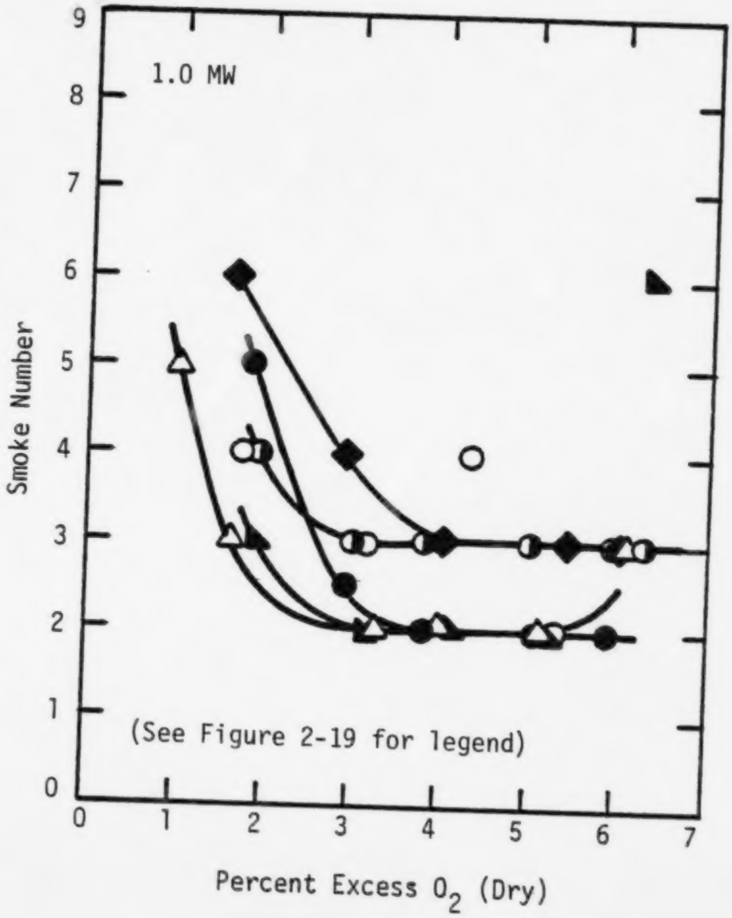

Figure 2-20. Smoke emissions for various fuels tested with commercial burner A.

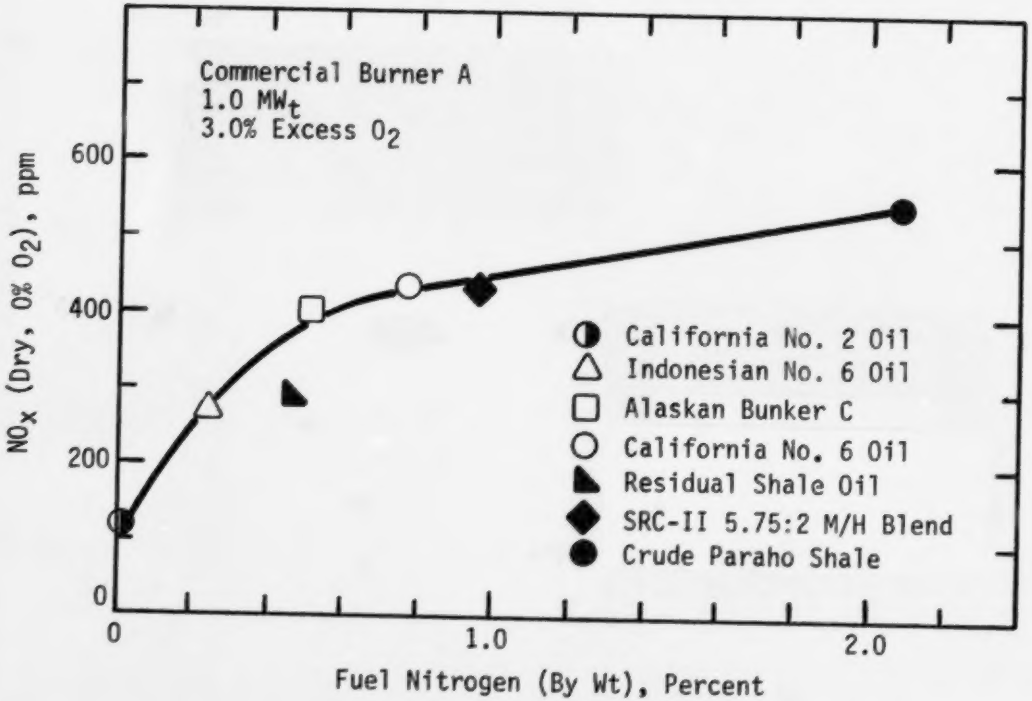

Figure 2-21. NO_x emissions versus fuel nitrogen content--Burner A.

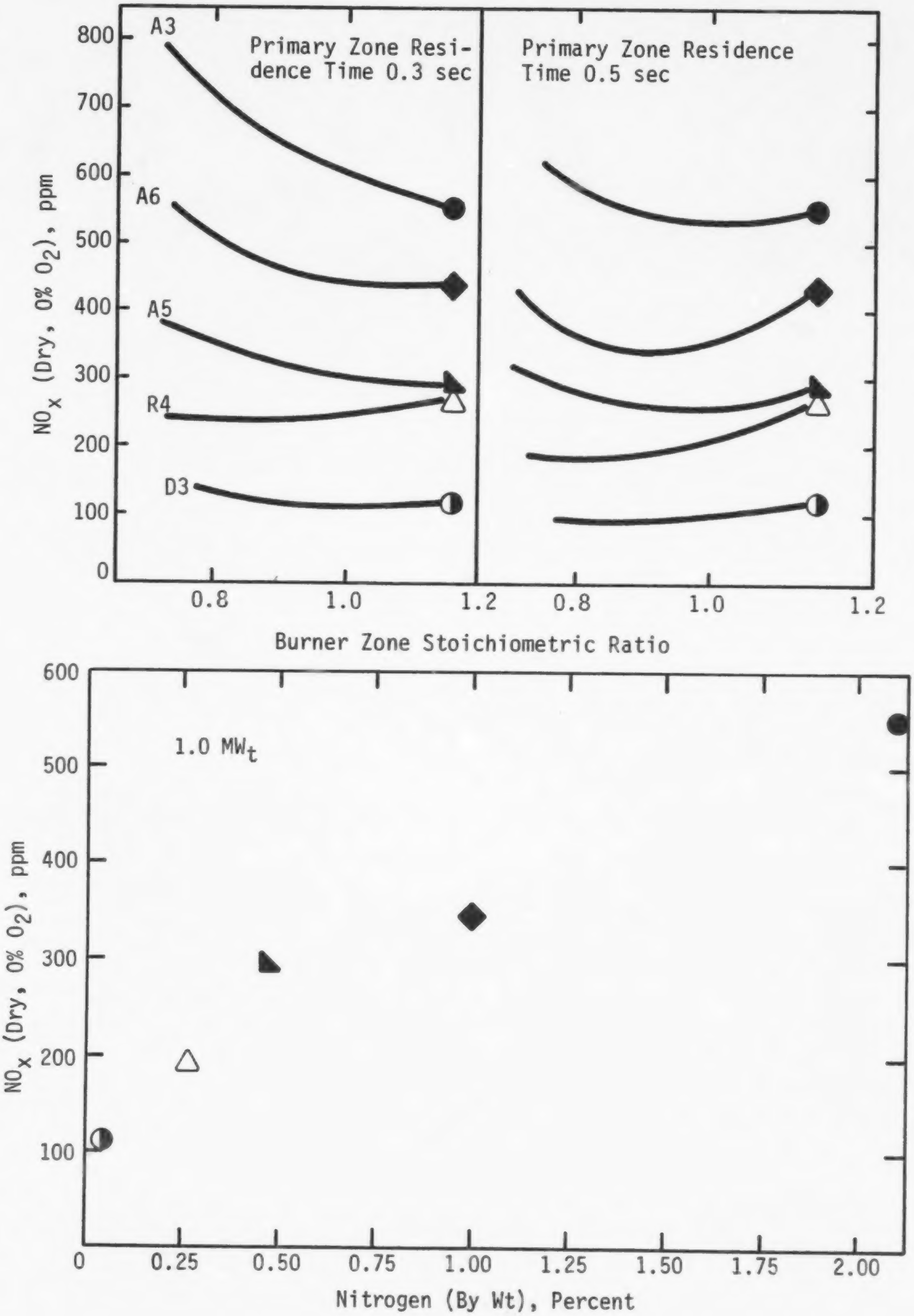

Figure 2-22. Effect of staged air addition on NO_x emission from Commercial Burner A.

NO_x emissions were seen to increase when staging air was injected close to the burner (residence time 0.3 seconds), except for the Indo/Malaysian residual oil which showed a slight decrease in NO_x. At residence time of 0.5 seconds, NO_x emissions decreased slightly for each fuel tested and reached a minimum as staging was increased. The NO_x reduction was greatest for the SRC-II blend (A6) at primary zone residence time of 0.5 seconds.

These results were somewhat surprising in light of results obtained in a previous study using a different, experimental burner. Those studies (England, et al, 1982) showed a significant decrease in NO_x emissions as staging air was increased. These results indicate that simple staging alone may actually increase NO_x emissions and point to the importance of optimizing the primary zone mixing and thermal environment.

2.3 Evaluation of Commercial Burner B

Burner B is illustrated in Figure 2-23. Nominal firing capacity is 1.2 MW (4.2×10^6 Btu/hr). The burner contains an integral blower and air damper, fuel-oil bypass control valve, gas pilot, twin-fluid atomizer, and flame safeguard and operating controls. The burner housing is cast iron with sheet metal components.

The Burner B fuel atomizer is a twin-fluid, internal-mixing type similar to that used in Burner A. This atomizer is designed for use with either air or steam as the atomizing fluid. Atomizing fluid consumption is rated at 8.2 kg/hr for air and 13.6 kg/hr for steam; however, the atomizing fluid consumption varies with load as shown in Figure 2-24. The burner was not tested with steam atomization.

The evaluation conducted on Burner B was less extensive than on the first burner and tests were oriented toward establishing the impact of fuels and operating conditions on NO_x and smoke emissions.

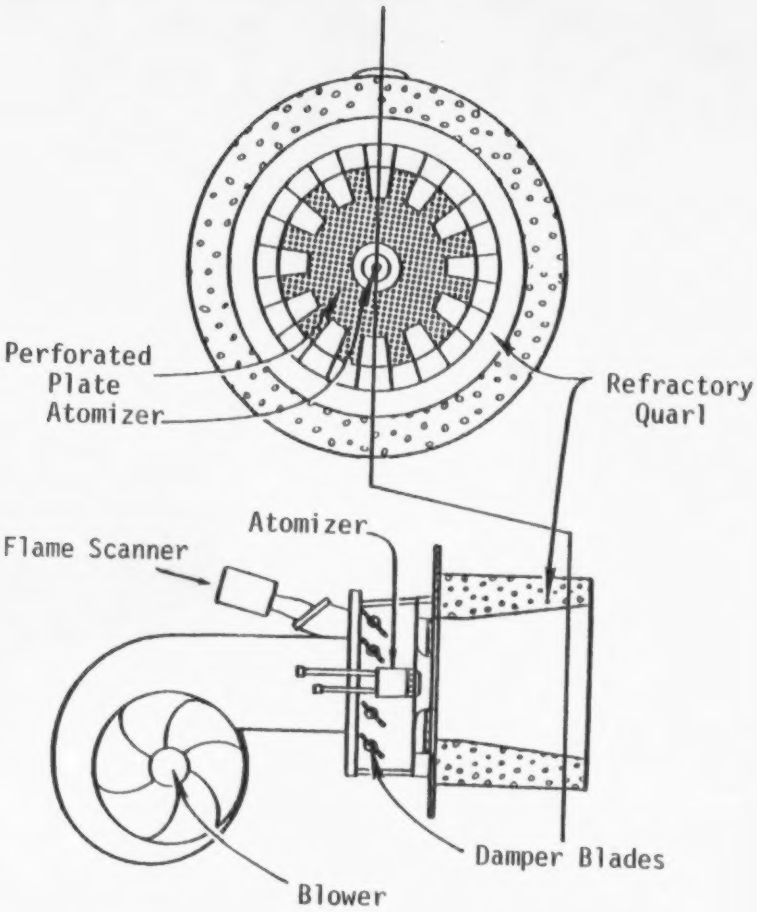
Perforated Plate
Atomizer
Refractory Quarl
Atomizer
Flame Scanner
Damper Blades
Blower

Figure 2-23. Commercial Burner B.

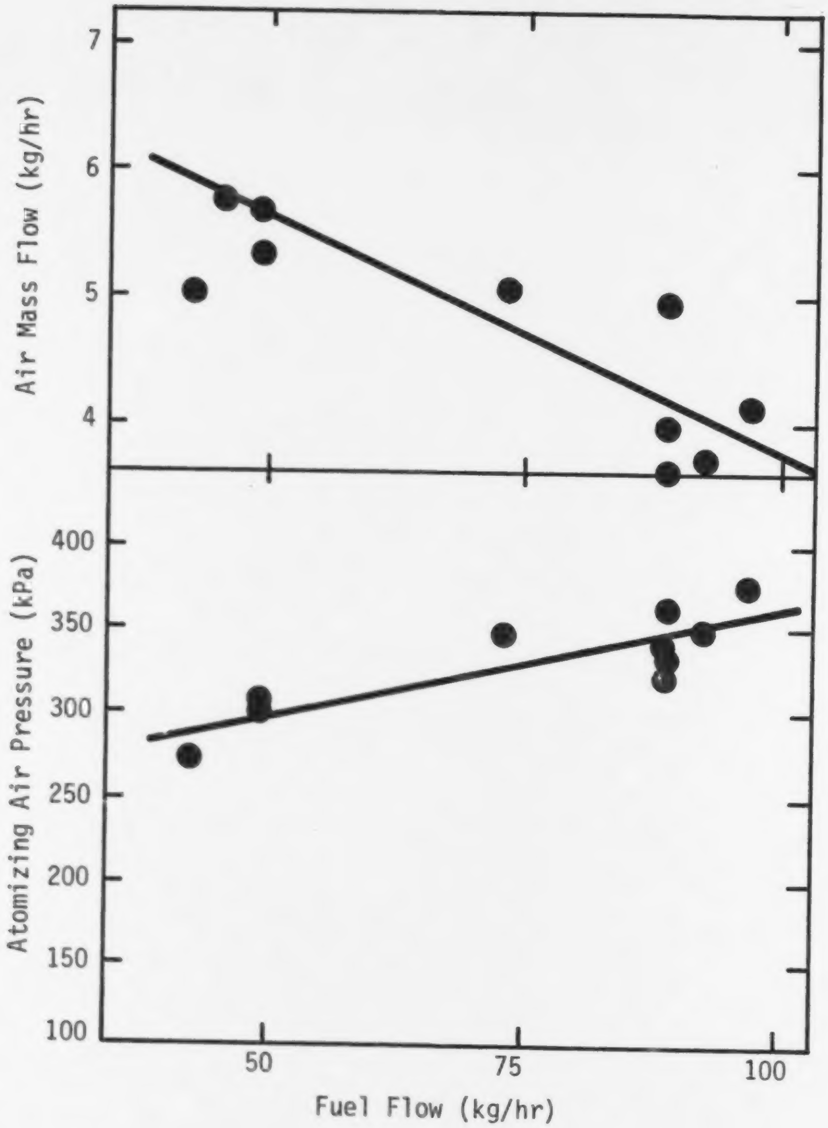

Figure 2-24. Atomizing air requirements of Burner B atomizer.

2.3.1 Baseline Characterization

NO_x and smoke emissions from Burner B are shown in Figures 2-25 and 2-26 for the Indo/Malaysian residual oil fired at three heat release rates. Emissions were only slightly dependent upon load over the range investigated. NO_x emissions increased sharply with excess O_2 from approximately 235 ppm at 0.5 percent excess O_2 to 315 ppm at 6 percent excess O_2. NO_x emissions are similar to the results presented earlier for Burner A (Figure 2-6) but appear to be more strongly dependent on excess O_2 level. Both NO_x and smoke emissions were less sensitive to turndown than Burner A, and smoke emissions at low load (0.6 MW) were lower. Burner B produced acceptable smoke emissions (smoke number less than 5) between 2 and 3 percent excess O_2 at all loads. Additionally, flame stability at high turndown ratio (2.6 to 1, equivalent to 0.47 MW) appeared to be superior. This illustrates the impact of burner design characteristics on NO_x and smoke emissions in a particular furnace configuration. Burner performance may vary somewhat in other applications depending on furnace characteristics such as confinement (L/D) and heat release per cooled surface area (Q/A).

The effect of atomizing air pressure on NO_x and smoke emissions is shown in Figures 2-27 and 2-28. Emissions were not strongly sensitive to atomization pressure. Smoke emissions tended to increase slightly at low atomization pressure, indicating deterioration of spray quality and fuel/air mixing. Burner stability appeared to be satisfactory over the range shown.

Figures 2-29 and 2-30 compare NO_x and smoke emissions from Burner B fired with several fuels fired previously in Burner A. NO_x emissions were strongly sensitive to fuel nitrogen content and ranged from approximately 90 ppm for distillate oil D3 to 1075 ppm for the crude shale oil A3 (at 3 percent excess O_2). NO_x emissions from the high nitrogen fuels (crude shale A3 and California residual oil R11) were much more sensitive to excess O_2 than the low nitrogen fuels. NO_x from the nitrogen-free distillate oil D3 were relatively insensitive to excess O_2. The same fuel trends were observed at reduced load. Figure 2-31 shows NO_x versus load for these same five

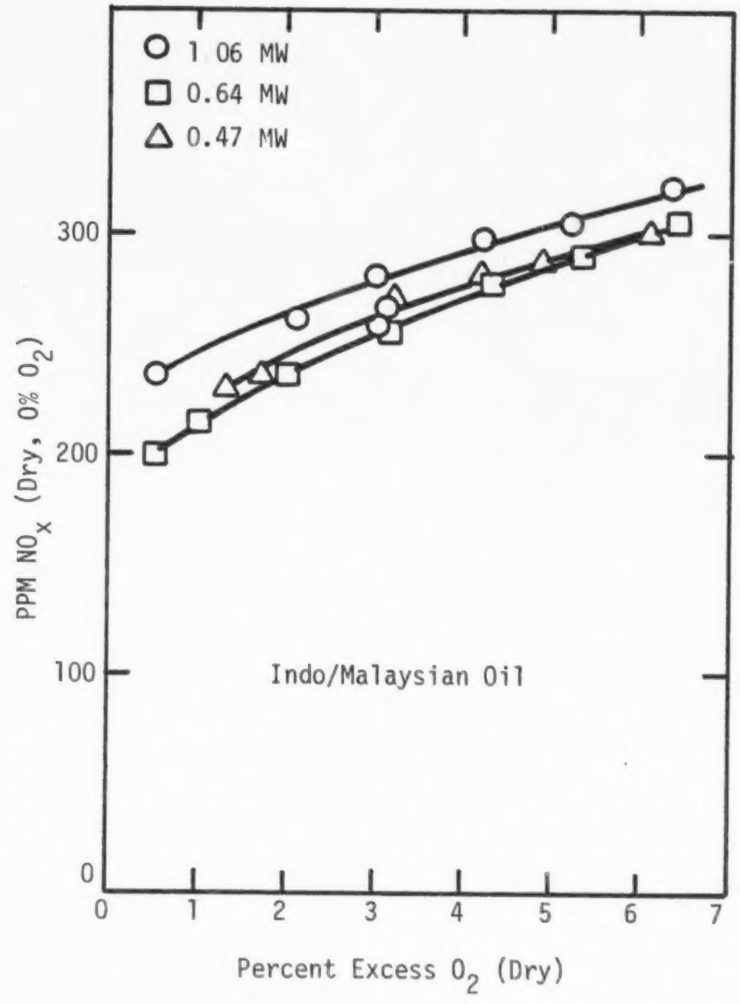

Figure 2-25. NO_x emissions from Burner B as a function of heat release rate.

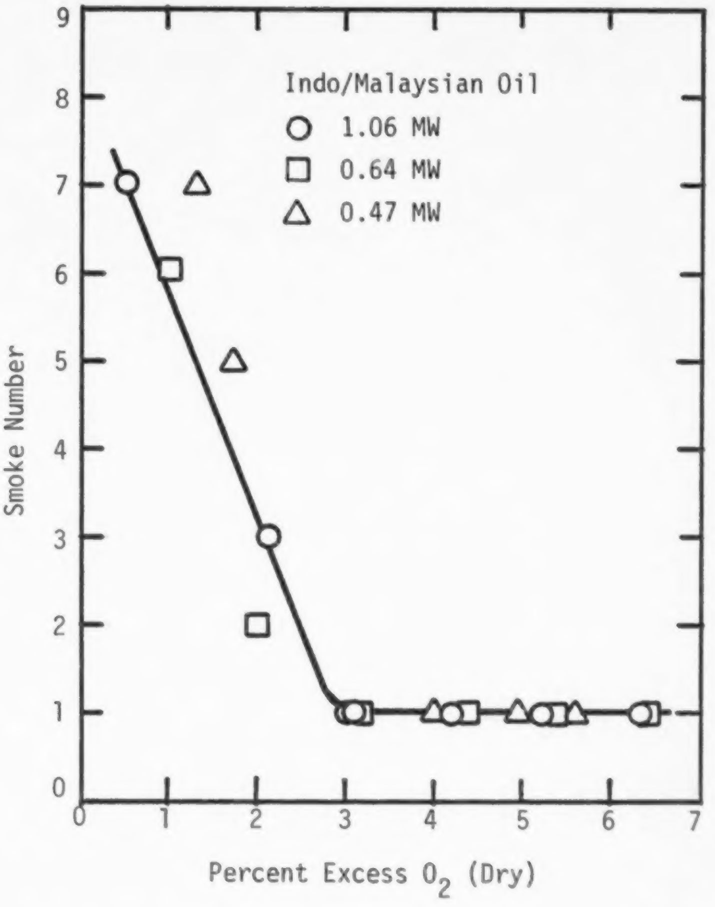

Figure 2-26. Smoke emissions from Burner B as a function of load.

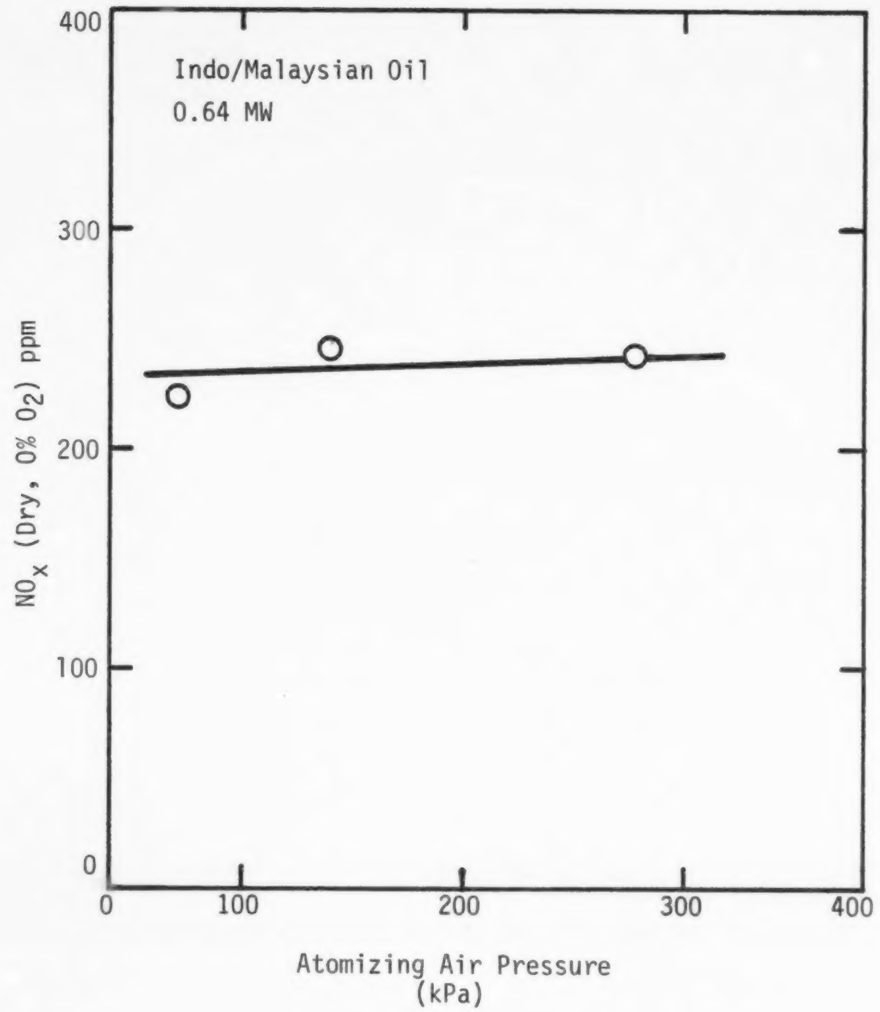

Figure 2-27. Effect of atomizing air pressure on NO$_x$ emissions from Burner B.

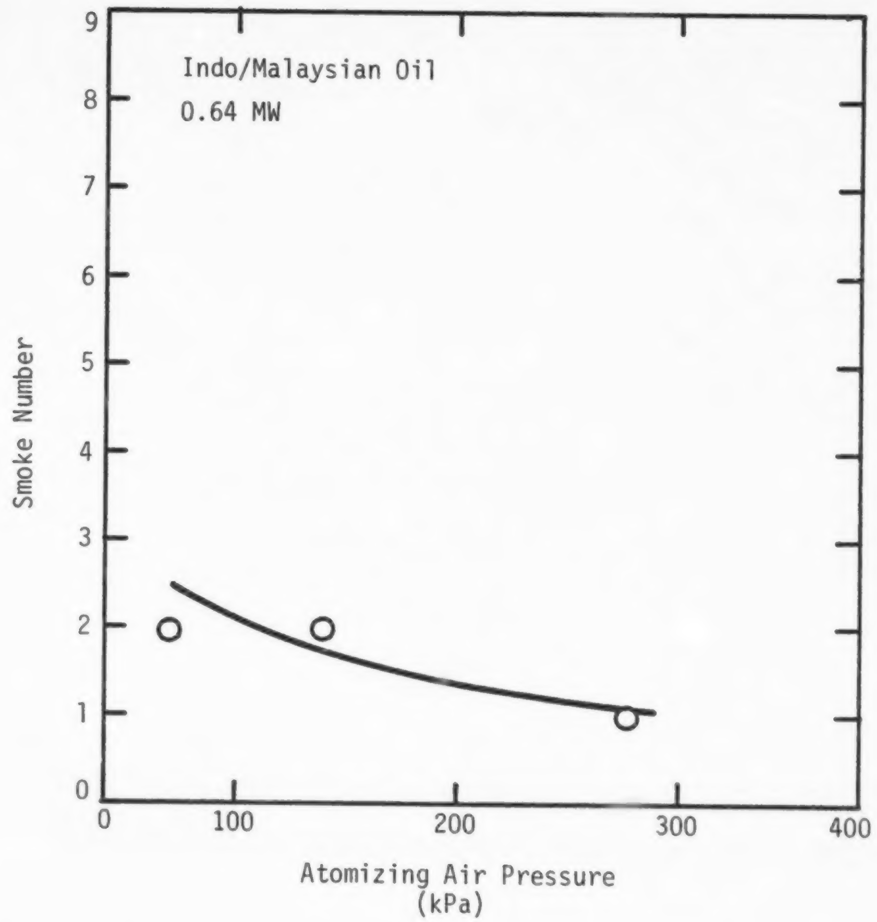

Figure 2-28. Effect of atomizing air pressure on smoke emissions from Burner B.

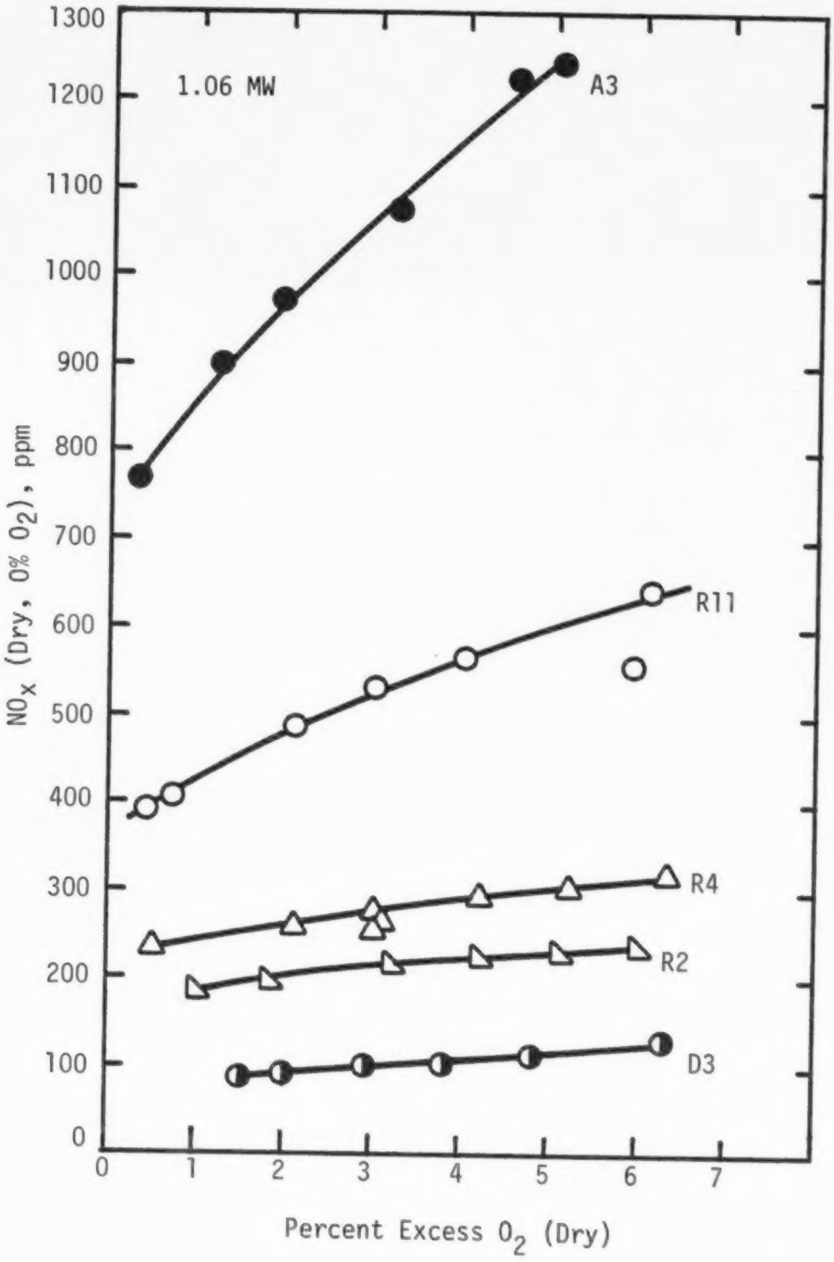

Figure 2-29. NO_x emissions for several fuels fired in Burner B.

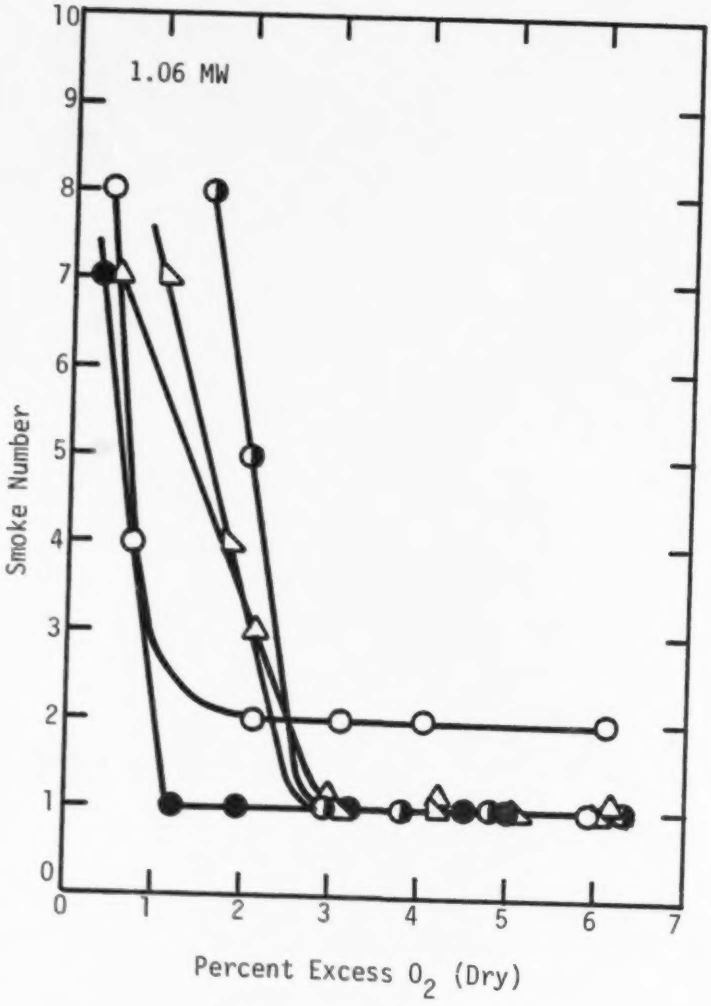

Figure 2-30. Smoke emissions for several fuels fired in Burner B.

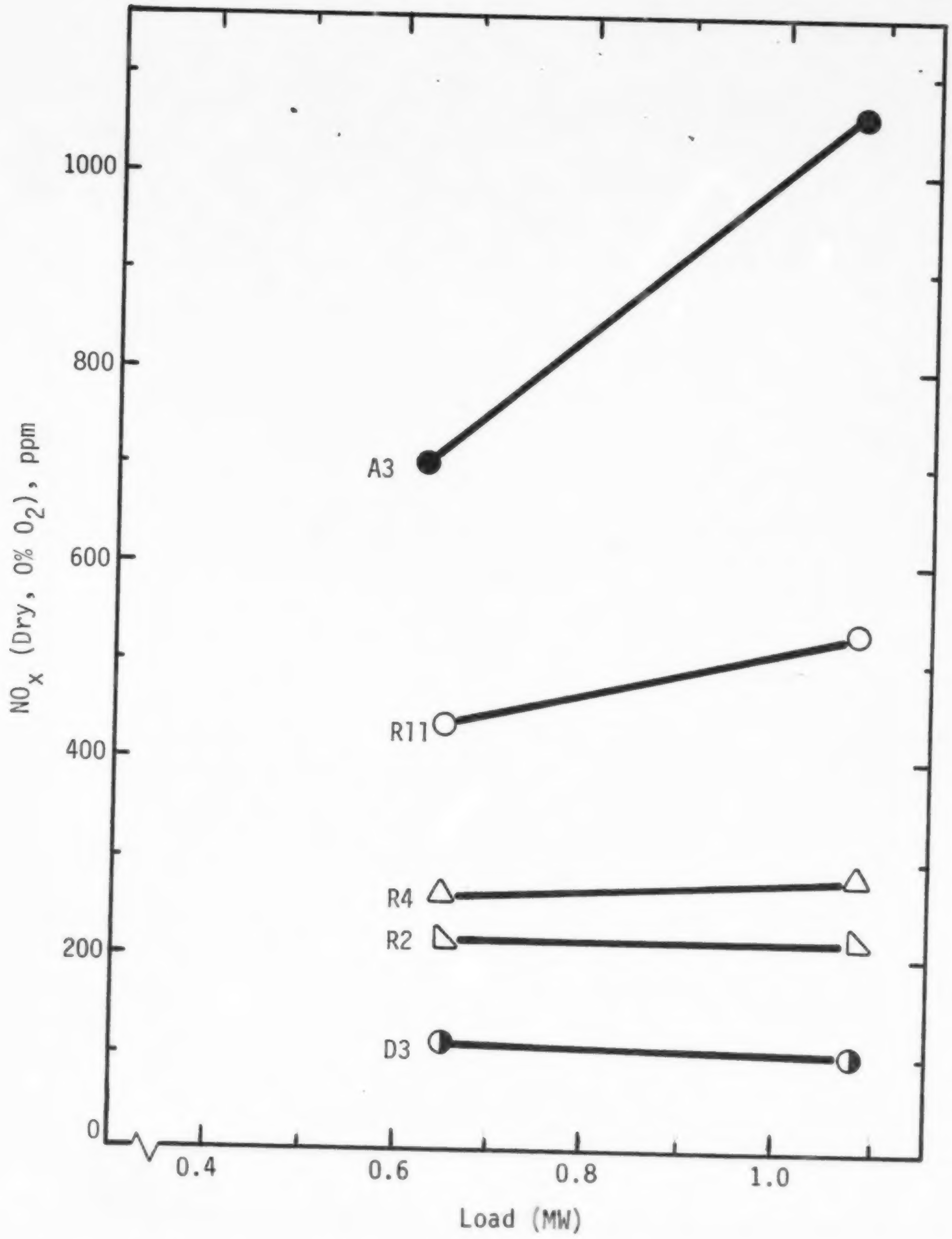

Figure 2-31. NO_x emissions from Burner B versus load for distillate, residual, and alternate fuel oils.

fuels. The distillate oil produced NO_x emissions insensitive to load, indicating that thermal NO_x was essentially constant at approximately 110 ppm. NO_x from the crude shale oil was much lower at reduced load. This illustrates the sensitivity of fuel NO_x formation to fuel/air mixing, since air velocity at the burner throat decreases with decreasing load. Estimated fuel nitrogen conversion decreases from about 28 percent at high load (1.06 MW) to about 18 percent at low load (0.64 MW) for the crude shale oil (assuming constant thermal NO_x). Similarly, estimated fuel nitrogen conversion for the California residual oil is approximately 34 percent and 27 percent at 1.06 and 0.64 MW, respectively.

2.4 Experimental Prototype Low-NO_x Oil Burner

An advanced low-NO_x burner concept suitable for high-nitrogen fuels based upon staged combustion with a high-temperature primary zone and a low-temperature secondary zone was derived from information obtained in the bench-scale studies. The bench-scale experiments were designed to supply information concerning the optimization of various parameters with respect to this concept and thus provided specific information necessary for scale-up. The burner concept is divided into three zones and the important features of each zone are defined as follows:

- Fuel Vaporization Zone
    - Fuel/air mixing
    - Fuel injection
    - Heat extraction
    - Geometry

- Fuel-Rich Hold-Up Zone
    - Residence time
    - Heat extraction
    - Geometry

- Second-State Burnout Zone
  - Secondary fuel/air mixing
  - Heat extraction

Table 2-5 summarizes the criteria which were used to design a pilot-scale burner with a nominal firing rate of 0.59 MW. The overall design approach was to build a primary zone of sufficient volume to provide at least 200 milliseconds residence time with minimum heat loss. Geometry was cylindrical with diameter based upon maximizing fuel/air mixing and minimizing heat loss. The baseline fuel injector provided small droplets. The second stage was designed to limit peak secondary flame temperatures to 2800°F.

The prototype test burner is illustrated in Figure 2-32. The burner consists of three sections:

1. A primary air/fuel injection section

2. A fuel-rich hold-up zone

3. A secondary injection section

Low NO_X emissions are achieved by operating the primary zone at an air/fuel ratio less than stoichiometric and injecting secondary or burnout air downstream of the primary zone in order to complete combustion. The design for each section was based upon the criteria in Table 2-5.

The primary zone is constructed from high-temperature refractories and insulation which minimize conductive heat loss through the walls and permit near-adiabatic conditions in the primary zone. Fuel and primary air are injected without swirl at the beginning of a divergent quarl section, which is followed by a fuel-rich holdup section. Residence time in the fuel-rich zone is approximately 560 msec at 0.59 MW Btu/hr, $SR_1 = 0.7$ and 1540°C. The primary combustion products are directed through a convergent section which

ABLE 2-5. DESIGN CRITERIA FOR SCALEUP OF LOW-NO_x CONCEPT

Parameter	Optimum Range Defined by Small Scale
A. Fuel Vaporization Zone	
1) Fuel/Air Mixing	Rapid mixing of fuel and air for maximum utilization of residence time.
2) Fuel Injection	Finely atomized droplets to allow rapid vaporization of fuel. 98% of droplets <50 μm.
3) Heat Extraction	Minimum heat loss to maximize droplet vaporization.
4) Geometry	Not defined.
B. Fuel Rich Holdup Zone	
1) Residence Time	Mean residence time >200 msec at high temperature.
2) Heat Extraction	Minimize heat extraction to maximize rate of decay of XN species to N_2. Preferably exit temperatures >1400K.
3) Geometry	Designed to maximize true residence time/volume ratio.
4) Stoichiometry	Variable from 0.4 to 1.16. Optimum at 0.65-0.85.
C. Second Stage Burnout	
1) Secondary fuel/air mixing	Slow to minimize peak flame temperature, thus minimizing second stage thermal NO_x formation.
2) Heat Extraction	Optimize to limit peak flame temperature <2800F

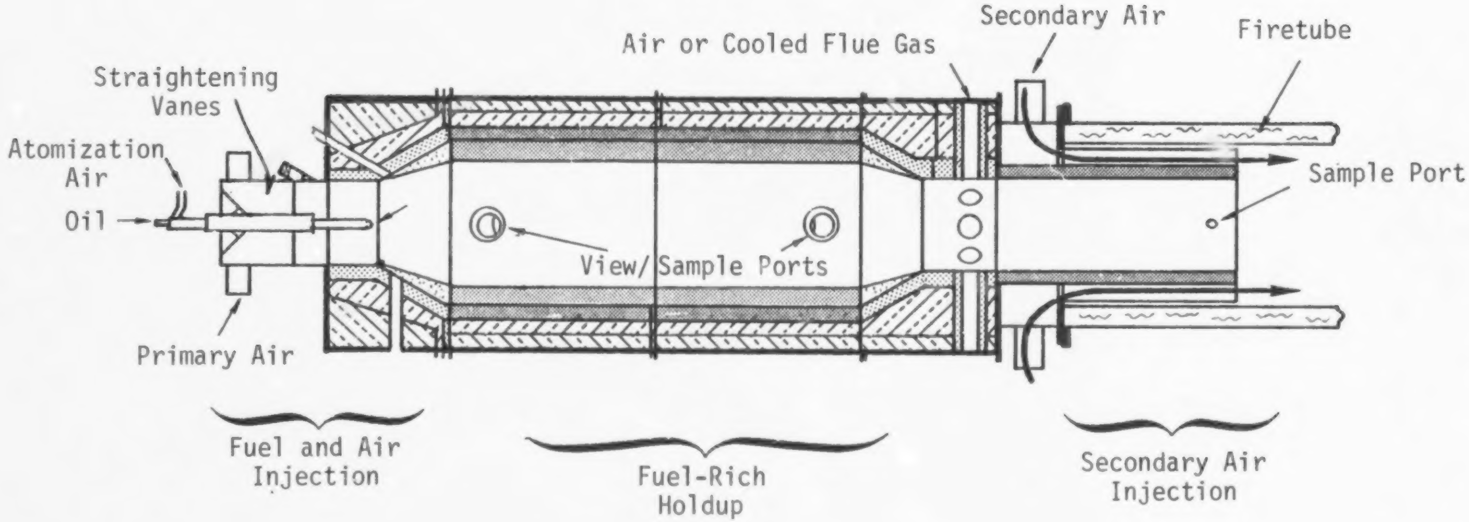
Straightening
Vanes
Atomization
Air
Oil
Primary Air
Air or Cooled Flue Gas
Secondary Air
Firetube
Sample Port
View/Sample Ports
Fuel and Air
Injection
Fuel-Rich
Holdup
Secondary Air
Injection

Figure 2-32. Prototype firetube boiler test burner.

serves to minimize radiative heat loss, ensure complete mixing of the primary products, and minimize backmixing of secondary air into the primary zone. Eight radial ports are provided immediately after the convergent section for sampling or interstage air addition. Secondary air is injected parallel to the burner axis annularly around the primary exit without swirl. A sample port is located at the burner exit for sampling gases from the primary zone.

The primary throat was designed to produce very low primary air velocity (1.5 m/sec) at the point of fuel injection. This was done to minimize recirculation of gases within the fuel-rich zone. Flame stabilization was achieved by radiation from the hot refractory walls. The primary zone exit velocity was designed for 17 m/sec (55 ft/sec) and the secondary air velocity was very low (1 m/sec) in order to produce a long, slow-mixing diffusion type flame.

Two different atomizer types were evaluated in the pilot-scale experiments. A Sonicore 188 T ultrasonic atomizer was chosen as the baseline atomizer for the fine spray produced at high atomization pressures and the relatively large oil orifices which would be unlikely to plug with viscous fuels. This atomizer is a larger version of the one used extensively in the bench-scale experiments which provided good atomization of a wide range of fuels. Initially the atomizer was used as received; however, the resonator cap was later removed to alleviate coking problems on the tip of the resonator. Drop size distribution measurements with a similar nozzle indicate that removing the resonator cap has only a small influence on the mean droplet diameter. The nozzle was used in this configuration for all testing. Air was used as the atomizing medium and 172 kPa (25 psig) was chosen as the baseline atomization pressure. A Todd CDS (constant differential steam) atomizer was also tested. This atomizer is an internal-mixing steam jet atomizer utilizing an internal mixing chamber with a drilled nozzle cap. The Todd atomizer and a nozzle similar to the Sonicore 188 T have been characterized with respect to drop-size distribution and spray pattern in a previous study (England et al, 1982). The results of the spray characterization (Figure 2-33) indicate a significant difference in drop-size distributions produced by the two atomizers when operated under normal

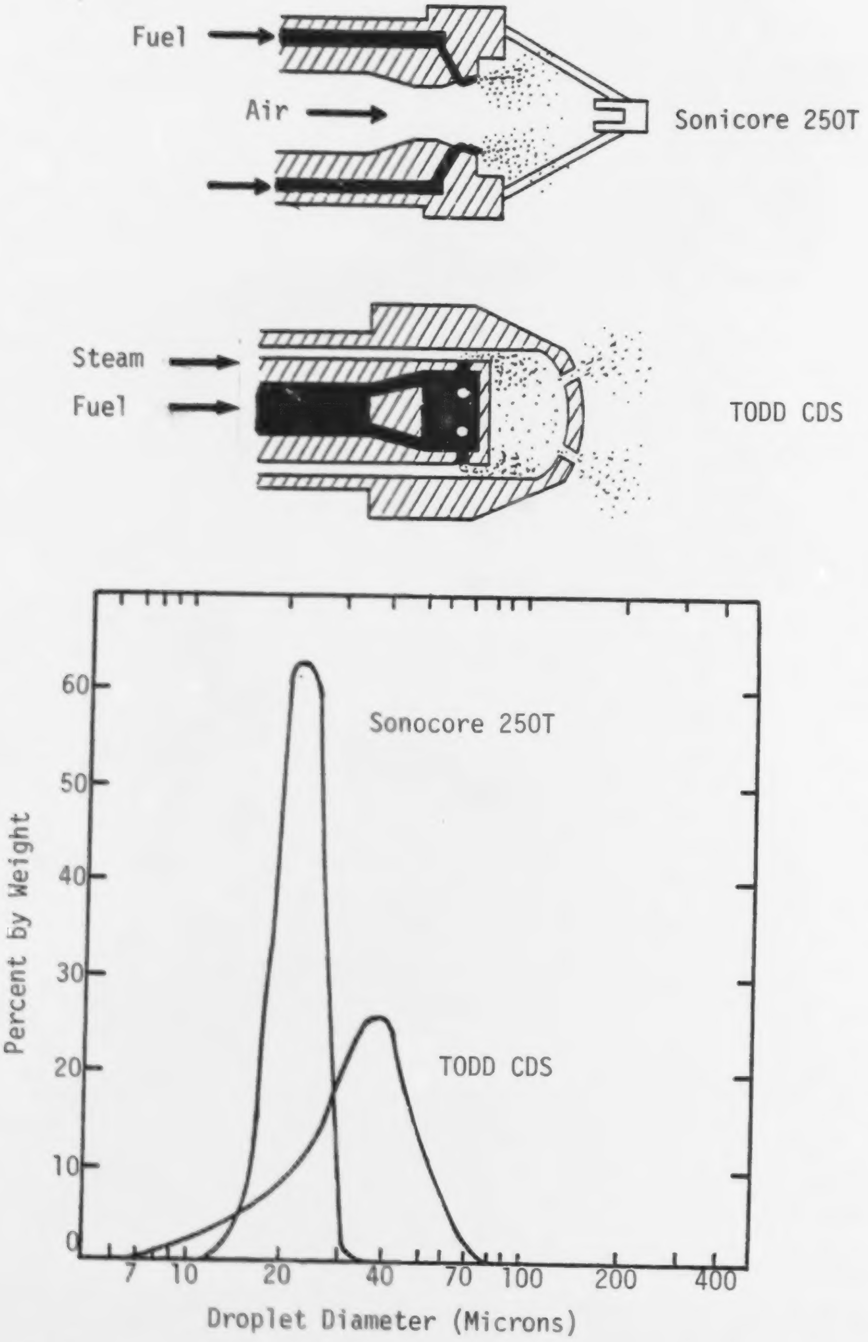

Figure 2-33. Spray characteristics of commercial atomizers used in prototype burner.

conditions. The drop-size distribution can be substantially changed by operating the atomizer at other atomization pressures.

A second primary throat was designed to produce a premixed fuel/air mixture prior to entering the fuel-rich zone. The design for this premixer is based upon a design developed by Pratt and Whitney (Pierce, et al, 1980) for low-NO_x gas turbine combustors. The premixer (Figure 2-34) mixes a swirling air flow (swirl number = 0.4) with the atomized fuel from a Sonicore 250 T atomizer in a venturi-type throat. The velocity in the throat is sufficiently high (30 m/sec) to prevent flashback into the premix tube. Flame stability was much better with this design, particularly when the burner refractory was cold.

The test plan objectives were to establish the emissions performance of the system under baseline conditions and to determine the sensitivity of exhaust NO_x emissions to fuel properties and to various operating parameters. The influence of atomizer configuration was investigated by individually operating two different atomizers at two assist fluid pressures each. A short series of detailed measurements (HCN, NH_3 NO, HC, CO, CO_2, and O_2) were made at the exit of the primary zone to assess the fraction of NO formed in the first and second stages. Tests were conducted with the burner installed on the Firetube Simulator described earlier in this section and in the Small Watertube Simulator (SWS) which is described in Section 3 of this report. Since the SWS is a much larger furnace (design load 2.9 MW_{th}) this allowed the impact of second-stage environment to be evaluated. Several different burner configurations were investigated on the SWS, directed mainly toward optimization of primary zone parameters (e.g. mixing, residence time, L/D). These configurations are identified in Figure 2-35.

Three liquid fuel oils and commercial-grade propane were used as test fuels. Analyses of the liquid fuel oils are presented in Table 2-6. The majority of tests were conducted using the California No. 6 oils R15a and R15b. An Alaskan diesel oil and a coal-derived liquid from the SRC-II process (5.75/1 middle/heavy distillate blend) were also tested. Doping experiments to vary fuel nitrogen content involved addition of technical

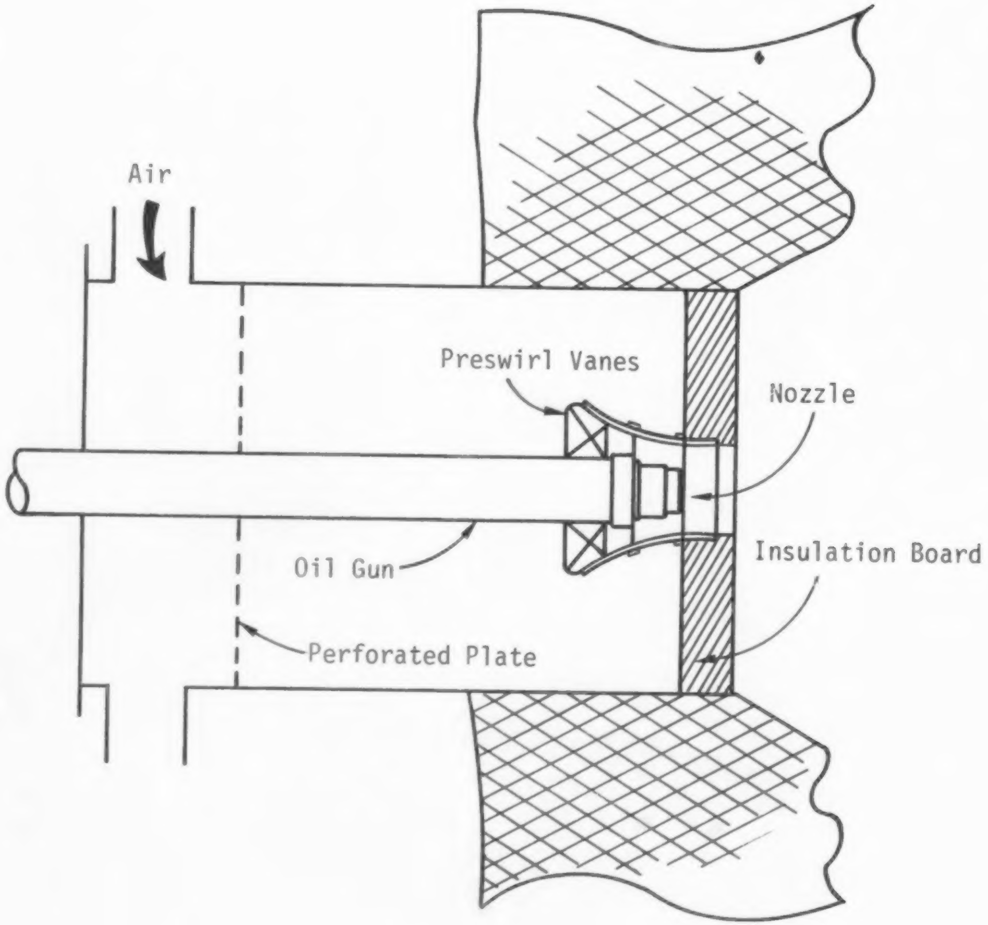
Air
Preswirl Vanes
Nozzle
Oil Gun
Insulation Board
Perforated Plate

Figure 2-34. Premixer assembly for experimental prototype burner.

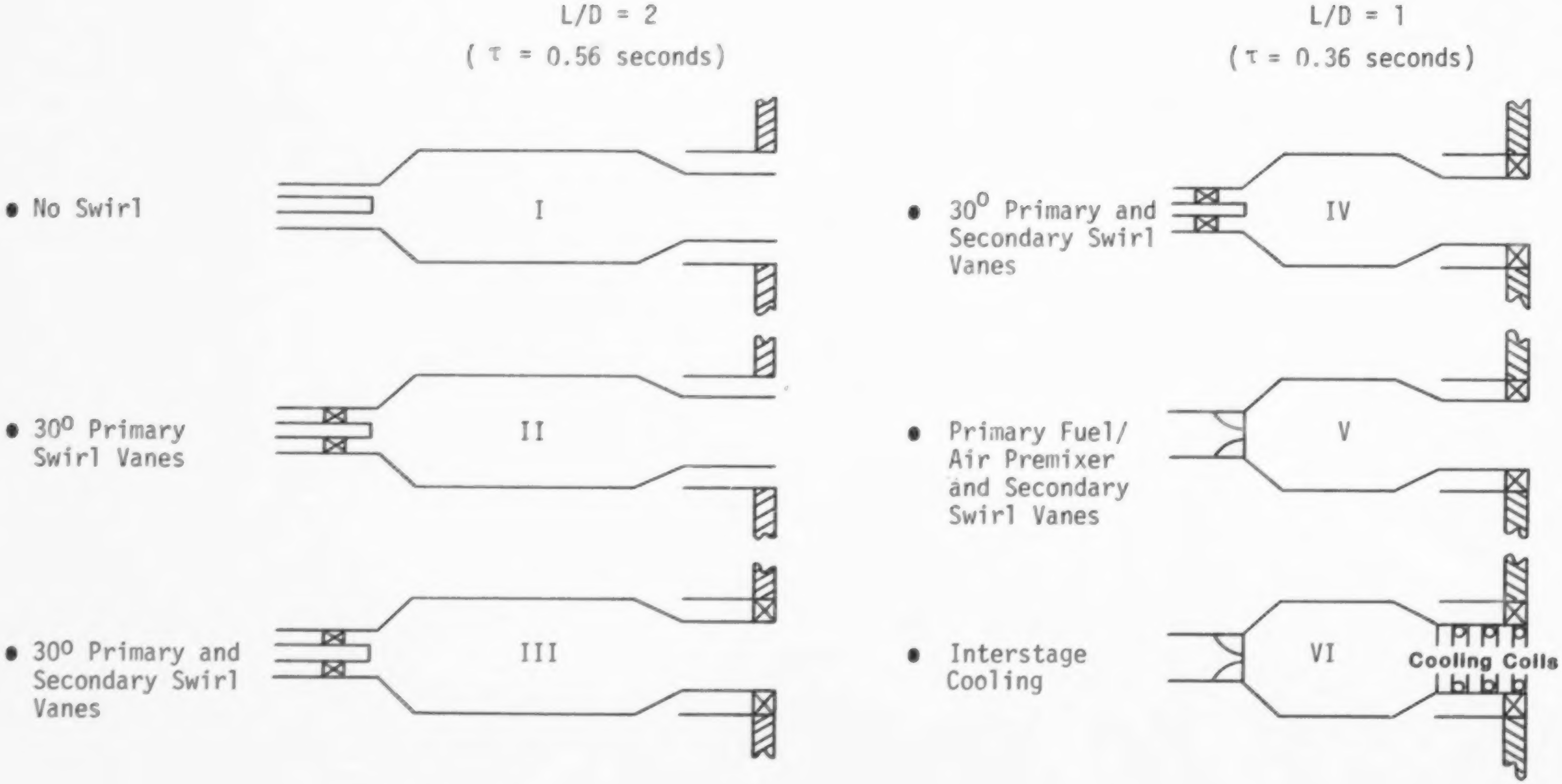
L/D = 2
(τ = 0.56 seconds)
L/D = 1
(τ = 0.36 seconds)
• No Swirl
I
• 30⁰ Primary Swirl Vanes
II
• 30⁰ Primary and Secondary Swirl Vanes
III
• 30⁰ Primary and Secondary Swirl Vanes
IV
• Primary Fuel/Air Premixer and Secondary Swirl Vanes
V
• Interstage Cooling
VI
Cooling Coils

Figure 2-35. Small pilot scale burner configurations evaluated on SWS facility.

TABLE 2-6. FUEL ANALYSIS

	D_1	R15a	$R15_b$	A6
	Alaskan Diesel	Cali-fornia	Cali-fornia	SRC-II
Ultimate Analysis:				
Carbon, %	86.99	87.01	86.62	85.91
Hydrogen, %	12.07	11.67	11.64	8.74
Nitrogen, %	0.008	0.62	0.70	0.96
Sulfur, %	0.31	0.47	0.80	0.30
Ash, %	<.001	0.017	0.04	0.04
Oxygen, %	0.62	0.21	0.20	4.08
Conradson Carbon Residue, %	-	4.9	-	0.51
Asphaltenes, %	-	1.84	-	1.73
Flash Point, °F	-	>350	-	-55
Pour Point, °F	-	30	-	
API Gravity at 60°F	33.1	16.4	16.9	39
Viscosity, SSU, at 140°F	33.0	484	1,160	
at 210°F	29.5	100	153	
Heat of Combustion:				
Gross Btu/lb	19,530	18,840	18,800	
Net Btu/lb	-	17,780	17,740	17,100
Calcium, ppm	-	2.7		-
Iron, ppm	-	1.7		-
Manganese, ppm	-	0.11		-
Magnesium, ppm	-	0.78		-
Nickel, ppm	-	16		-
Sodium, ppm	-	1.5		-
Vanadium, ppm	-	0.94		-

grade pyridine (C_5H_5N) to the diesel fuel and in some tests anhydrous ammonia was injected with propane.

2.4.1 First-Stage Parameters

Typical results showing the influence of primary zone stoichiometric ratio (SR_1) upon exhaust NO_x emissions are shown in Figure 2-36 for the California residual fuel oil (R15) at 0.59 MW. Exhaust O_2 concentration was held constant at 3 percent (SR_t = 1.16). NO_x emissions at SR_1 equal to 1.16 (unstaged) were generally greater than 400 ppm for most of the conditions tested. As is decreased, NO_x emissions decrease rapidly until a minimum is reached, and then rise with further decreases in SR_1. The SR_1 at which minimum NO_x is achieved is dependent upon both fuel type and burner configuration but generally lies in the range from 0.65 to 0.75. In Figure 2-37 the behavior of CO and smoke emissions with SR_1 are presented. Smoke and CO are generally low for SR_1 >0.7. Near the SR_1 where minimum NO_x is achieved, CO and smoke emissions begin to rise rapidly. CO is less than 100 ppm and smoke number generally less than 5 at the point where the minimum NO_x level occurs. At stoichiometries richer than the optimum, CO and smoke are high.

NO_x emissions were found to be sensitive to load under both staged and unstaged conditions (Figure 2-38). Unstaged NO_x emissions firing the California residual oil decreased sharply from 875 ppm to 430 ppm as load was increased from 0.29 to 0.88 MW (1×10^6 to 3×10^6 Btu/hr). Propane produced the opposite behavior unstaged, NO_x emissions showing an increase with increasing load. However, under staged conditions, NO_x emissions were much less sensitive to load and similar trends were observed with both fuels. NO_x emissions increased slightly as load was increased at constant first-stage stoichiometry (SR_1 = 0.7). Figure 2-39 shows the minimum achievable NO_x emissions for both fuels as a function of load. Emissions at 0.29 MW and 0.59 MW with the residual oil were approximately equal;, however emissions were higher at 0.88 MW. The SR_1 at which minimum NO_x was achieved was observed to shift toward more fuel-rich conditions as load was increased.

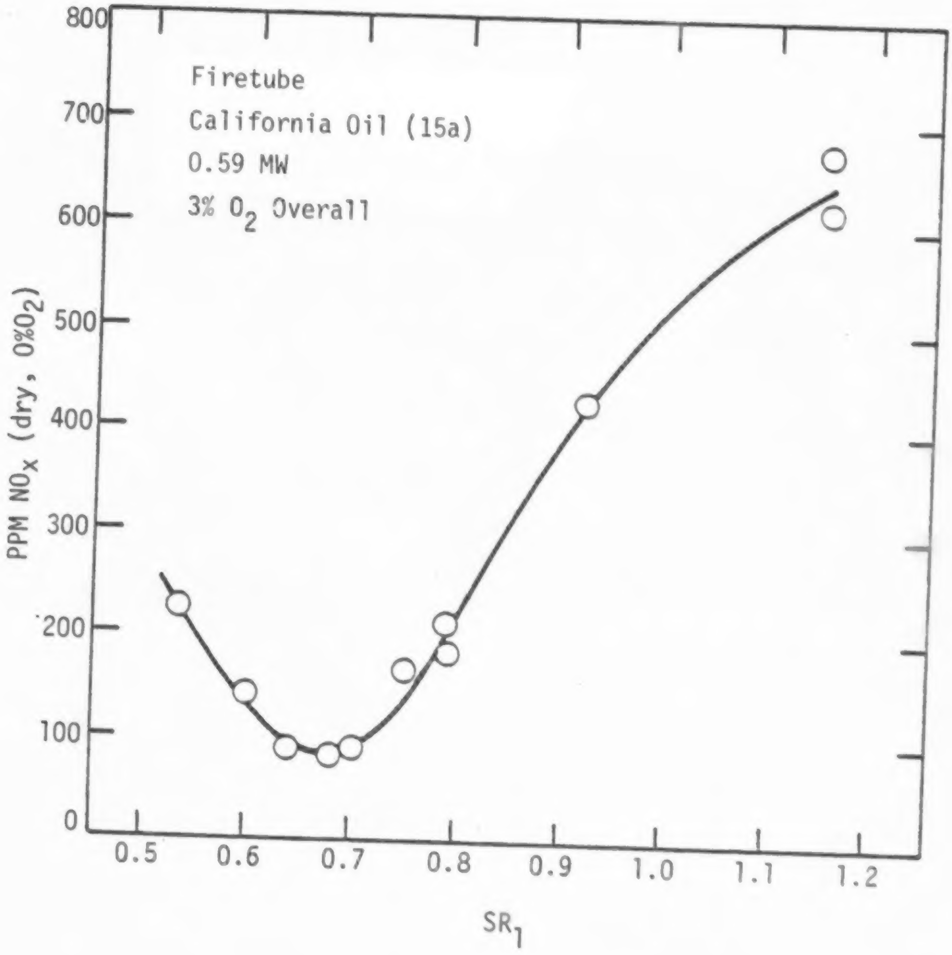

Figure 2-36. Effect of SR_1 Upon NO_x Emissions.

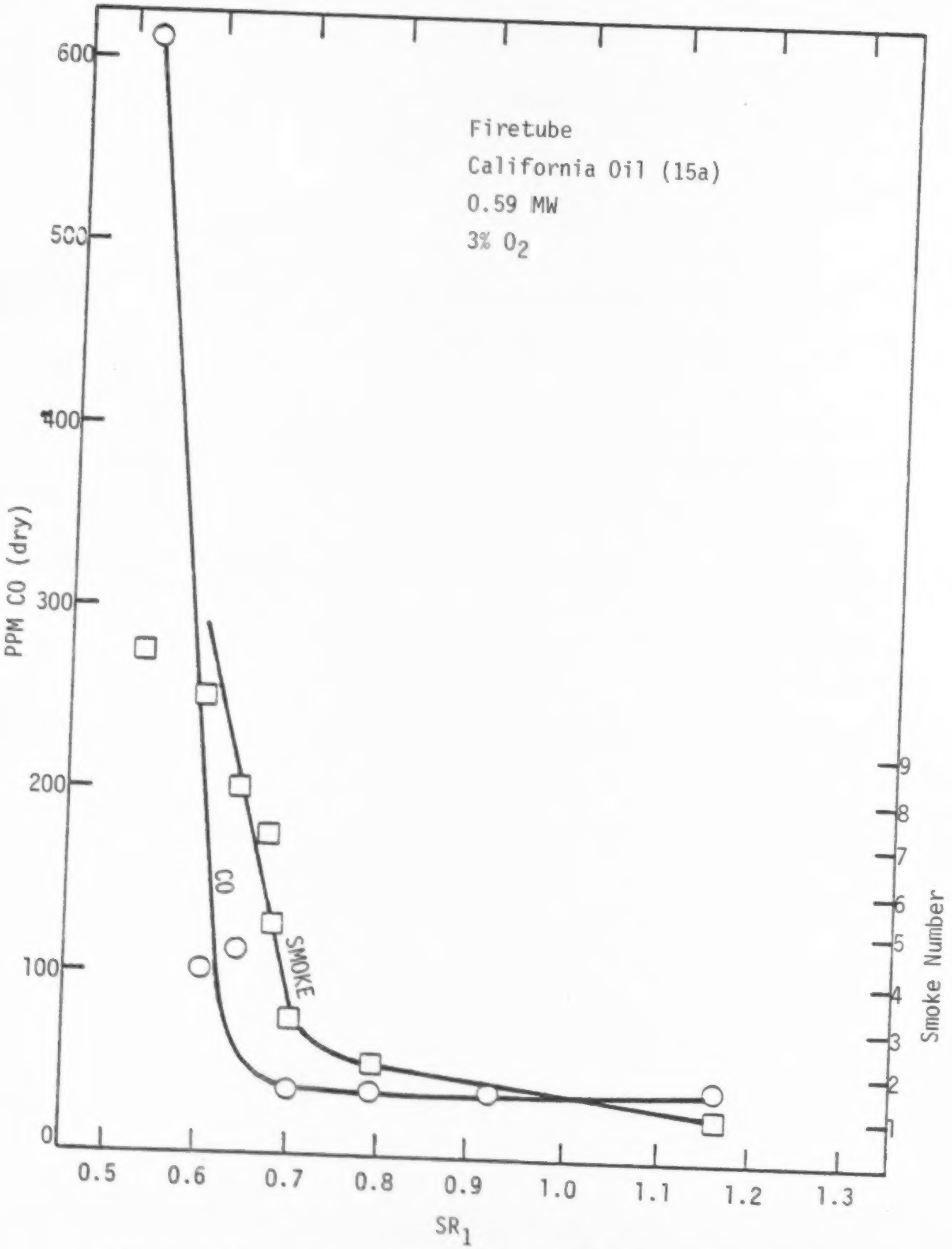

Figure 2-37. Effect of SR_1 upon CO and smoke emissions.

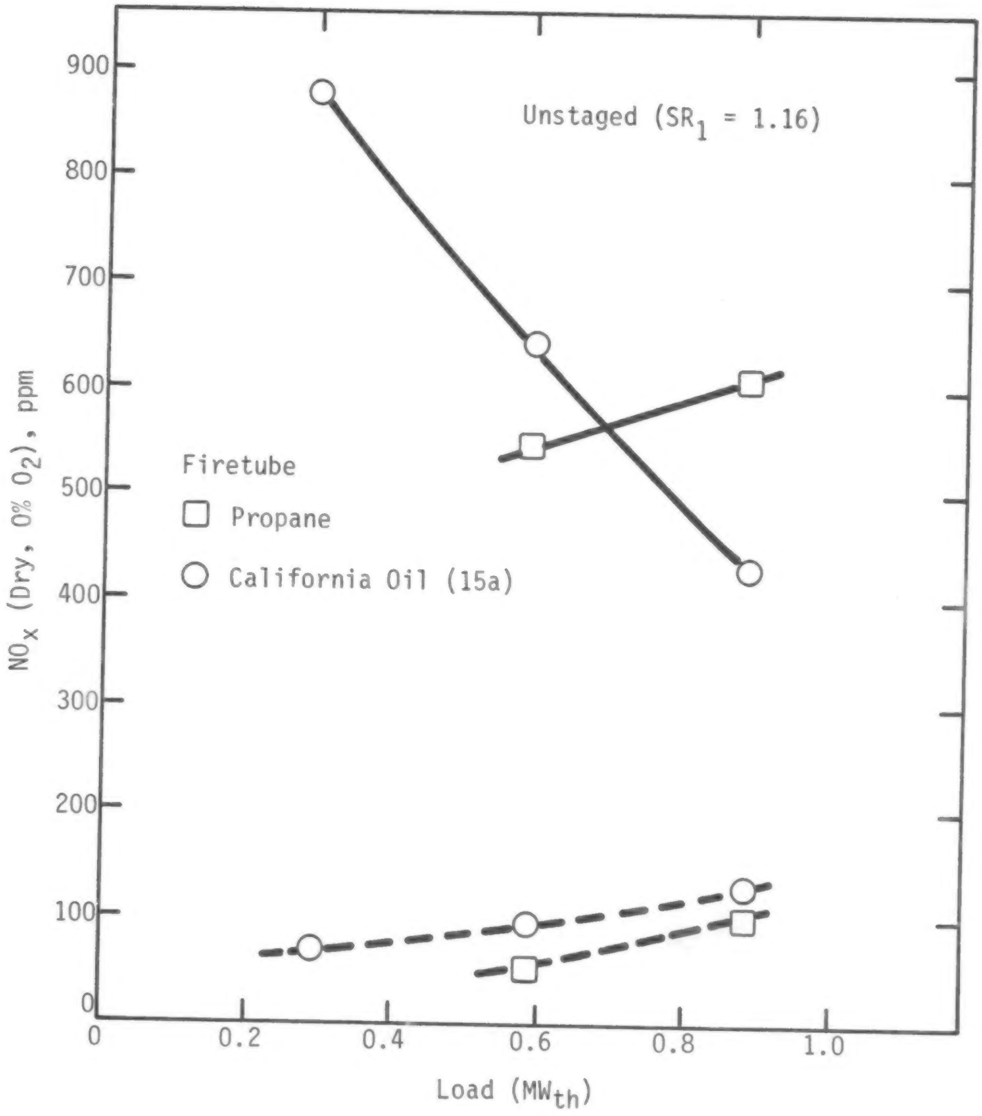

Figure 2-38. Effect of load upon NO_x emissions (staged and unstaged).

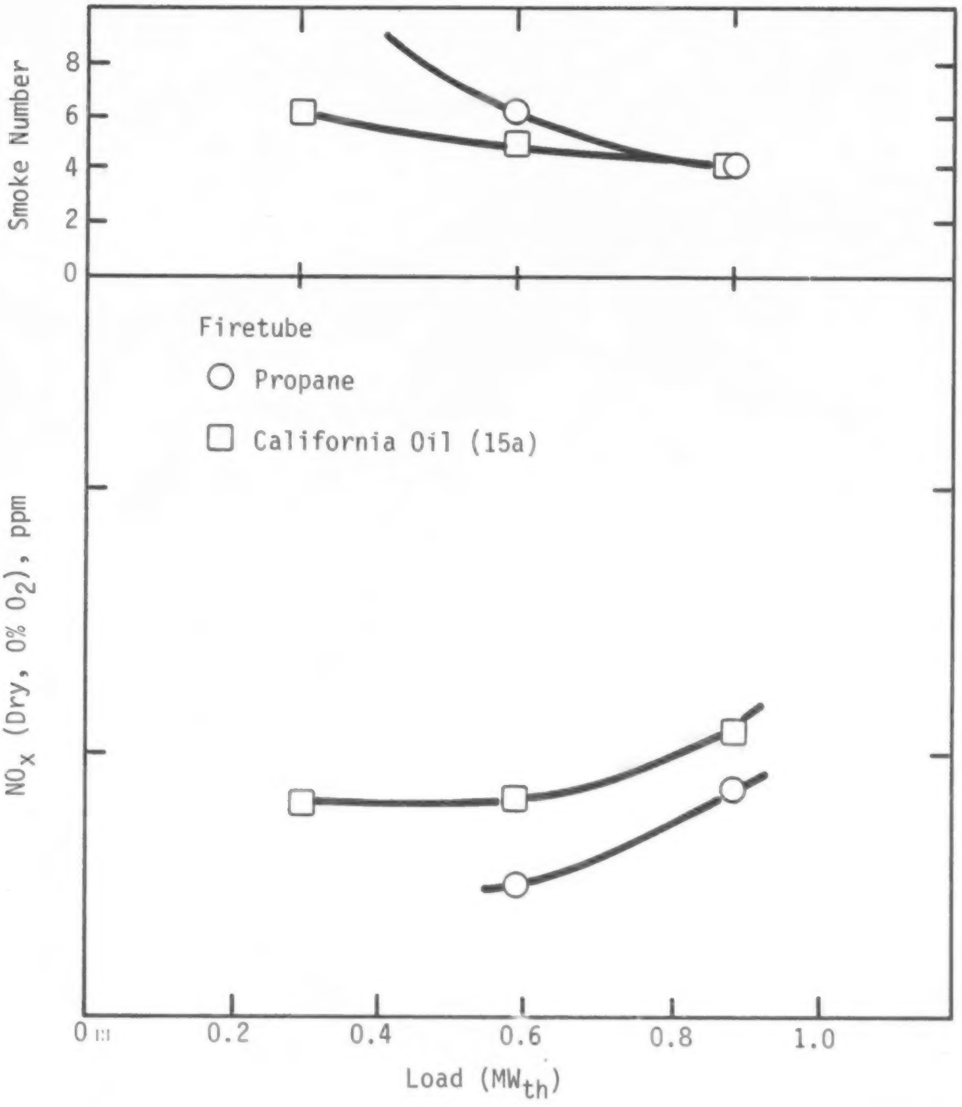

Figure 2-39. Effect of load on minimum NO_x and smoke emissions.

Smoke emissions are also shown in the figure. It can be seen that smoke emissions were also very sensitive to load.

The major effect of load is believed to be on gas-phase residence time in the primary zone. An increase in load from 0.29 MW to 0.88 MW decreases first-stage residence time from approximately 1.14 seconds to 0.38 seconds. Gas temperature does not change significantly in the primary zone since it is nearly adiabatic. Another way to vary residence time is to change the length of the primary zone. The effect of removing one of the burner sections is shown in Figure 2-40. Residence time at 0.59 MW, SR_1 = 0.7, and 2800°F was decreased from approximately 0.56 seconds to 0.36 seconds. Minimum NO_x emissions were higher in the short primary configuration than in the long primary configuration by approximately 25 ppm out of 95 ppm. The optimum SR_1 was also shifted to slightly leaner stoichiometry, which may reflect a different mixing conditions between the long and short primary configurations. NO_x emissions appear to decrease with increasing residence time in the primary zone. This trend is consistent with the bench-scale tunnel furnace results reported by England, et al (1982).

It should be pointed out that the results shown in Figure 2-40 were obtained in the Small Watertube Simulator (SWS) furnace. It can be seen that NO_x emissions compare favorably between the two furnaces in spite of substantial differences in furnace shape and thermal environment. Comparison of emissions between the two furnaces is discussed later in this section. Since NO_x emissions were similar in both furnaces, the following discussions regarding the influence of individual parameters do not distinguish between the two furnaces.

The results of testing two different atomizers at two assist-fluid pressures are presented in Figure 2-41. Variations in atomizer design resulted in NO_x emissions from 340 ppm to 670 ppm unstaged with the California oil. Under staged conditions, the NO_x emissions varied over a narrower range but smoke emissions varied significantly. NO_x emissions ranged from 90 to 125 ppm at SR_1 = 0.7 while smoke emissions varied from Bacharach smoke number of 3 to a visible plume of smoke rising from the

Smoke emissions are also shown in the figure. It can be seen that smoke emissions were also very sensitive to load.

The major effect of load is believed to be on gas-phase residence time in the primary zone. An increase in load from 0.29 MW to 0.88 MW decreases first-stage residence time from approximately 1.14 seconds to 0.38 seconds. Gas temperature does not change significantly in the primary zone since it is nearly adiabatic. Another way to vary residence time is to change the length of the primary zone. The effect of removing one of the burner sections is shown in Figure 2-40. Residence time at 0.59 MW, $SR_1 = 0.7$, and 2800°F was decreased from approximately 0.56 seconds to 0.36 seconds. Minimum NO_x emissions were higher in the short primary configuration than in the long primary configuration by approximately 25 ppm out of 95 ppm. The optimum SR_1 was also shifted to slightly leaner stoichiometry, which may reflect a different mixing conditions between the long and short primary configurations. NO_x emissions appear to decrease with increasing residence time in the primary zone. This trend is consistent with the bench-scale tunnel furnace results reported by England, et al (1982).

It should be pointed out that the results shown in Figure 2-40 were obtained in the Small Watertube Simulator (SWS) furnace. It can be seen that NO_x emissions compare favorably between the two furnaces in spite of substantial differences in furnace shape and thermal environment. Comparison of emissions between the two furnaces is discussed later in this section. Since NO_x emissions were similar in both furnaces, the following discussions regarding the influence of individual parameters do not distinguish between the two furnaces.

The results of testing two different atomizers at two assist-fluid pressures are presented in Figure 2-41. Variations in atomizer design resulted in NO_x emissions from 340 ppm to 670 ppm unstaged with the California oil. Under staged conditions, the NO_x emissions varied over a narrower range but smoke emissions varied significantly. NO_x emissions ranged from 90 to 125 ppm at $SR_1 = 0.7$ while smoke emissions varied from Bacharach smoke number of 3 to a visible plume of smoke rising from the

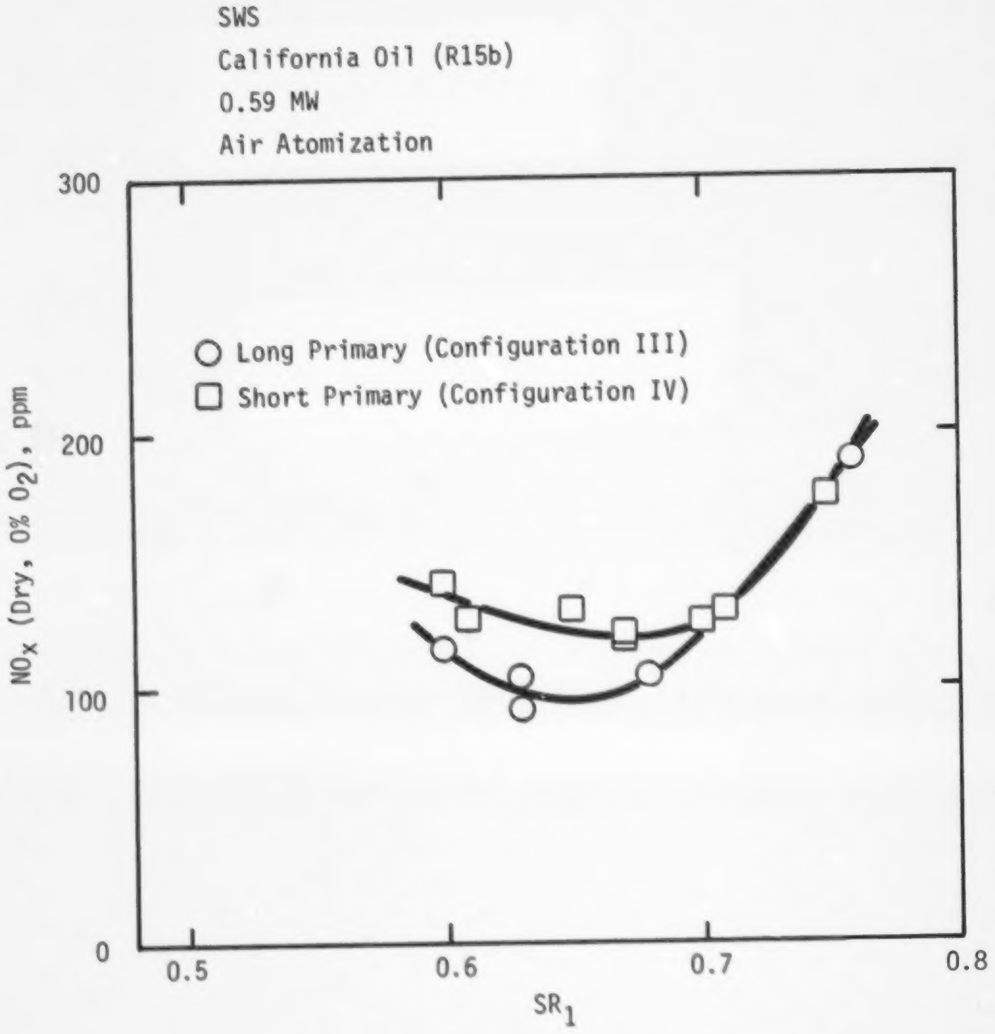

Figure 2-40. Influence of primary zone length on NO_x emissions.

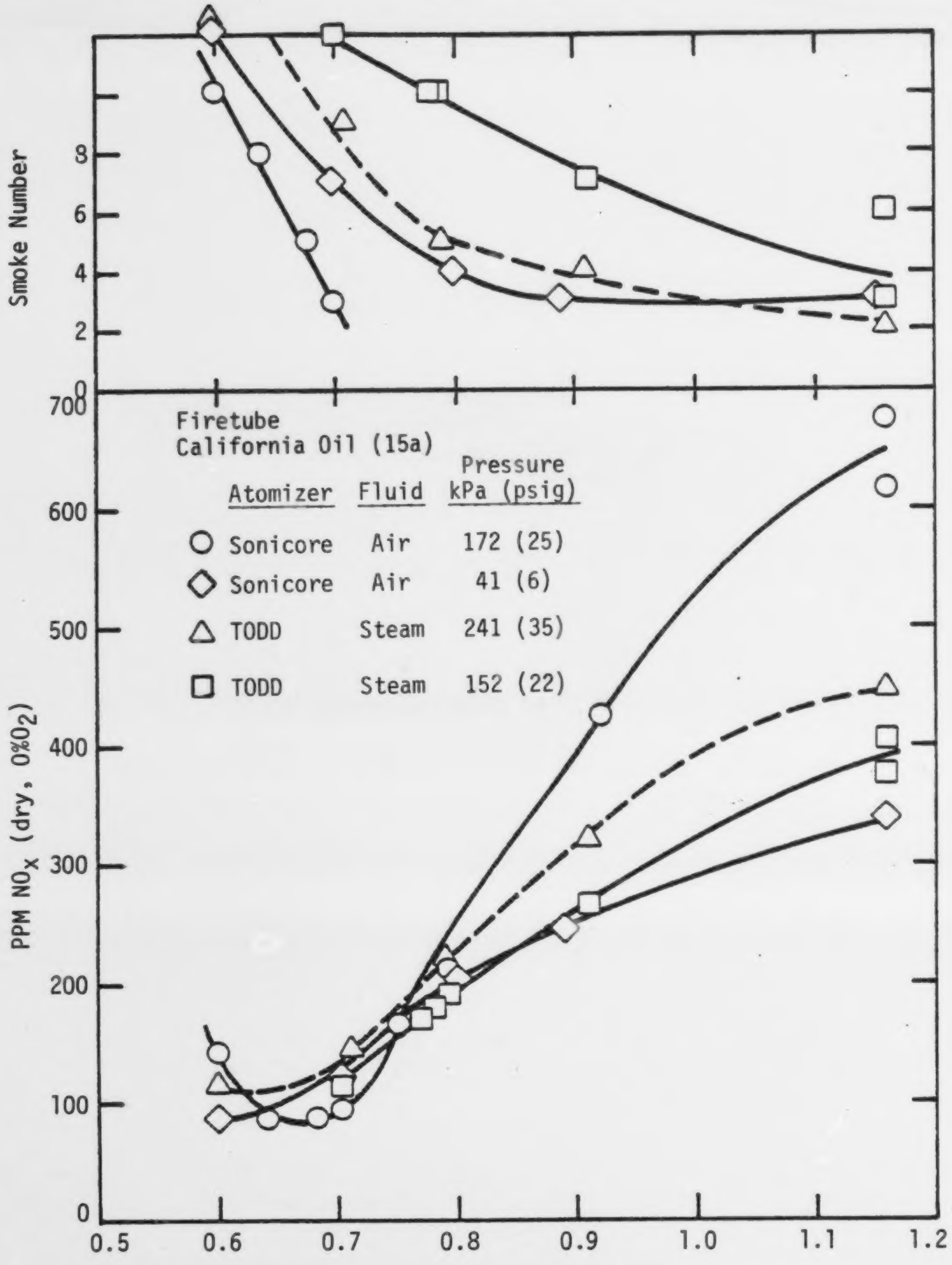

Figure 2-41. Effect of atomizer type and pressure upon NO$_x$ and smoke emissions (0.59 MW$_{th}$).

stack. The high smoke levels prevented acquisition of complete NO_x data near the optimum SR_1. It is significant to note that the same minimum NO_x level was achieved with the Sonicore atomizer at 41 kPa (SR_1 = 0.6) and at 172 kPa (SR_1 = 0.68), but that smoke levels were very different.

Figure 2-42 compares NO_x emissions produced using the ultrasonic atomizer atomized with steam and air. The same minimum NO_x level was achieved with both atomizing fluids; however, the optimum SR_1 was shifted from approximately 0.65 to 0.74 by switching from air to steam atomization. This may reflect improved near-burner fuel/air mixing as a result of increased fuel jet momentum with steam atomization.

Figure 2-43 compares NO_x emissions for two different primary air mixing configurations. A set of 30° angle fan-type swirl vanes was placed in the primary air throat in order to improve flame stability under cold-furnace conditions (during startup). NO_x emissions were not affected by this modification although cold-furnace flame stability was considerably improved (flame stability was always satisfactory under hot-furnace conditions because flame stability is enhanced by radiation from the furnace walls). Also shown are emissions with 30° swirl vanes attached in the secondary air annulus. The objective of this modification was to reduce second-stage flame length. Adding the secondary swirl vanes also had no impact on NO_x emissions or flame shape. This was attributed to the extremely low secondary-to-primary momentum ratio at the point of secondary air injection. Under these conditions, the primary jet characteristics can be expected to dominate mixing.

As first-stage residence time was decreased, the importance of the fuel injection system design became more apparent. Figure 3-44 compares data obtained with the premixed burner to that obtained with the low primary air velocity arrangement. Both sets of data were obtained with the burner mounted on the watertube simulator. In the short first-stage residence time configuration (360 msec at SR_1 = 0.7), the premixer slightly reduced the exhaust NO emissions, and broadened the SR_1 for minimum emissions. A similar conclusion was reached by comparing data for a propane/NH_3 fuel (which

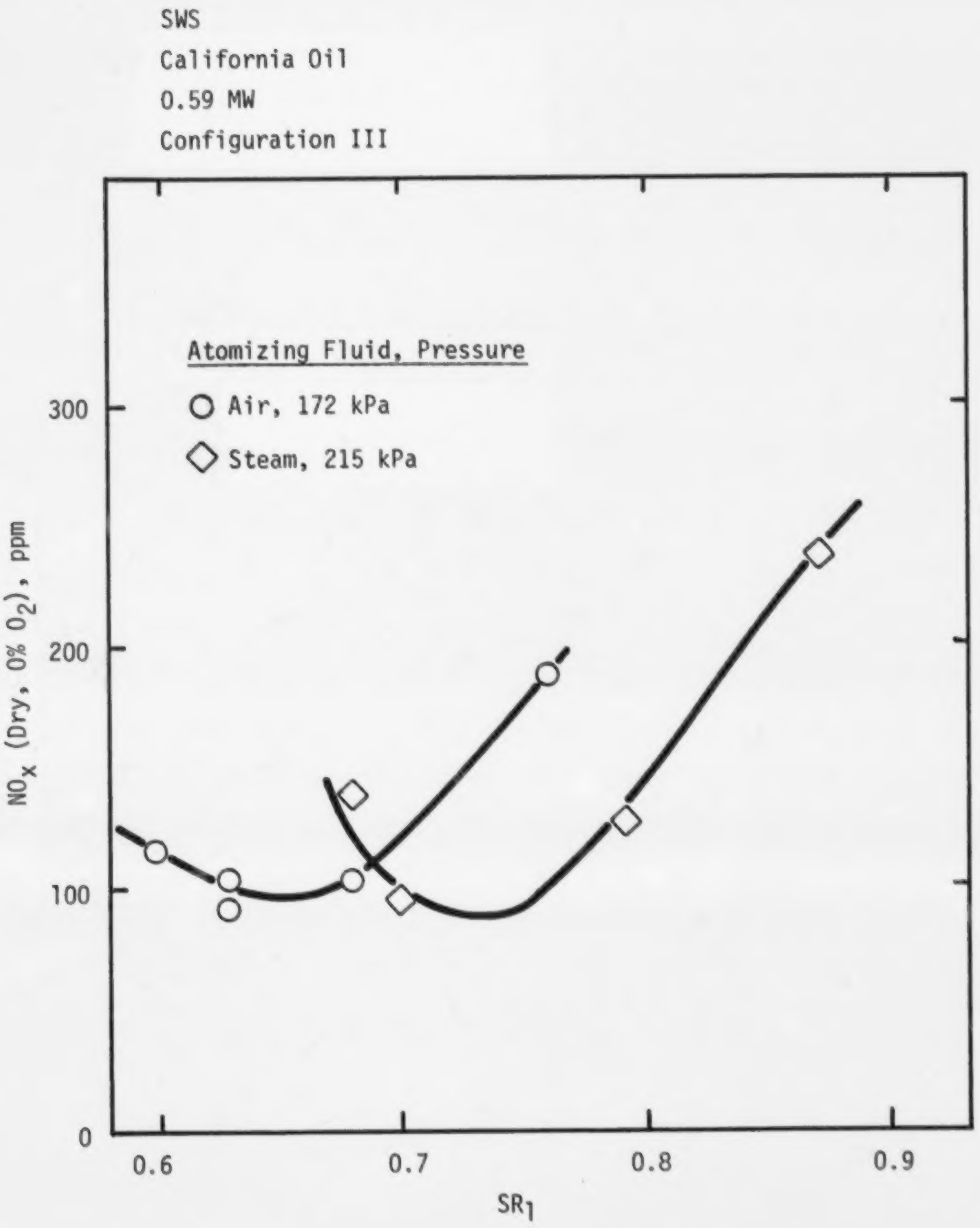

Figure 2-42. Influence of atomizing fluid on NO_x emissions.

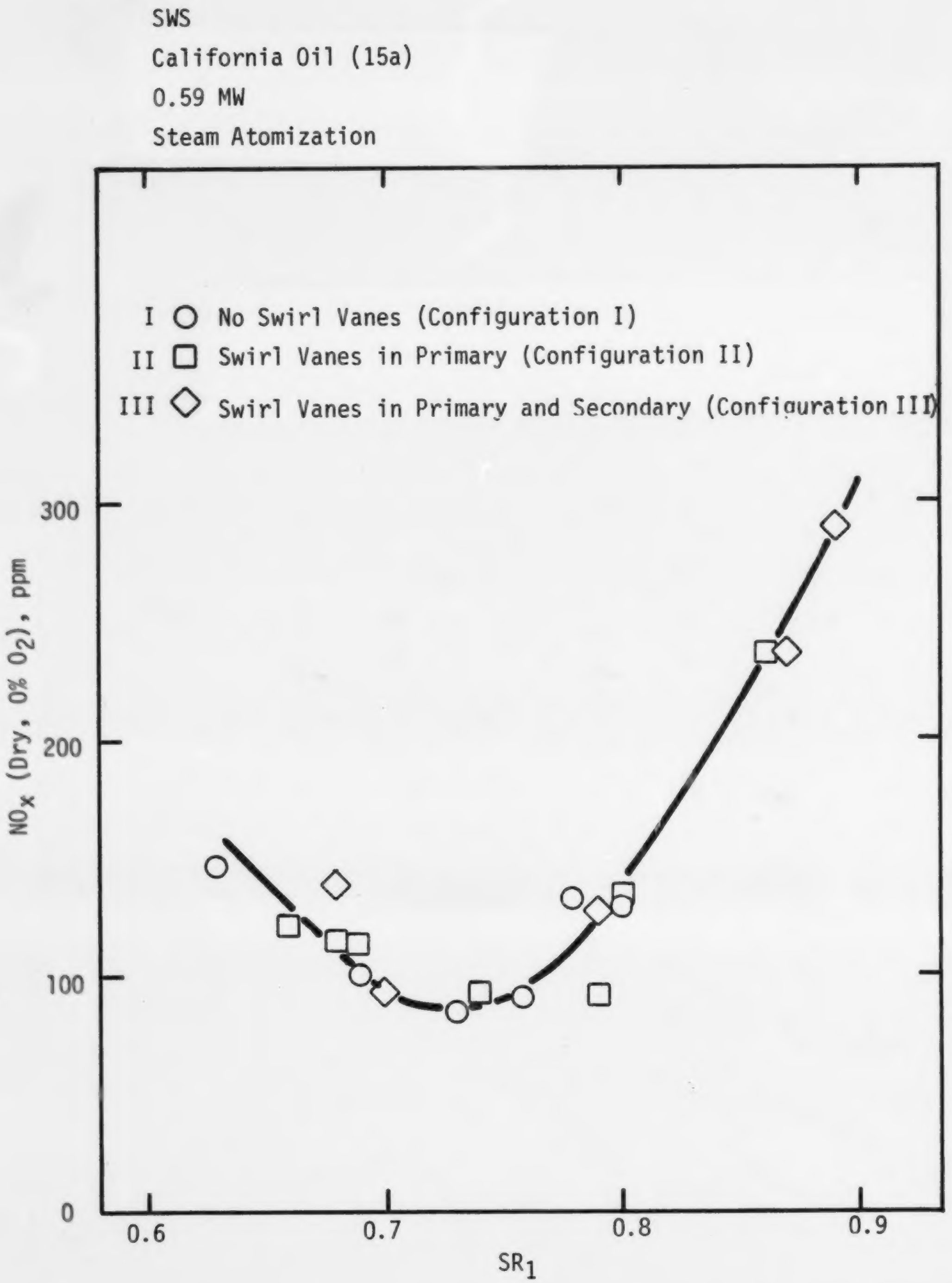

Figure 2-43. Influence of primary and secondary air swirl on NO_x emissions.

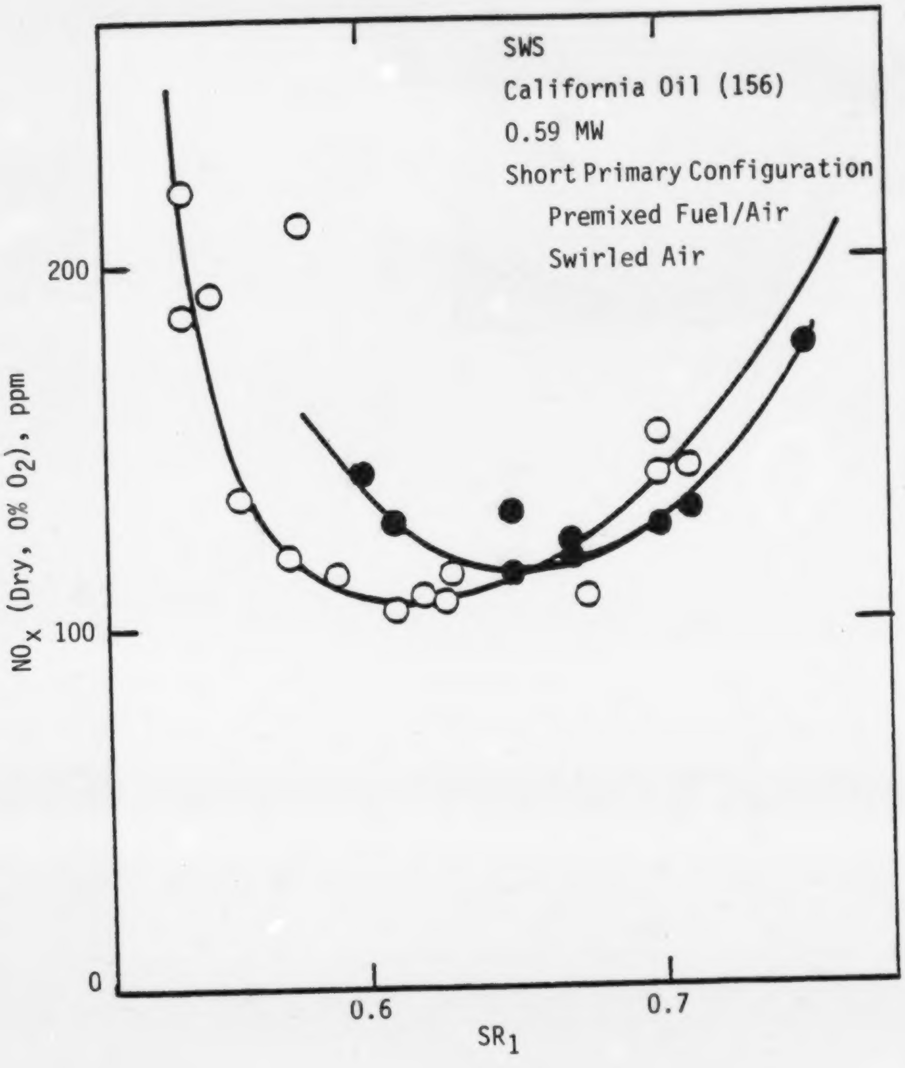

Figure 2-44. Effect of primary fuel/air mixing on NO_x emissions with short primary zone residence time.

represents a limit of instant fuel vaporization) to the California residual oil with the standard fuel nozzle. Thus, unless the first-stage residence time is extremely short (>200 msec), the characteristic time for fuel vaporization and mixing is small relative to the rich-zone residence time and hence atomizer design has a much greater effect on smoke formation than on minimum NO.

A short series of tests were conducted in order to assess the fate of fuel nitrogen in the primary zone and the influence of primary zone gas composition upon exhaust NO_x emissions. Measurements were taken with the California residual oil at 0.59 MW and 0.88 MW and with propane at 0.88 MW. Species measured at the first-stage exit included O_2, CO, CO_2, HCN, NH_3, and total hydrocarbons. HCN and NH_3 were determined by specific ion electrodes as described in Volume I of this report.

Figure 2-45 shows the results of the detailed measurements with the California oil at 0.59 MW. The data taken at the primary exit (open symbols) are presented as measured and exhaust NO_x data (solid symbols) are corrected to 0 percent O_2. The general trend of the data is similar to that observed in the bench-scale studies (Volume I). The dominant fixed nitrogen species under very rich conditions are NH_3 and HCN. As SR_1 is increased, the NH_3 and HCN concentration decreased and NO concentration increases. A minimum in TFN (total fixed nitrogen = $NO+NH_3+HCN$) occurs due to a tradeoff between decreased oxidizable fixed nitrogen species (HCN and NH_3) and increased NO formation. This minimum in TFN corresponds approximately to a minimum in exhaust NO_x formation. Figure 2-46 shows the results of similar measurements with the California oil at 0.88 MW. The data are similar to the 0.59 MW results except for greater amounts of HCN and HC under very rich conditions, resulting in higher TFN than at 0.59 MW. This results directly in higher exhaust NO_x emissions.

Figure 2-47 presents data obtained with propane fuel and shows that reactive XN species can be formed under fuel-rich conditions in significant amounts even when burning a nitrogen-free fuel. The minimum in TFN

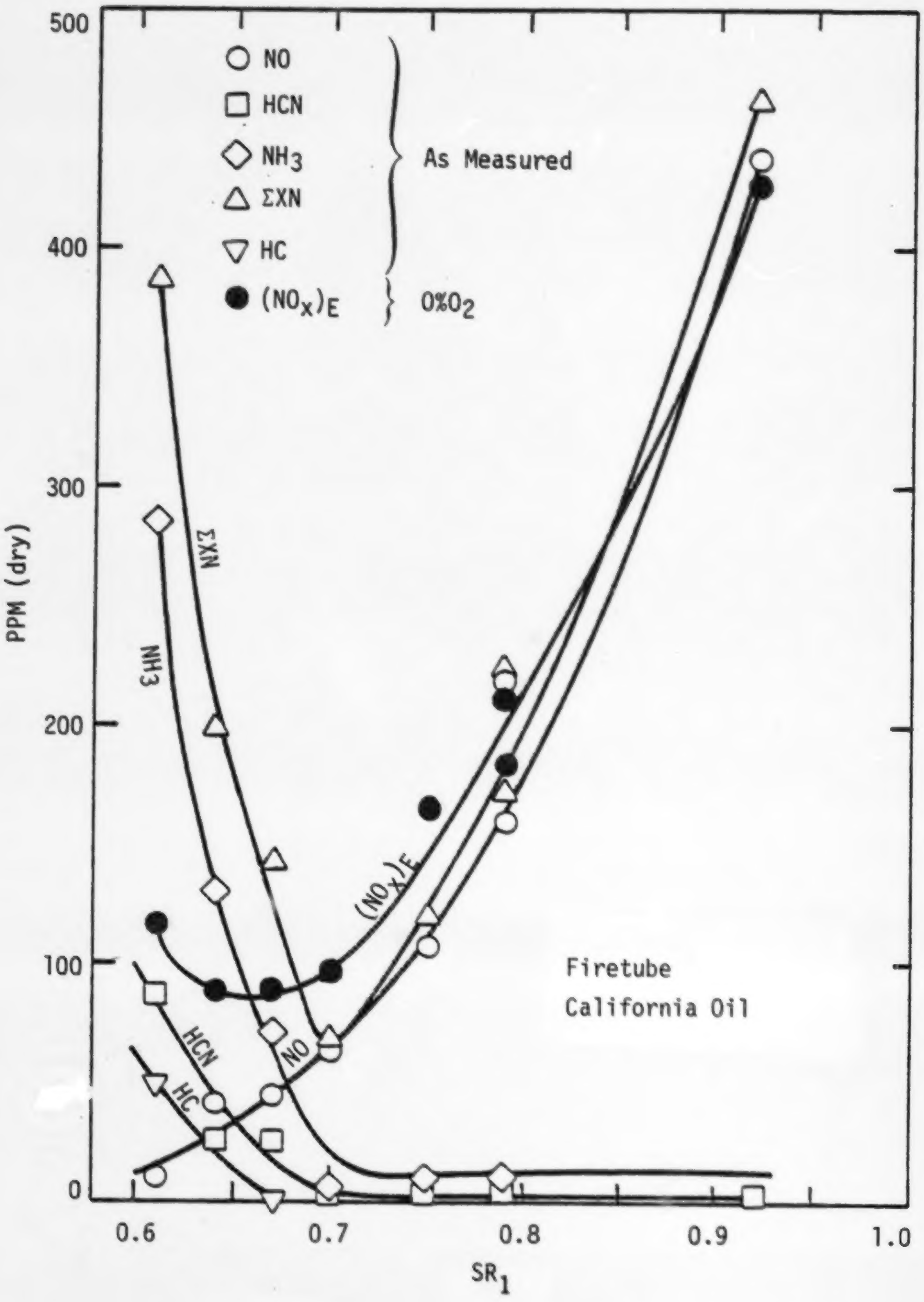

Figure 2-45. Detailed measurements at first-stage exit--California oil at 0.59 MW_{th} (2×10^6 Btu/hr).

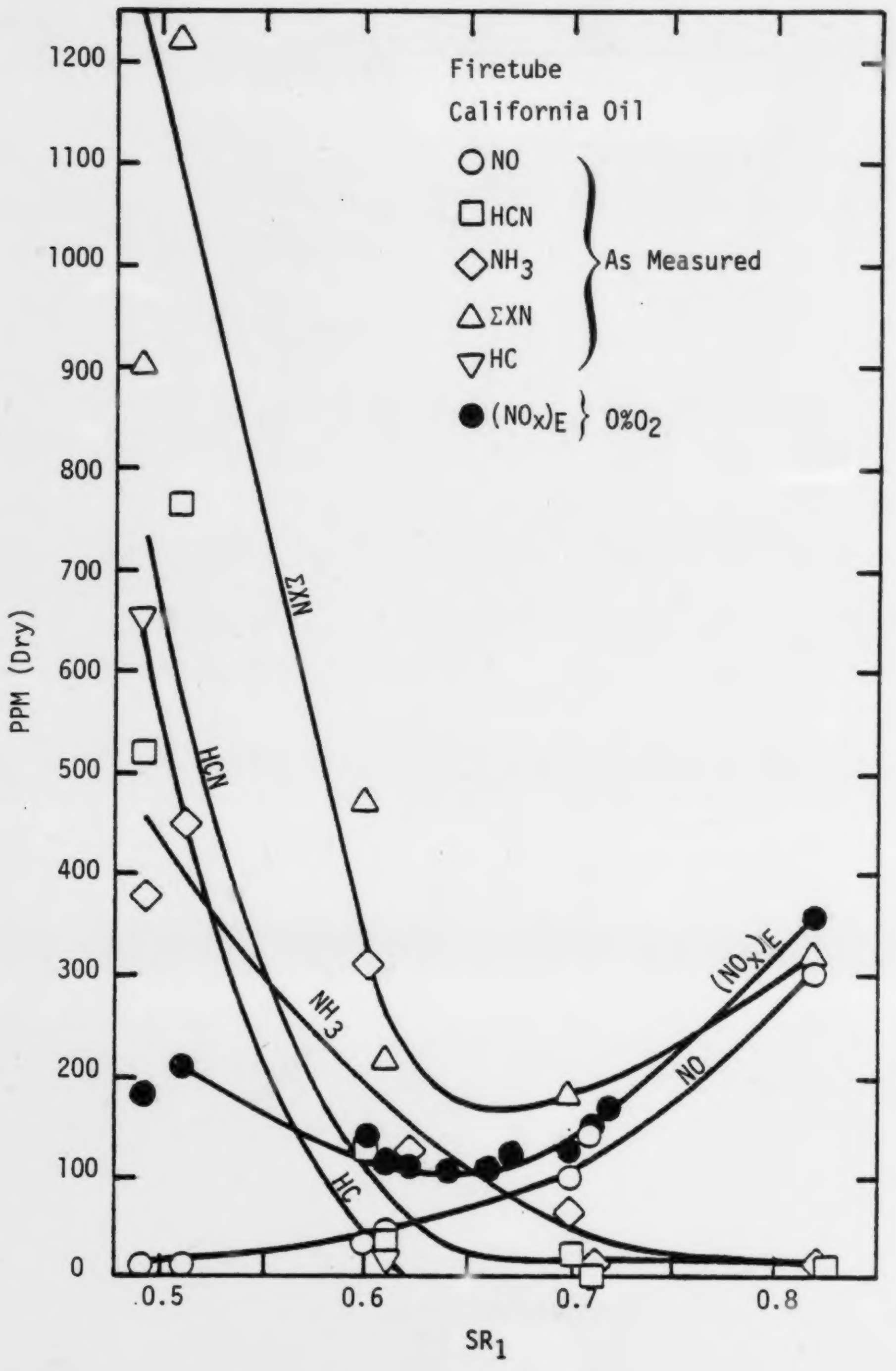

Figure 2-46. Detailed measurements at first-stage exit-- California oil at 0.88 MW_{th} (3×10^6 Btu/hr).

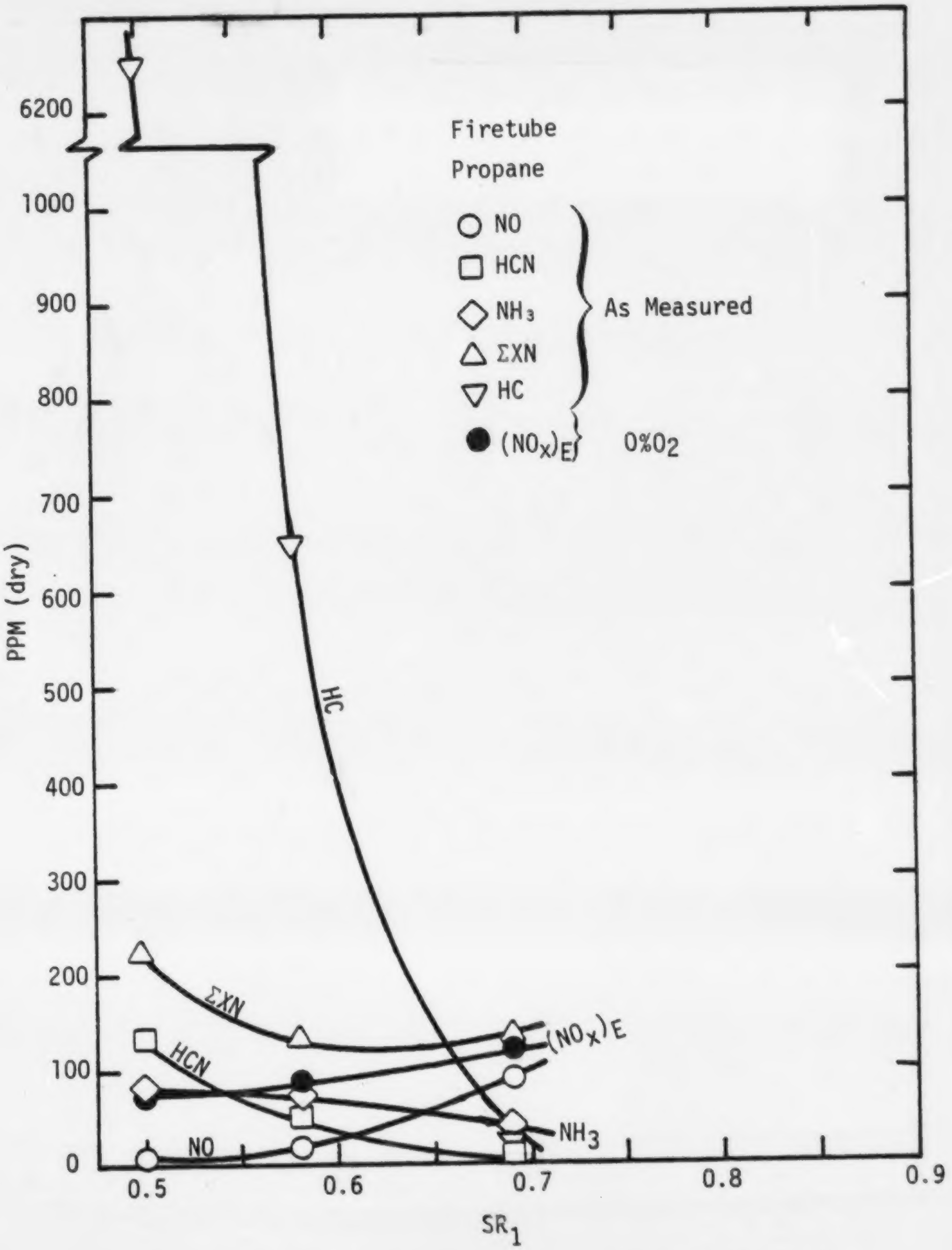

Figure 2-47. Detailed measurements at first-stage exit--propane at 0.88 MW$_{th}$ (3×10^6 Btu/hr).

concentration is much less pronounced than with nitrogen-containing fuels and thus exhaust NO_x emissions do not show a definite minimum.

2.4.2 Second-Stage Parameters

Two methods of secondary air injection were investigated to determine the sensitivity of emissions to changes in secondary fuel/air mixing. The annular (parallel) air injector provided a relatively slow mixing rate nd a water-cooled air injection boom provided a relatively fast mixing rate. This boom was inserted along the axis of the firetube through an access port at the rear. The secondary air was injected radially outward at the exit plane of the first stage. The results of varying the split of secondary air between these two injectors is shown in Figure 2-48. There is very little effect of secondary mixing upon NO_x emissions at $SR_1 = 0.7$; however, smoke emissions are substantially decreased as secondary air is transferred from the parallel injector to the radial injector.

Overall excess O_2 level in the second stage can be expected to influence NO_x emissions through mixing and through flame temperature. Figure 2-49 illustrates the influence of varying overall stoichiometry while maintaining first-stage stoichiometry constant. Increasing exhaust O_2 from 2 to 5 percent has no effect upon NO_x emissions near the optimum first-stage stoichiometry ($SR_1 = 0.7$) and results in a slight increase at $SR_1 = 0.8$; however, it can be seen that exhaust O_2 has a very significant effect upon smoke emissions. At both first-stage stoichiometries, increasing exhaust O_2 produced a substantial decrease in smoke emissions. Thus overall stoichiometry is not significant with respect to NO_x emissions but may be very important to smoke emissions. Since the second-stage flame is basically a diffusion type flame, the lack of a pronounced effect of excess O_2 on NO_x is not entirely surprising.

All the TFN which exists at the first stage exit does not result in NO in the combustion products of the second stage. Thus, it is important to design the second-stage air injection system to minimize NO formation from conversion of TFN species. In addition, thermal NO formation must be

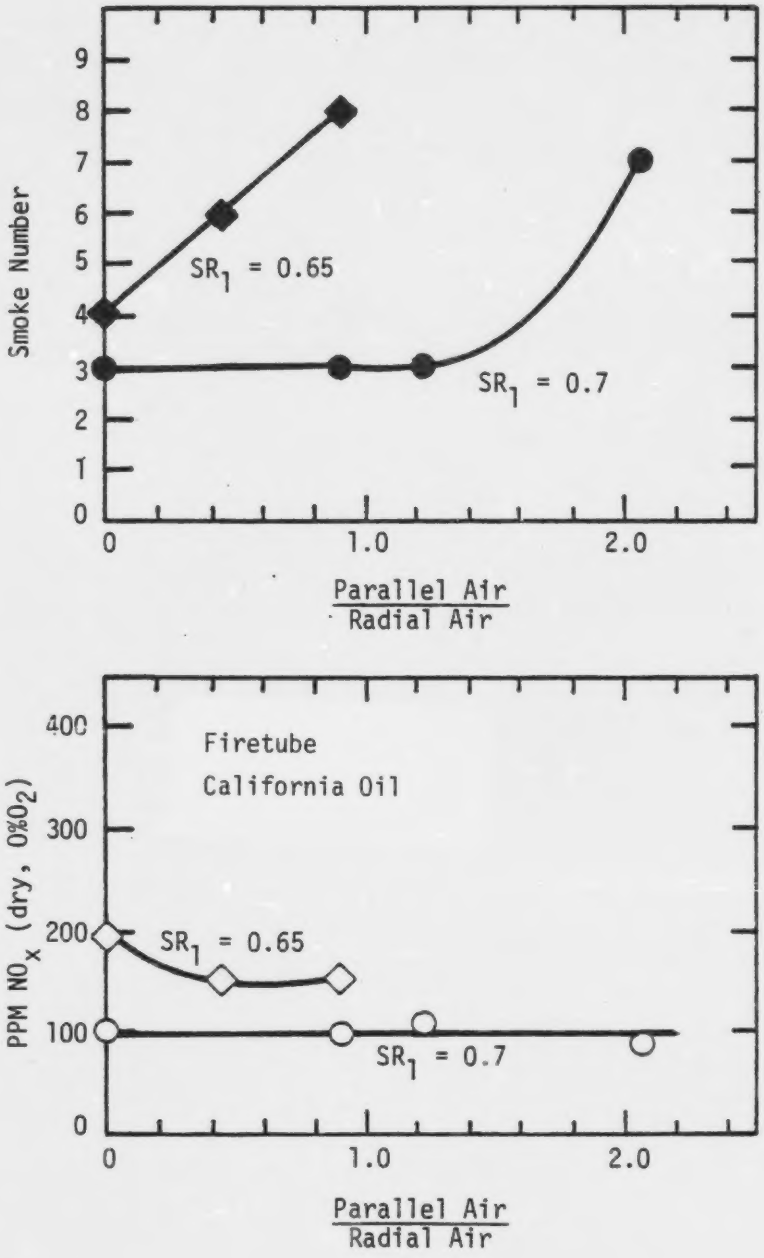

Figure 2-48. Effect of rapid secondary air injection upon NO$_x$ and smoke emissions (0.59 MW$_{th}$).

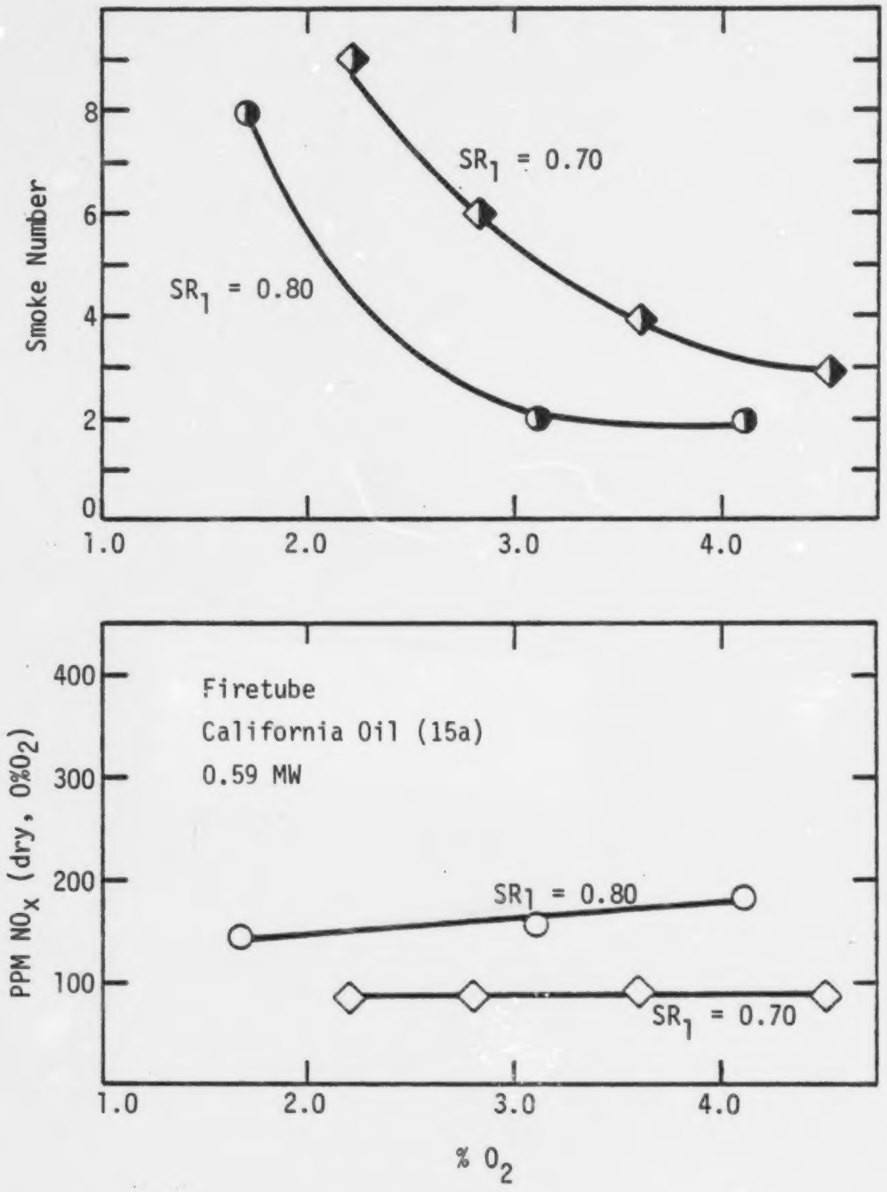

Figure 2-49. Effect of exhaust O_2 upon NO_x and smoke emissions.

minimized which requires that second-stage flame temperatures must be maintained below some critical threshold. Heat extraction between the fuel-rich zone and the secondary air injection system allows some control over temperature in the second-stage. Figure 2-50 presents results obtained when water-cooling tubes were placed around the periphery of the second-stage throat. This cooling removed approximately 6 percent of the heat input, and decreased the minimum exhaust NO_x by approximately 20 ppm. There was a minor impact on smoke emissions; thus, it appears that at the optimum operating conditions, second-stage thermal NO formation accounts for approximately 20 percent of the total exhaust NO emissions. Use of interstage cooling may become more important in subsequent scale-up if air preheat is added and/or rich-zone heat loss is reduced further.

Another way to evaluate the impact of second-stage temperature is to compare emissions in the Firetube Simulator and in the SWS under equivalent conditions. The Firetube Simulator has a nominal design capacity of 0.88 MW_{th} and at 0.59 MW the heat release per cooled furnace surface area is approximately 0.104 MW/m^2. The SWS has a nominal design capacity of 2.9 MW and at 0.59 MW the heat release per cooled furnace surface area is approximately 0.084 MW/m^3. A rough estimate of furnace temperature (Perry and Chilton, 1973) yields 810°C for the Firetube Simulator and 680°C for the SWS under the same firing conditions. Figure 2-51 compares NO_x emissions achieved in both furnaces with nearly identical burner configurations. NO_x emissions were similar in both furnaces and there appeared to be a slight shift in the optimum SR_1. This suggests that thermal NO_x formation is very low and approximately the same in both cases. Thus, for relatively cold furnaces, furnace geometry and flame confinement have a negligible impact on NO_x emissions with this burner. Smoke emissions were significantly higher in the SWS under most conditions, which limits the minimum NO_x level which can be achieved practically. Figure 2-52 shows NO_x emissions as a function of smoke number for the Firetube Simulator and the SWS. Smoke number was significantly higher in the SWS than in the Firetube Simulator except under minimum NO_x conditions. The high smoke conditions in the Firetube were generally obtained at SR_1 on the rich side of the optimum. NO_x levels below 100 ppm with smoke number less than 7 were not possible in the SWS.

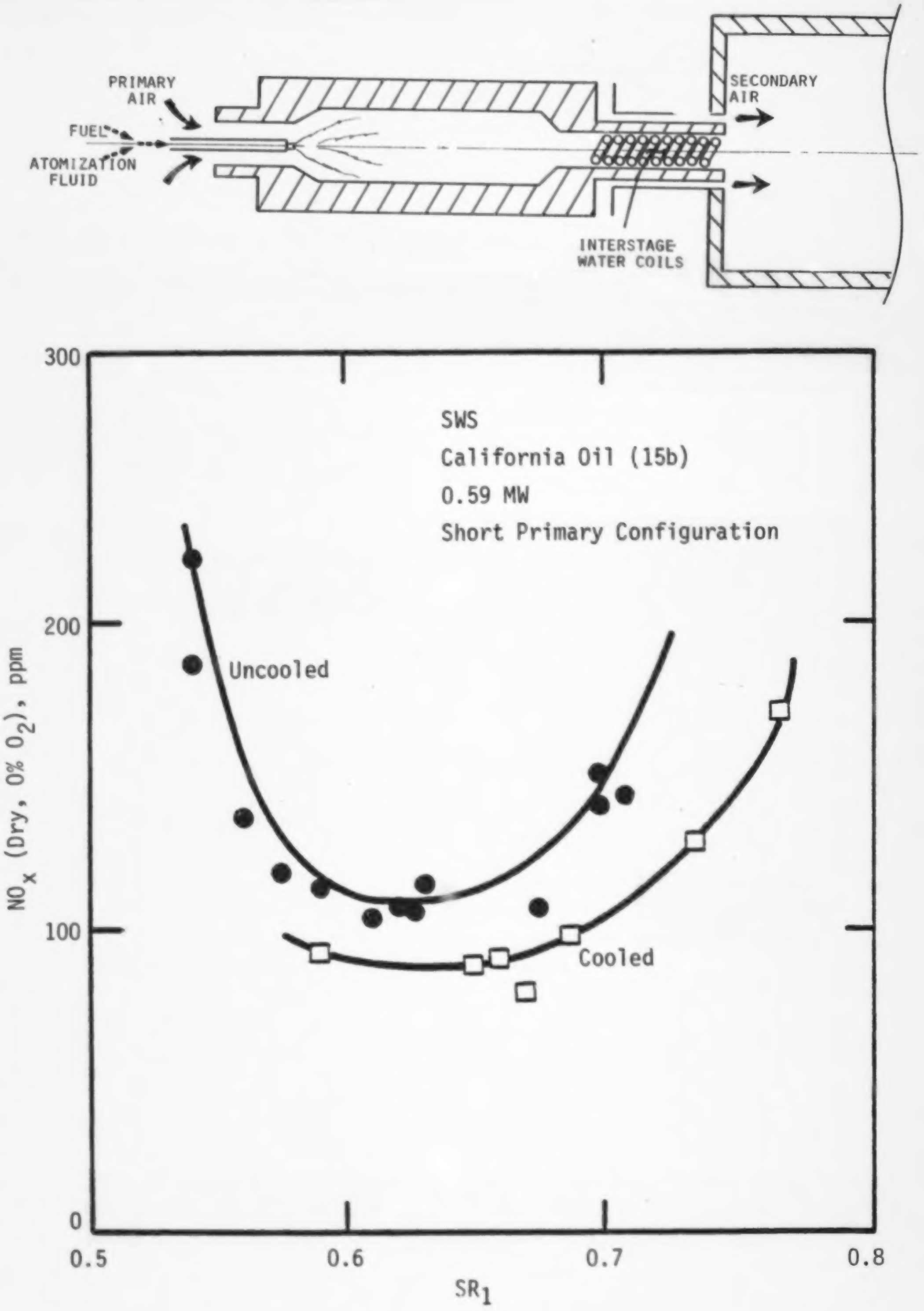

Figure 2-50. Influence of interstage heat extraction on NO_x.

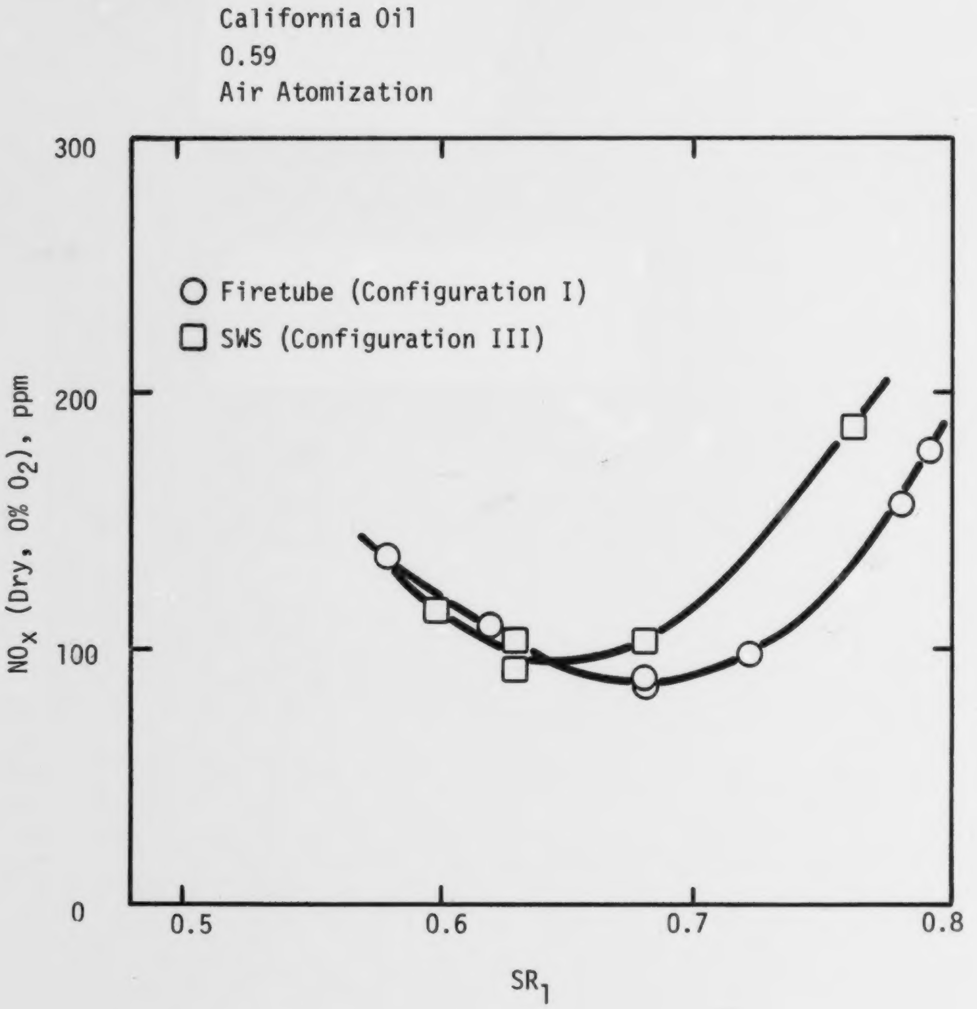

Figure 2-51. Comparison of NO_x emissions in Firetube Simulator and Small Watertube Simulator.

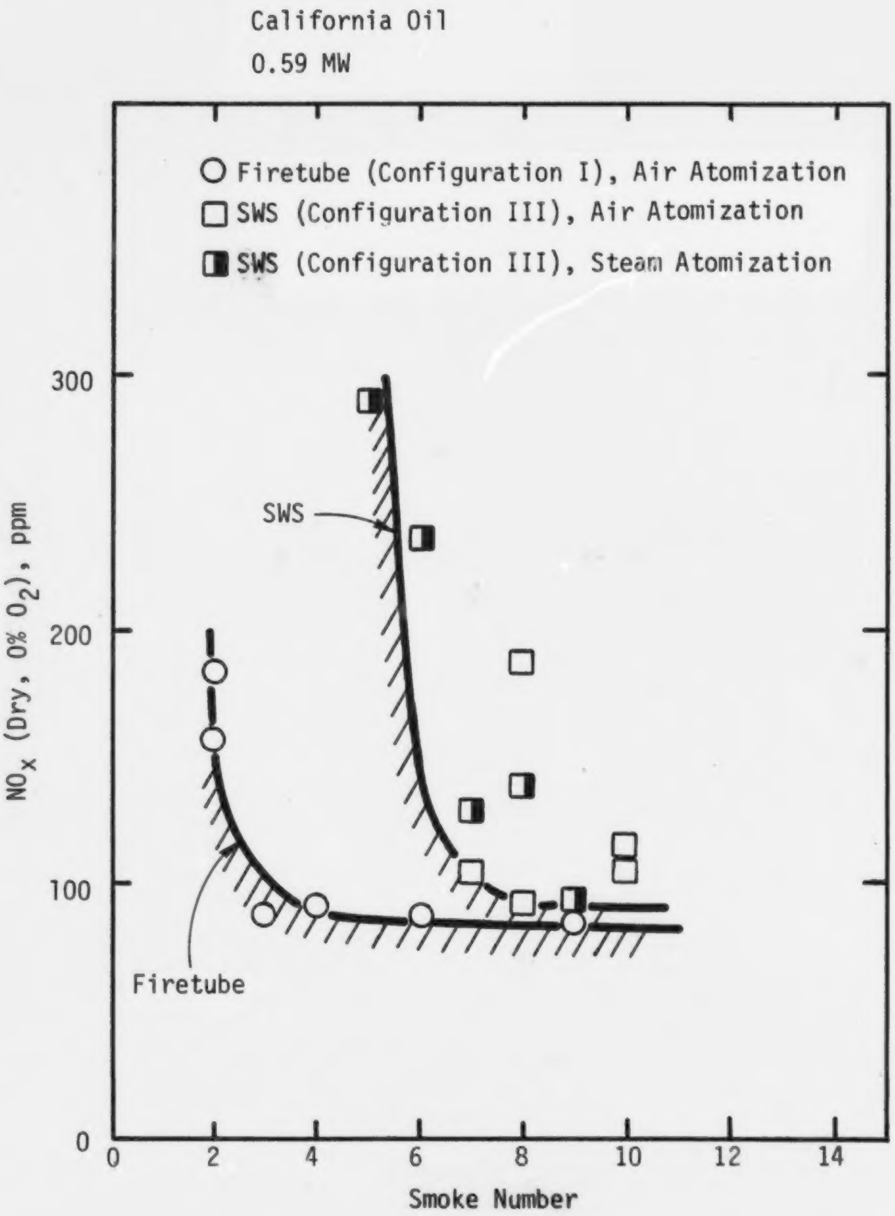

Figure 2-52. Impact of furnace environment on emissions performance.

Therefore it can be seen that although NO_x emissions were not sensitive to furnace environment, burnout of smoke (soot) in the final stages of combustion was.

2.4.3 Process Parameters

The preceding sections have described the impact of various parameters on the low-NO_x concept as defined in Table 2-5. In addition to those parameters, several variations on the process itself were investigated; specifically, use of flue gas recirculation (FGR) and multiple staging of the combustion air.

Recirculation of combustion products into the burner provides another way to limit flame temperature and local oxygen availability because the products have high heat capacity (specific heat) and low oxygen concentration. FGR has traditionally been used to control NO_x emissions from gas and distillate oil fired systems where thermal NO_x is the dominant source of NO_x NO_x emissions. FGR could potentially be applied to the current low-NO_x concept to suppress thermal NO_x formation in the second stage. Figure 2-53 shows the impact of FGR in the Firetube Simulator when added to the annular secondary air. Approximately 39 percent of the secondary flow is recycled flue gas (20 percent of the total air plus FGR flow). Minimum NO_x emissions decreased slightly from approximately 88 ppm to 80 ppm, or approximately 9 percent, with the addition of FGR to the secondary air. This suggests that thermal NO_x formation is relatively low without FGR since the benefit of FGR was minor. FGR may be more beneficial in hotter furnace environments.

Also shown in Figure 2-53 are data with FGR added to the primary air. This produced a large increase in minimum NO_x emissions from 88 ppm to 208 ppm. This can be attributed to two factors: (1) reduced gas temperature in the first stage and (2) reduced residence time due to the increased mass throughput. Both factors independently result in high TFN (total fixed nitrogen) species concentrations at the exit of the first stage which is subsequently converted to NO_x in the second stage.

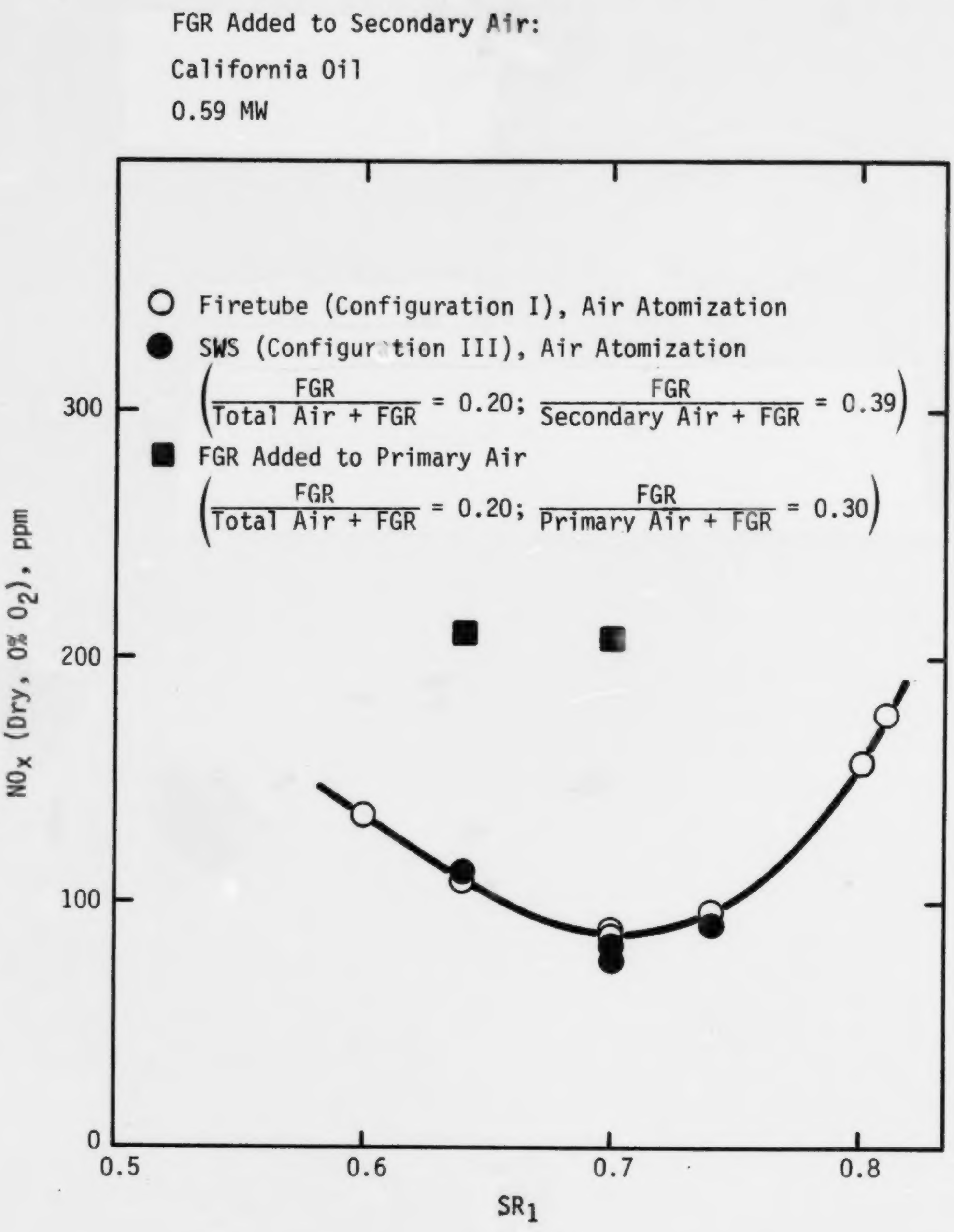

Figure 2-53. Effect of flue gas recirculation in primary and secondary air.

FGR was also added to the primary combustion products near the primary zone exit before secondary air addition as an alternative way to reduce control second-stage flame temperatures. The FGR was added through eight 5-cm diameter ports around the circumference of the primary exit section. Figure 2-54 shows NO_x emissions versus recyle ratio at $SR_1 = 0.70$. At low FGR rates, NO_x emissions were higher than the baseline level. At higher FGR rates, NO_x returned to approximately the same level as baseline. There was no apparent benefit to interstage FGR addition.

Flue gas recirculation did not prove to be beneficial in further reducing NO_x emissions from the low-NO_x burner because thermal NO_x formation was not significant; in fact, FGR increased NO_x emissions substantially when added to the primary air. Thus, although the application of FGR may be beneficial in hot furnace environments where thermal NO_x formation in the second stage is high, it will be beneficial only if added to the secondary air.

The concept for multiple (i.e., more than two) staging to achieve low-NO_x emissions was also investigated. Combustion air was divided into primary, interstage, and secondary air streams. Interstage air was added through the eight radial ports upstream of the primary exit. Figure 2-55 shows NO_x emissions versus SR_2 for SR_1 of 0.51, 0.70, and 0.76. SR_2 is defined as the total mixture stoichiometric ratio after the addition of interstage air. The figure shows minimum NO_x levels of 128 ppm at $SR_1 = 0.70$ and $SR_2 = 0.88$. It is clear that interstage air is detrimental to the low-NO_x concept as tested. Mixing and temperature conditions in the interstage region favor high conversion of TFN species to NO_x and possibly some thermal NO_x may be formed in locally fuel-lean regions.

2.4.4 Fuel Nitrogen Effects

Two petroleum oils (distillate and residual), one coal-derived liquid (SRC-II) and one doped oil (distillate and pyridine) were screened under baseline conditions in the prototype test burner. Fuel nitrogen content for the liquid fuels ranged from 0 to 1.0 percent N. Propane and propane plus

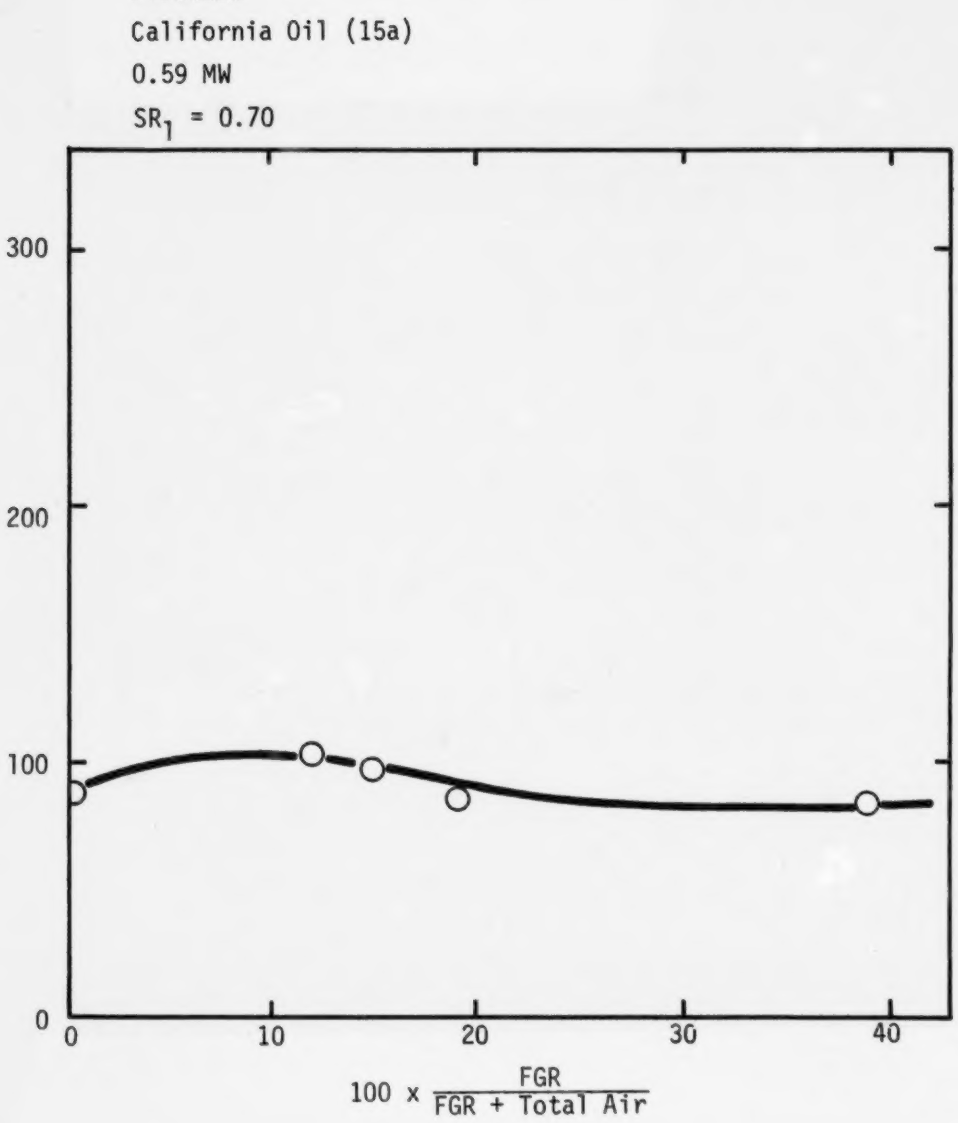

Figure 2-54. Effect of interstage FGR injection.

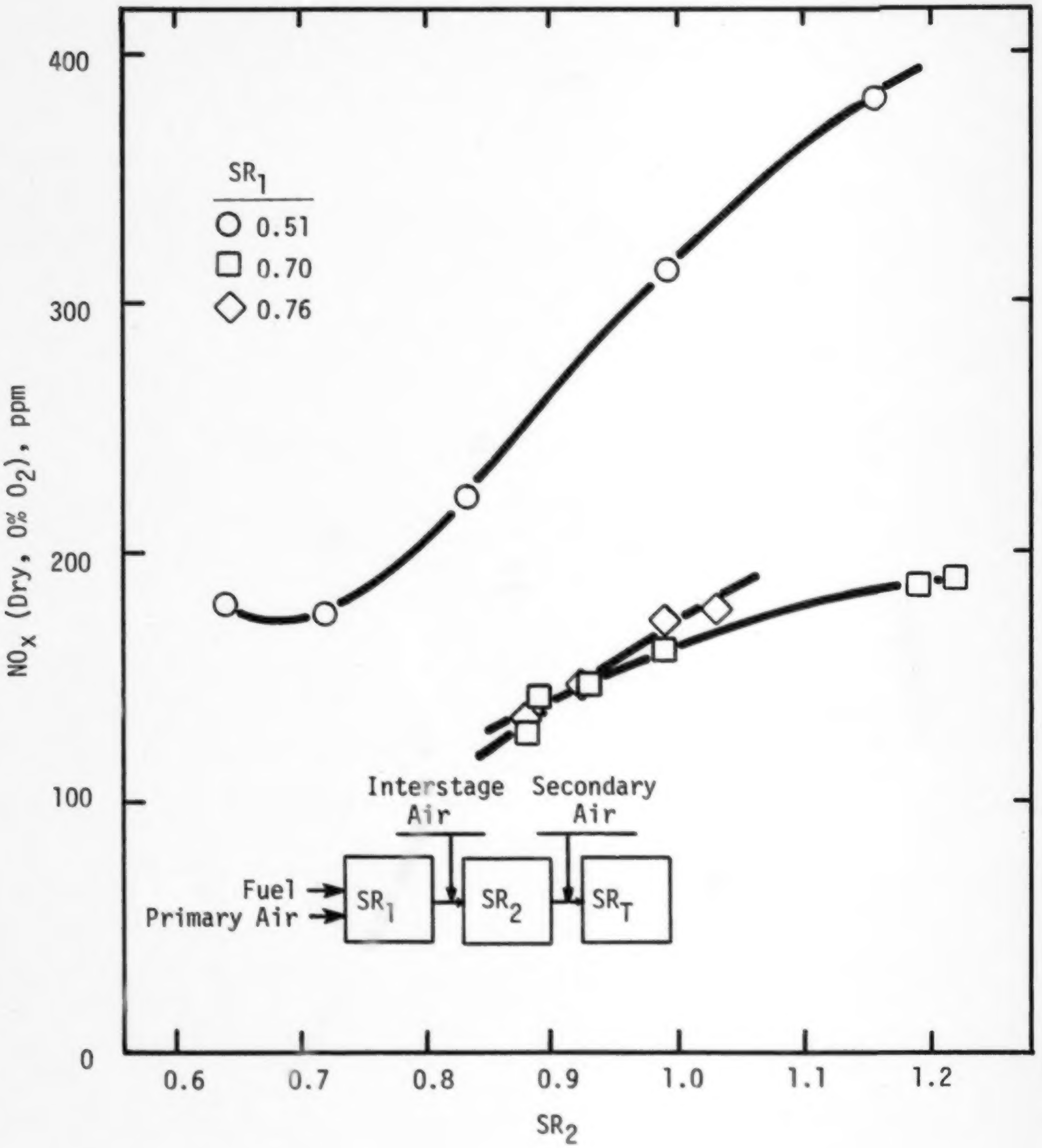

Air Added to Radial Interstage Ports
Firetube
California Oil (15a)
0.59 MW
SR_T = 1.16

Figure 2-55. NO_x emissions with interstage air injection.

ammonia were also fired to simulate an instantaneously volatilized oil. Figure 2-56 compares NO_x and smoke emissions from the four liquid fuels tested. A wide range of NO_x emissions were observed under unstaged conditions (SR_1 = 1.16) and, depending upon the fuel, ranged from a minimum of 610 ppm with the residual petroleum oil to a maximum of 990 ppm with the coal-derived liquid. NO_x emissions under staged conditions varied over a much narrower range and appeared to be only slightly dependent upon fuel nitrogen content. For instance, the SRC-II containing 0.98 percent N produced NO_x emissions lower than the California residual fuel (65 ppm vs. 85 ppm) and the diesel oil doped to the same nitrogen level as the residual oil resulted in lower NO_x emissions than the simulated oil (74 ppm vs. 85 ppm). This suggests the importance of other fuel properties (e.g., viscosity, volatility) at very low NO_x levels. Figure 2-56 also shows that smoke emissions from the burner are only slightly dependent upon fuel type for equivalent conditions.

Figure 2-57 shows NO_x and smoke emissions from propane and propane/NH_3 mixtures. In this experiment NH_3 was mixed with the propane prior to injection into the burner to simulate the nitrogen levels of the residual petroleum oil an a crude shale oil. NO_x emissions decrease with decreasing SR_1 for the undoped propane and reach a steady level below SR_1 = 0.7. In the absence of fuel nitrogen, NO_x emissions are derived from thermal NO formation which is strongly dependent upon temperature (and residence time at high temperature). In Figure 2-58, NO_x emissions from propane are shown at two loads and it can be seen that thermal NO_x formation is more significant at 0.88 MW than at the lower load, and in fact can account for a major fraction of the NO_x emissions from nitrogen-containing fuels.

When NH_3 is injected with the propane (Figure 2-57), NO_x emissions follow the same trend with SR_1 as with liquid fuels. A minimum in NO_x occurs near SR_1 = 0.7 and the NO_x level increases slightly with increasing nitrogen content.

These results illustrate that by maintaining optimum first-stage stoichiometry NO_x emissions of 55 ppm (3 percent O_2) can be achieved with

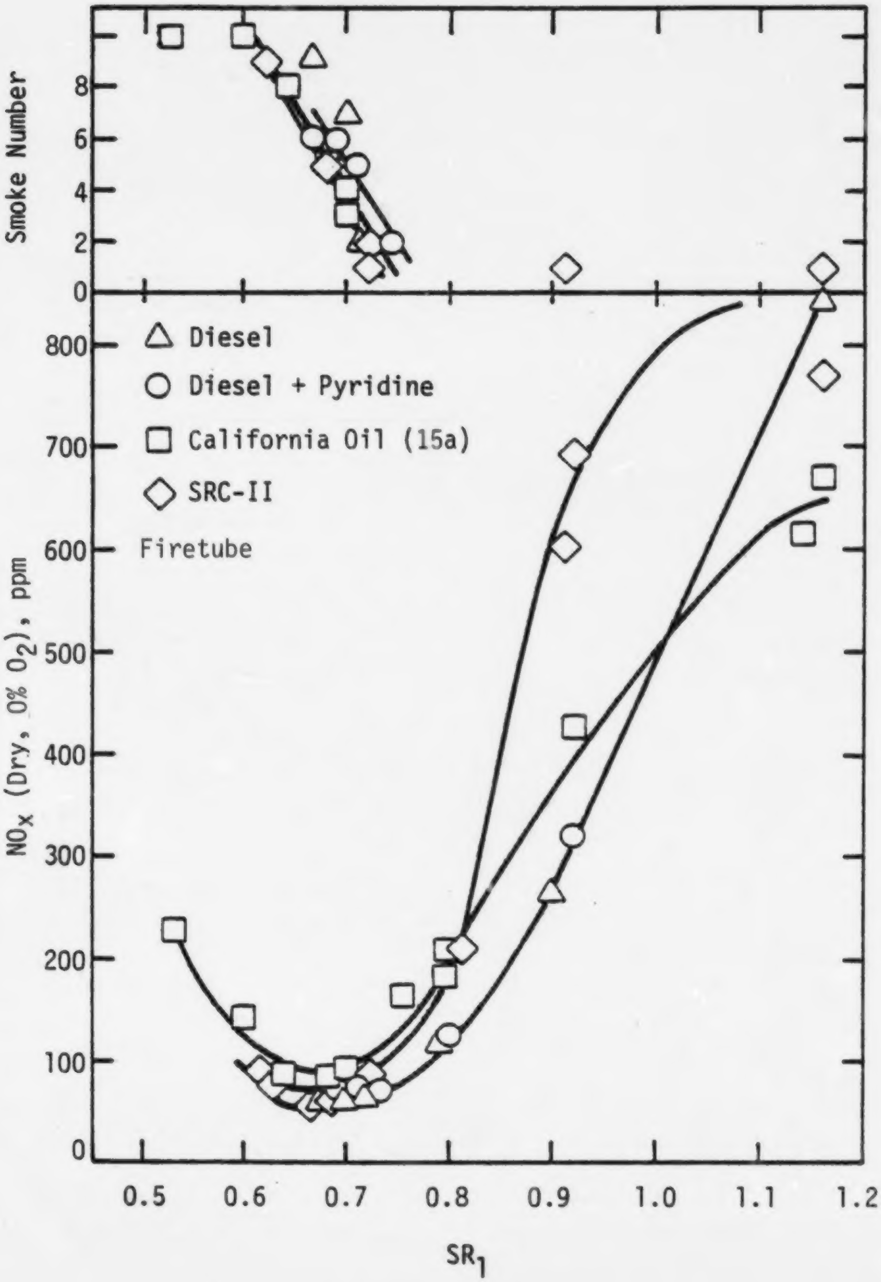

Figure 2-56. Influence of fuel type on NO$_x$ and smoke emissions from liquid fuels (0.59 MW).

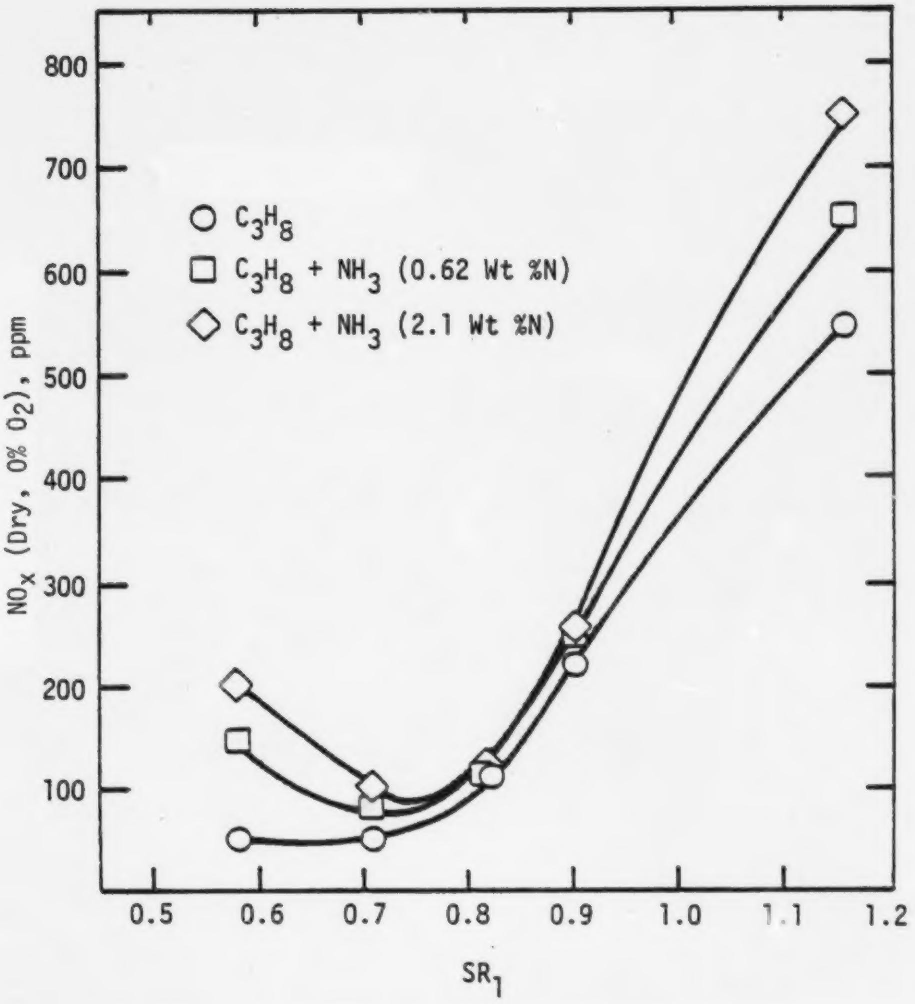

Figure 2-57. Effect of nitrogen content upon NO_x emissions from gaseous fuels (0.59 MW).

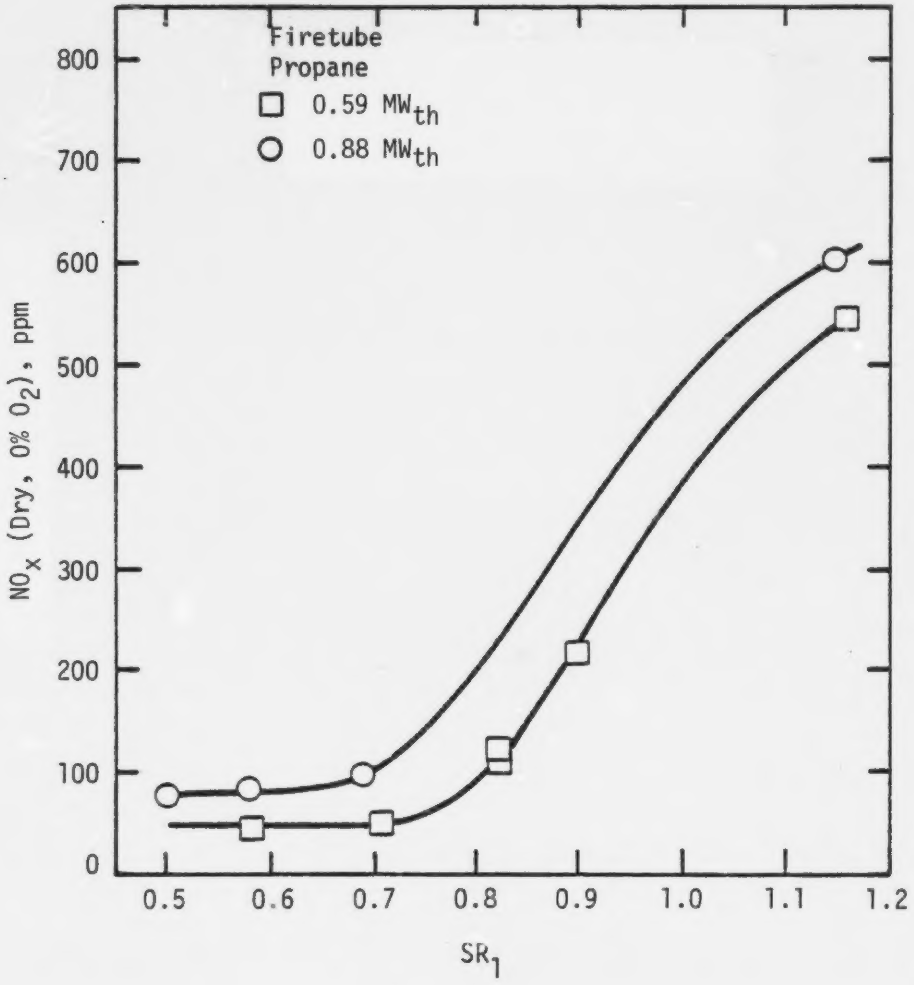

Figure 2-58. Effect of load upon thermal NO_x formation (propane).

acceptable CO and smoke emissions. Figure 2-59 shows that low emissions are not strongly dependent upon fuel nitrogen content but that other fuel properties have a second order effect. Thus, a wide range of fuels from gas to heavy petroleum oils and alternative liquids can be utilized in this burner concept without significantly affecting emissions.

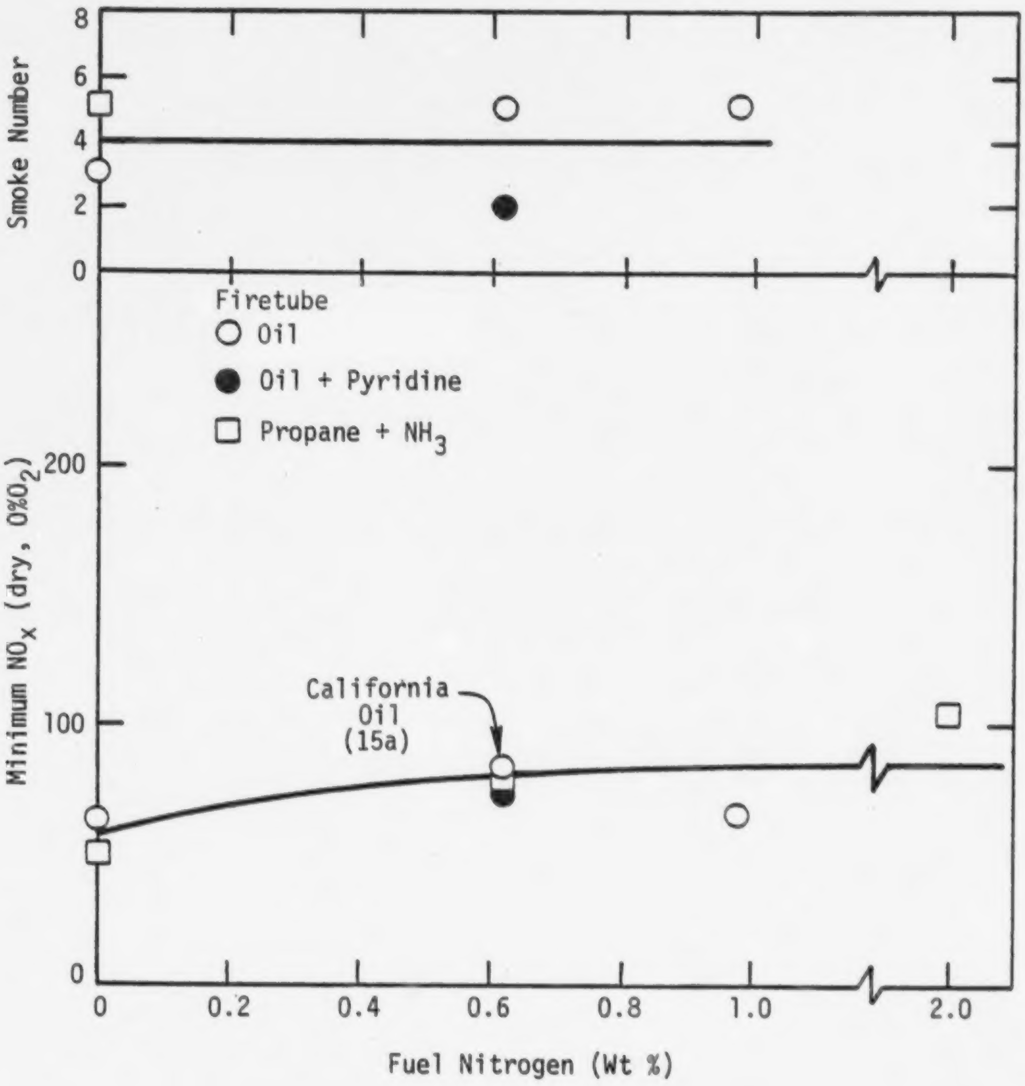

Figure 2-59. Effect of fuel nitrogen content upon minimum NO_x emissions (0.59 MW_{th}).

3.0 WATERTUBE BURNER STUDIES

The objectives of these studies were to:

- Evaluate NO_x production in flames similar to those found in industrial watertube boilers.
- Investigate the effects of scale and burner design on NO_x emissions.
- Develop scaling criteria for low-NO_x burner concepts.

The intermediate pilot scale studies were conducted in the EPA small watertube simulator (SWS) facility operated by EER in Santa Ana, California. The nominal furnace capacity is 3 MW (10 x 10^6 Btu/hr) and is designed to simulate the thermal environment of an industrial watertube boiler.

Three heavy oil burners were tested in the SWS:

- A commercial watertube boiler burner.
- A prototype distributed mixing, externally-staged burner.
- A scaled-up version of the advanced prototype burner developed in the small pilot scale studies.

The commercial watertube boiler burner was used to establish baseline furnace emission levels. The externally staged distributed mixing burner represents current generation low-NO_x burner design, and the advanced prototype burner is a result of this research effort. Thus, the level of NO_x control achievable with burners ranging in design and complexity (and cost) is represented.

3.1 Small Watertube Simulator (SWS)

The SWS furnace is illustrated in Figure 3-1. The furnace is a horizontal cylinder 1.83 meters inside diameter by 5.17 meters long. Burners are mounted on one end and the exhaust exits through the cylindrical wall at the rear of the furnace. The flue gases are exhausted to an air heater which permits air preheat levels to approximately 200°C. The furnace is cooled by external water sprays. Thermal environment is determined by a partial refractory lining installed inside the furnace. Furnace temperatures can be varied by varying the amount of refractory on the furnace wall. Table 3-1 lists the nominal characteristics of the furnace.

Fuel oil is supplied to the furnace from an underground tank by a rotary gear pump. Residual fuel oil flow was metered by a positive displacement flowmeter which was calibrated gravimetrically for each fuel or by a calibrated turbine flowmeter. Distillate fuel oil flow was metered by rotameter. Flow control is achieved using pressure regulators and globe values. Residual fuel oil lines are steam traced to control fuel temperature. Atomizing air is supplied by a facility air compressor and steam for atomization and heat tracing is supplied by a small firetube boiler.

Flue gas is sampled and conditioned using the sampling train shown in Figure 3-2. Samples are withdrawn from the exhaust duct with a water-cooled stainless steel probe. The sample passes through a cyclone for particulate removal, a glass wool filter, Teflon-lined diaphragm pump, refrigerated water trap and a Teflon fiber filter to provide a dry, clean sample to the continuous monitors. All materials in contact with the sample are Teflon or stainless steel.

Table 3-2 lists the flue gas analyzers used to monitor O_2, CO_2, CO, NO/NO_x, and SO_2 concentrations. Instrument accuracy is maintained by frequent calibration with certified calibration gases. There is provision for a zero gas and two span gases for each instrument. The usual calibration involves adjusting each instrument to read identical to the specified zero and span

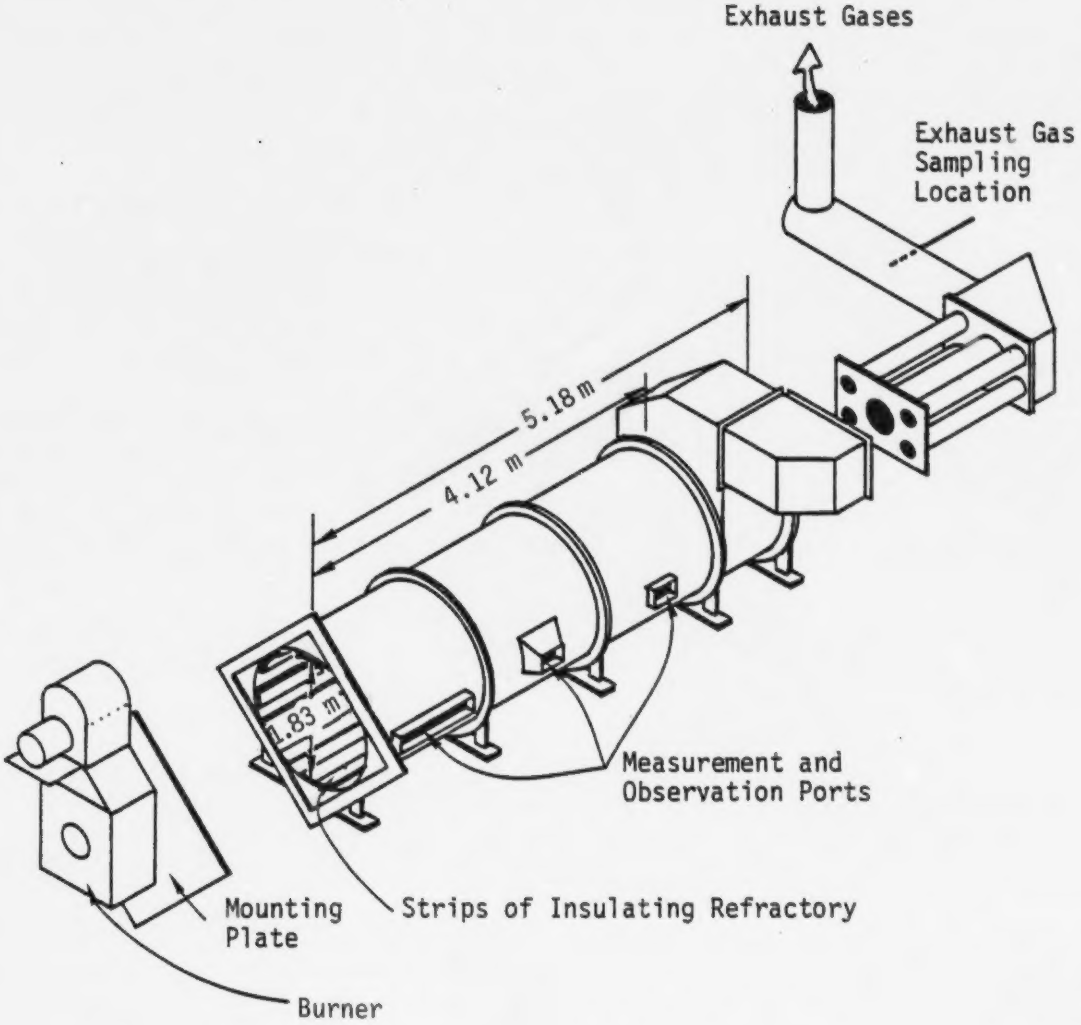
Exhaust Gases
Exhaust Gas Sampling Location
5.18 m
4.12 m
1.83 m
Measurement and Observation Ports
Mounting Plate
Strips of Insulating Refractory
Burner

Figure 3-1. Small watertube boiler simulator test facility.

TABLE 3-1. NOMINAL SPECIFICATIONS OF SWS TEST FURNACE

Parameter	Small Watertube Boiler Simulator
Firing	
Configuration	Single Wall
Nominal Firing Rate	2.93 MW (10 x 10^6 Btu/hr)
Dimensions	
Shape	Cylinder
Diameter	1.83 m (6 ft)
Length	5.18 m (17 ft)
Surface Area	
Total	41.8 m^2 (450 ft^2
Insulated (axial strips around circumference and rear wall)	19.0 m^2 (204 ft^2)
Cooled	22.9 m^2 (246 ft^2
Volume	19.7 m^3 (696 ft^3)
Cooling	Water spray cooled on all surfaces
Thermal Environment	
Heat Release/Cooled Surface	0.13 MW/m^2 (40,650 Btu/hr/ft^2)
Heat Release/Volume	0.15 MW/m^3 (14,368 Btu/hr/ft^3)

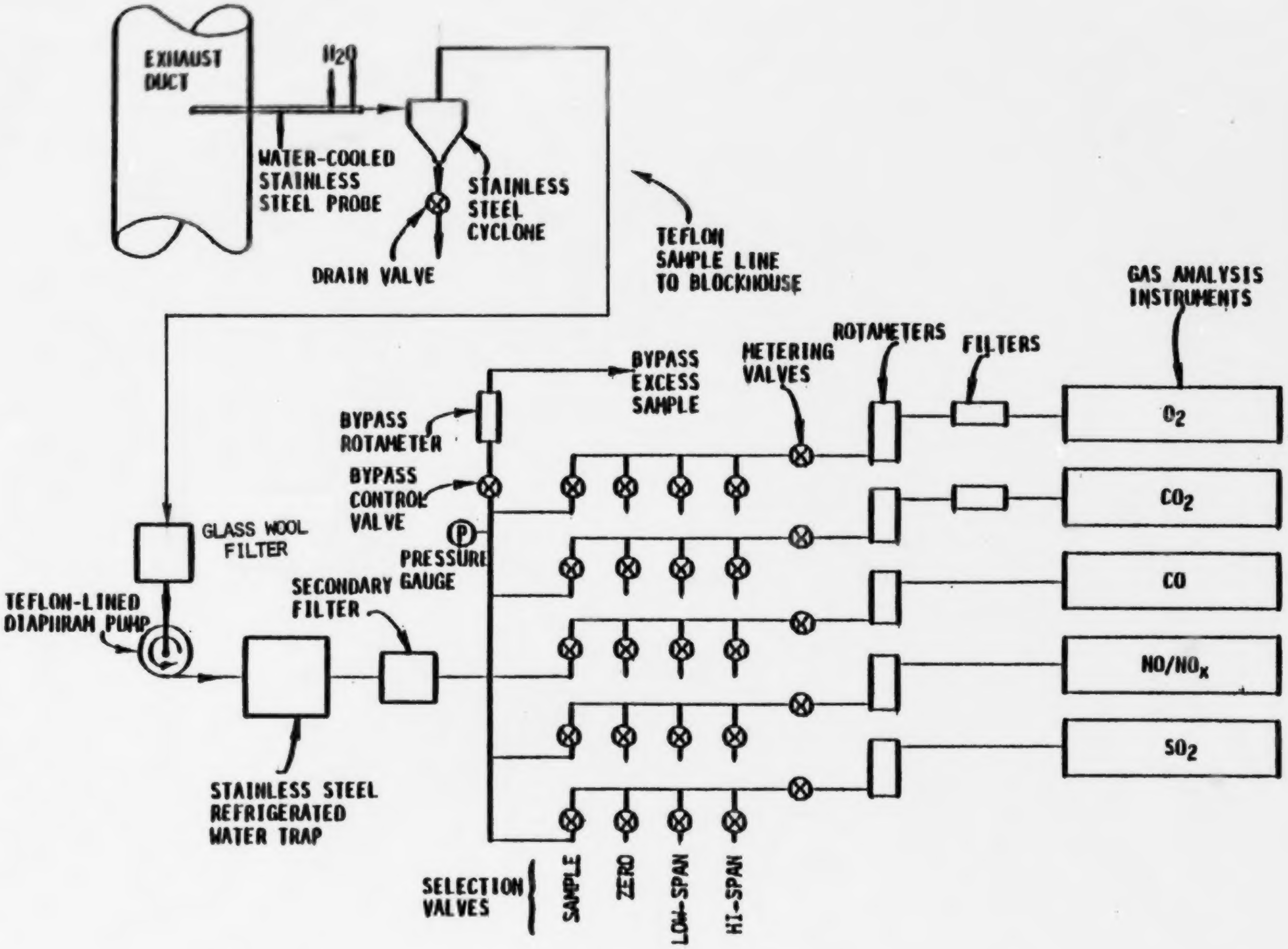
EXHAUST DUCT
H_2O
WATER-COOLED STAINLESS STEEL PROBE
STAINLESS STEEL CYCLONE
DRAIN VALVE
TEFLON SAMPLE LINE TO BLOCKHOUSE
GAS ANALYSIS INSTRUMENTS
ROTAMETERS
FILTERS
METERING VALVES
BYPASS EXCESS SAMPLE
BYPASS ROTAMETER
BYPASS CONTROL VALVE
PRESSURE GAUGE
GLASS WOOL FILTER
SECONDARY FILTER
TEFLON-LINED DIAPHRAM PUMP
STAINLESS STEEL REFRIGERATED WATER TRAP
O_2
CO_2
CO
NO/NO_x
SO_2
SELECTION VALVES
SAMPLE
ZERO
LOW-SPAN
HI-SPAN

Figure 3-2. Continuous gas analyzer sample train.

TABLE 3-2. CONTINUOUS EMISSIONS ANALYZERS USED FOR FLUE GAS ANALYSIS

Species	Operating Principal	Instrument	Model No.
O_2	Paramagnetic	Beckman	755
CO_2	Nondispersive Infrared	Anarad	AR-500
CO	Nondispersive Infrared	Anarad	AR-500
NO/NO_x	Chemiluminescence	Thermo Electron	10
SO_2	Pulsed Fluorescence	Thermo Electron	40

gas concentrations. The zero gas is N_2 and is certified to have less than one percent of the full range concentration of each gas species being measured with the continuous analyzers. The span gases are certified to be accurate within two percent. In addition, new span gases are compared with old ones to assure continuity of data.

The sampling locations for the gas-phase measurements and particle sampling are located in the two-foot diameter exhaust duct located downstream of the SWS exhaust gas exit. The lengths of straight ducting upstream and downstream of the sampling location correspond to approximately eight- and two-duct diameters, respectively. This meets the requirements of EPA Method 1 for the minimum number of points to be sampled. The temperature and gas velocity at the sampling location vary with test conditions. The temperature is generally in the range of 500 to 1500°F. The gas velocity is in the range of 15 msec (50 ft/sec).

3.2 Commercial Watertube Burner Tests

Figure 3-3 illustrates the main features of the commercial burner selected for the baseline evaluation. The burner is designed for firing No. 6 oil or No. 2 oil at 3.5 MW thermal input. The burner assembly includes an integral air fan, circular air registers, air damper, pilot/igniter assembly, control linkages, and fuel oil/atomizing steam piping trains.

The burner air register assembly consists of two air vane assemblies which divide the combustion air into core and annular air flows. The air vanes impart swirl to the combustion air which varies with load to maintain satisfactory flame stability and shape over a 10:1 turndown ratio. Combustion air is not preheated.

The burner throat is constructed of prefired refractory tiles. The throat diverges at approximately 25° half angle and has an L/d ratio of approximately 0.96. The tile surface is rippled. The oil gun assembly is located on the axis of the burner throat. A diffuser cone is attached to the end of the oil gun guide pipe to provide flame stability.

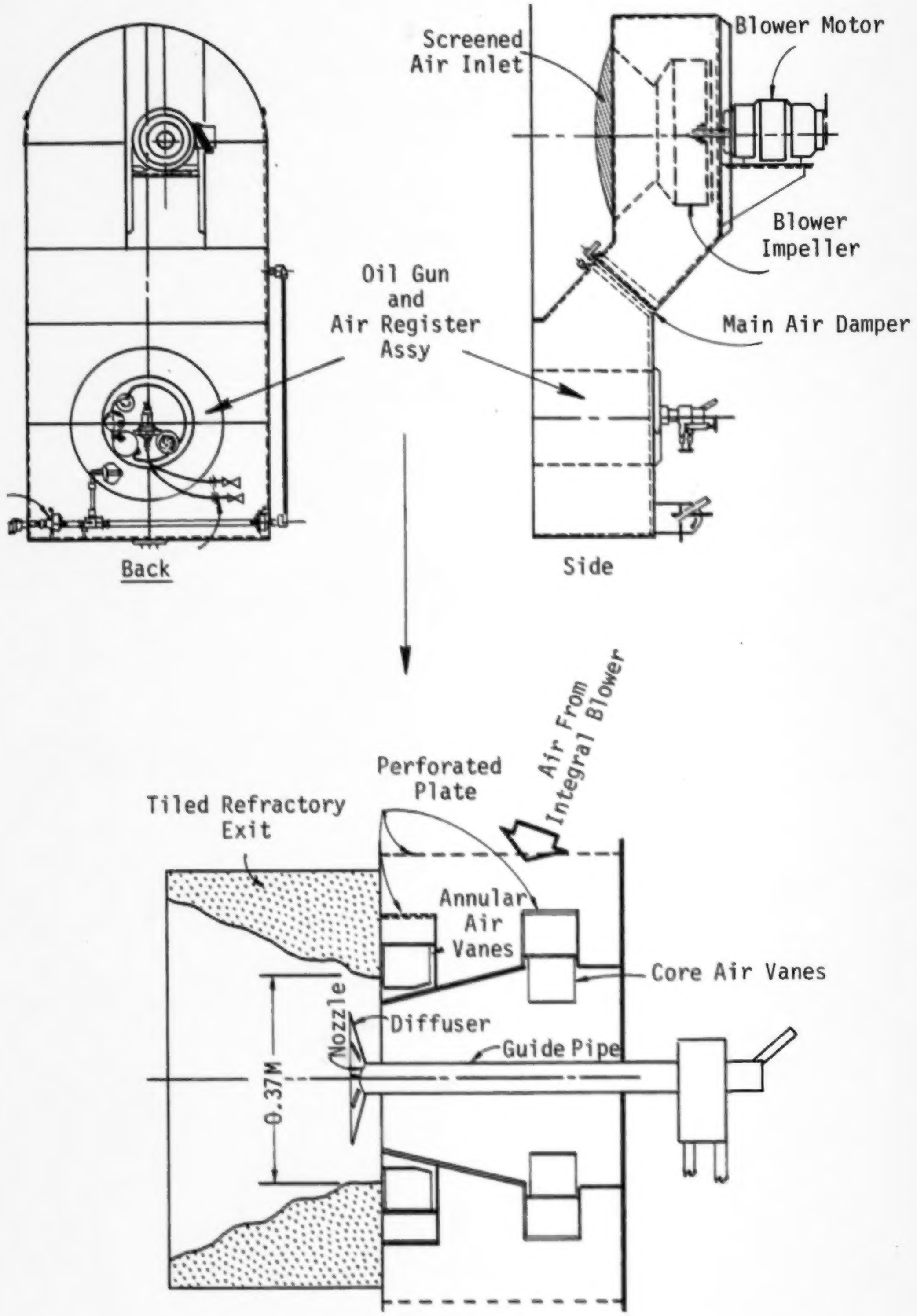
Screened Air Inlet
Blower Motor
Blower Impeller
Oil Gun and Air Register Assy
Main Air Damper
Back
Side
Air From Integral Blower
Perforated Plate
Tiled Refractory Exit
Annular Air Vanes
Core Air Vanes
Nozzle
Diffuser
Guide Pipe
0.37M

Figure 3-3. Commercial watertube boiler burner.

Figure 3-4 illustrates the two atomizers utilized for firing distillate and residual fuel oils. The same basic atomizer is used for both fuels with the exception of a different nozzle body and cap. The atomizer is a twin-fluid, internal mixing type nozzle which is designed to use steam as the atomizing fluid. Steam and oil is directed into a mixer assembly which causes several pairs of steam and oil jets to impinge at a 90° angle, shearing the oil jet to produce small droplets. The atomized steam/oil mixture then passes through the nozzle body and cap. Holes are drilled in the cap to produce the desired spray angle. Spray angle for the residual oil cap was 55° (included angle) and was 60° for the distillate oil cap.

3.2.1 Commercial Watertube Burner Characterization

Tests were conducted in the SWS with two furnace configurations:

- Uninsulated--without any refractory inside the furnace.
- Insulated--with approximately 45 percent of the interior surface covered with insulating refractory.

Comparison of the two configurations allowed the effect of thermal environment to be determined.

Three fuels were tested, ranging in fuel nitrogen content from 0.053 (distillate oil) to 0.74 (residual oil). The residual shale oil is a product of a previous Air Force program which refined Paraho process crude shale oil to military grade fuel (diesel fuel marine) specifications. The residual shale oil was a secondary product and has been extensively hydrotreated. Analysis of all three fuels is presented in Table 3-3. The residual fuels were heated to produce 21 cs oil viscosity at the burner.

Figure 3-5 shows NO_x emissions versus excess oxygen level for the three fuels fired in the uninsulated furnace at 3.1 MW load. Burner air registers were adjusted according to manufacturers recommendations, and excess O_2 was varied by adjusting the total air damper. NO_x emissions from the No. 2 fuel

3/25 Final

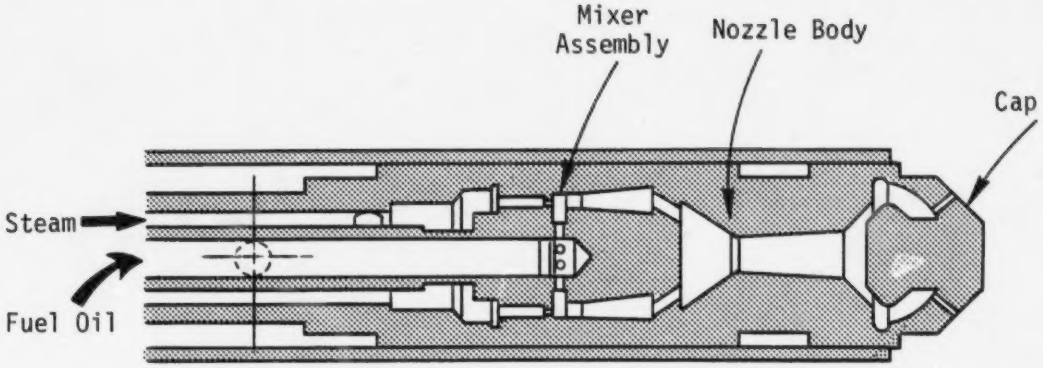
Mixer Assembly
Nozzle Body
Cap
Steam
Fuel Oil

(a) Heavy Oil Nozzle Assembly

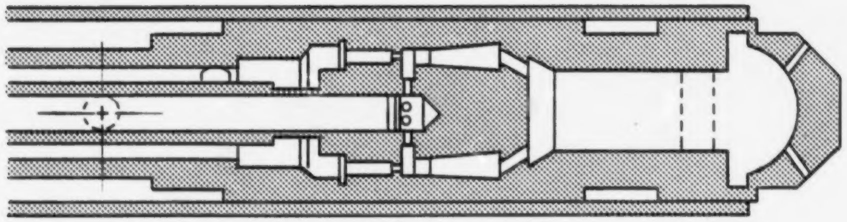

(b) Light Oil Nozzle Assembly

Figure 3-4. Atomizer assemblies used in commercial watertube boiler burner.

TABLE 3-3. FUEL PROPERTIES

	California No. 2 Oil	California No. 6 Oil	Residual Shale Oil
Ultimate Analysis:			
Carbon, %	86.8	85.40	86.71
Hydrogen, %	12.52	11.44	12.76
Nitrogen, %	0.053	0.74	0.46
Sulfur, %	0.27	1.63	0.28
Ash, %	<0.001	0.043	0.009
Oxygen, %	0.36	0.71	0.03
Conradson Carbon Residue, %	-	8.72	0.19
Asphaltenes, %	-	5.18	0.083
Flash Point, °C	-	-	113
Pour Point, °C	-	3>	32>
Specific Gravity	0.86	0.96	0.88
Viscosity, CS:			
At 60°C	0.7	180	8.8
At 99°C	0.6	27.5	4
Trace Metals, ppm:			
Calcium	-	21	4.2
Iron	-	73	<0.5
Manganese	-	0.8	<0.5
Magnesium	-	5.1	0.15
Nickel	-	65	<0.5
Sodium	-	21	2.51
Vanadium	-	44	<1.0
Heat of Combustion:			
Gross kJ/g	45.0	43.0	45.0
Net kJ/g	-	40.5	42.3

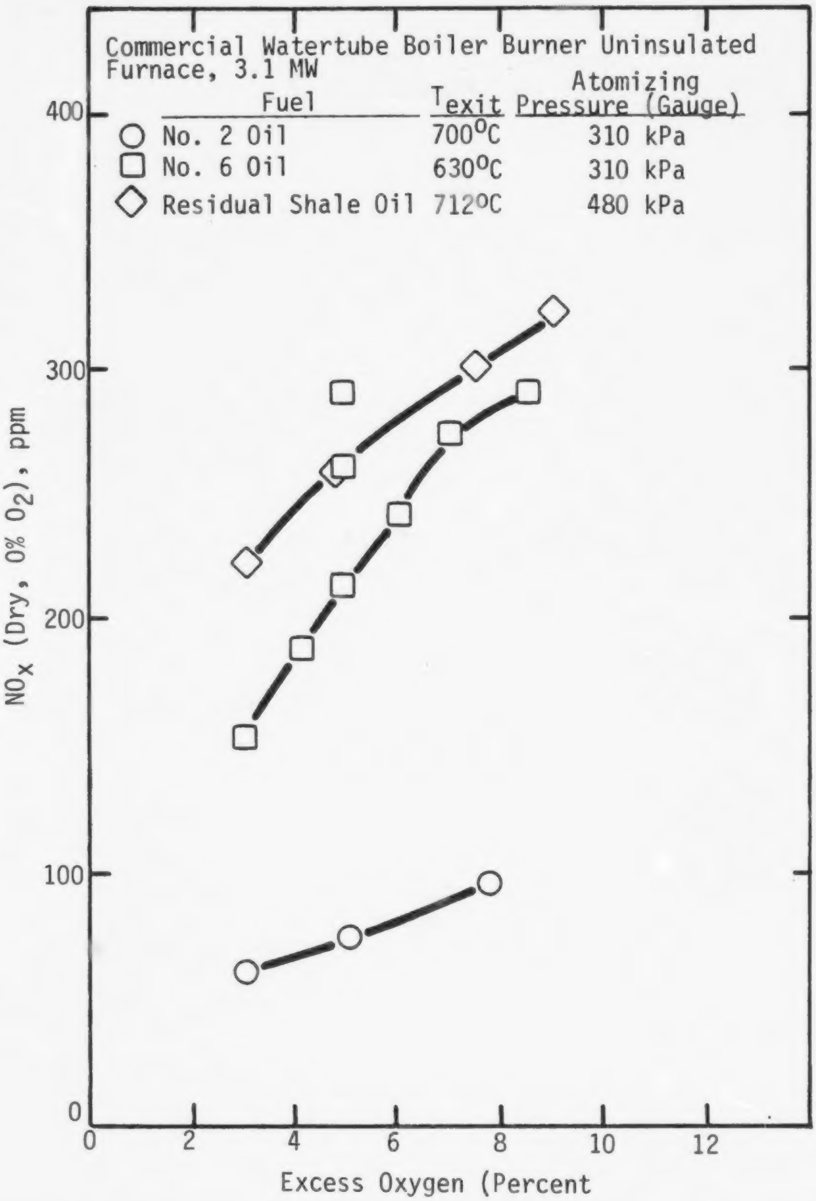

Figure 3-5. Effect of excess oxygen for distillate, residual, and shale derived fuel oils fired in commercial watertube burner (3.1 MW, uninsulated furnace).

oil were mildly sensitive to excess oxygen, increasing from 61 ppm at 3 percent excess oxygen to 96 ppm at 7.9 percent excess oxygen. NO_x emissions were much higher and more sensitive to excess oxygen level for the residual No. 6 oil, increasing from approximately 150 ppm at 3 percent excess oxygen to greater than 280 ppm at 8 percent excess oxygen. The residual shale oil produced the highest NO_x emissions, surprisingly, and emissions were also very sensitive to excess oxygen level. Previous results had shown that NO_x emissions from petroleum-derived fuels generally increased with fuel nitrogen content (bench-scale studies, Volume I); however, several synthetic fuels from coal and shale liquifaction processes appeared to produce higher levels of thermal NO_x than petroleum-derived fuels of equal nitrogen content. This was attributed to higher fuel volatility for synthetic fuels which can cause higher peak flame temperatures due to increased local combustion intensity.

Figure 3-6 shows similar data obtained in the insulated SWS configuration. Trends were similar to those observed in the uninsulated case; however, NO_x emissions from the No. 6 oil and residual shale oil were higher by approximately 70 and 100 ppm, respectively, relative to the uninsulated case. This is probably due to an increase in fuel NO_x formation. NO_x emissions from the No. 2 oil were similar in both furnace configurations, which suggests that thermal NO_x formation was not affected by furnace temperatures. The increase in NO_x emissions for the residual fuels could be a result of more rapid fuel vaporization which would evolve fuel nitrogen earlier in flames where higher oxygen concentrations exist. This would be expected to lead to greater conversion of fuel nitrogen to NO_x.

The effect of load on NO_x emissions produced by No. 2 oil is shown in Figure 3-7 for both insulated and uninsulated furnace configurations. Load was varied by adjusting the burner oil valve which is linked to both core and annular air registers and to the total air damper; thus, swirl level varied as load was adjusted to maintain flame stability and shape. NO_x emissions decreased as load decreased in the insulated furnace. NO_x emissions varied with load in the uninsulated furnace configuration but not monotonically or as significantly as in the insulated furnace. This may be due to slightly different burner settings between the two runs.

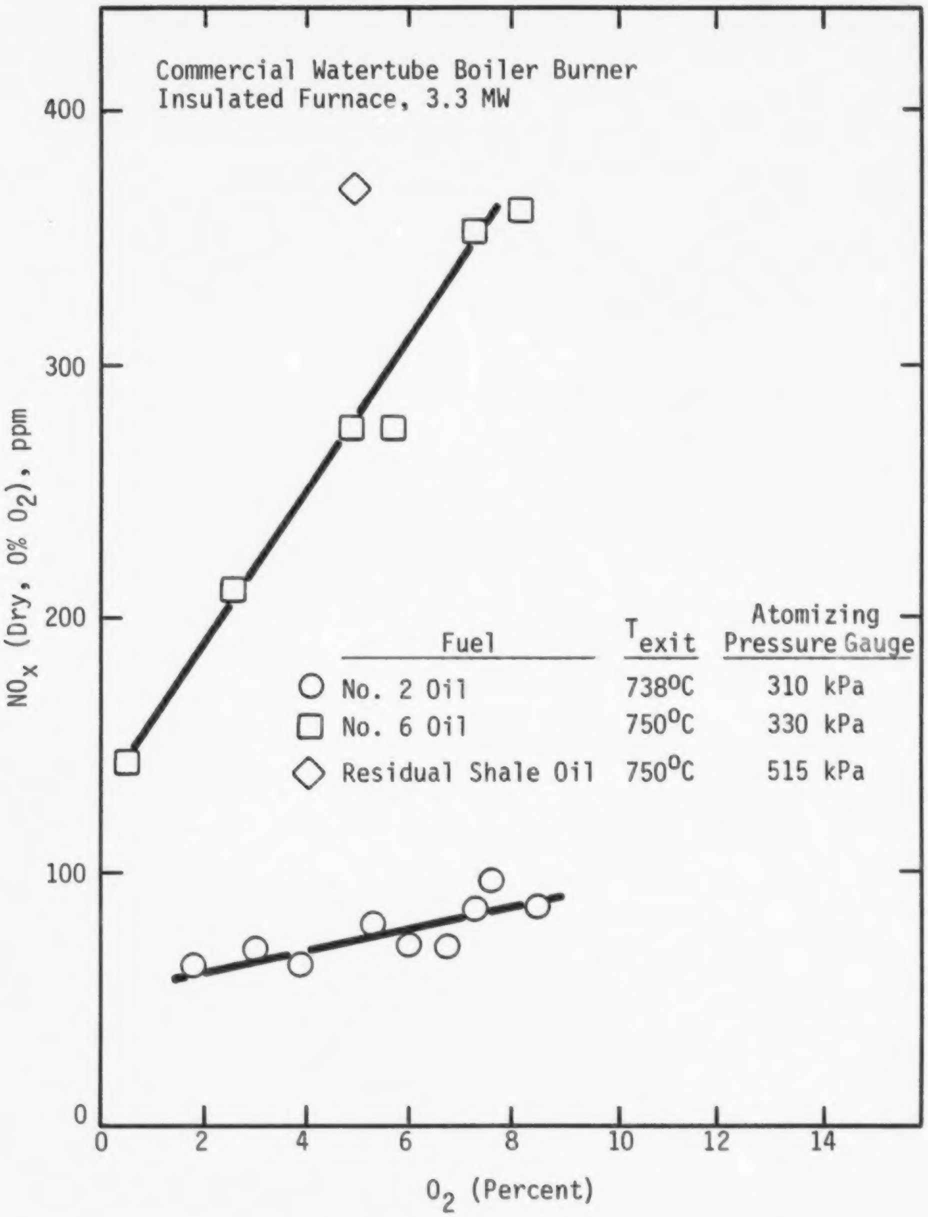

Figure 3-6. Effect of excess oxygen for different fuels fired in commercial watertube burner (3.3 MW, insulated furnace).

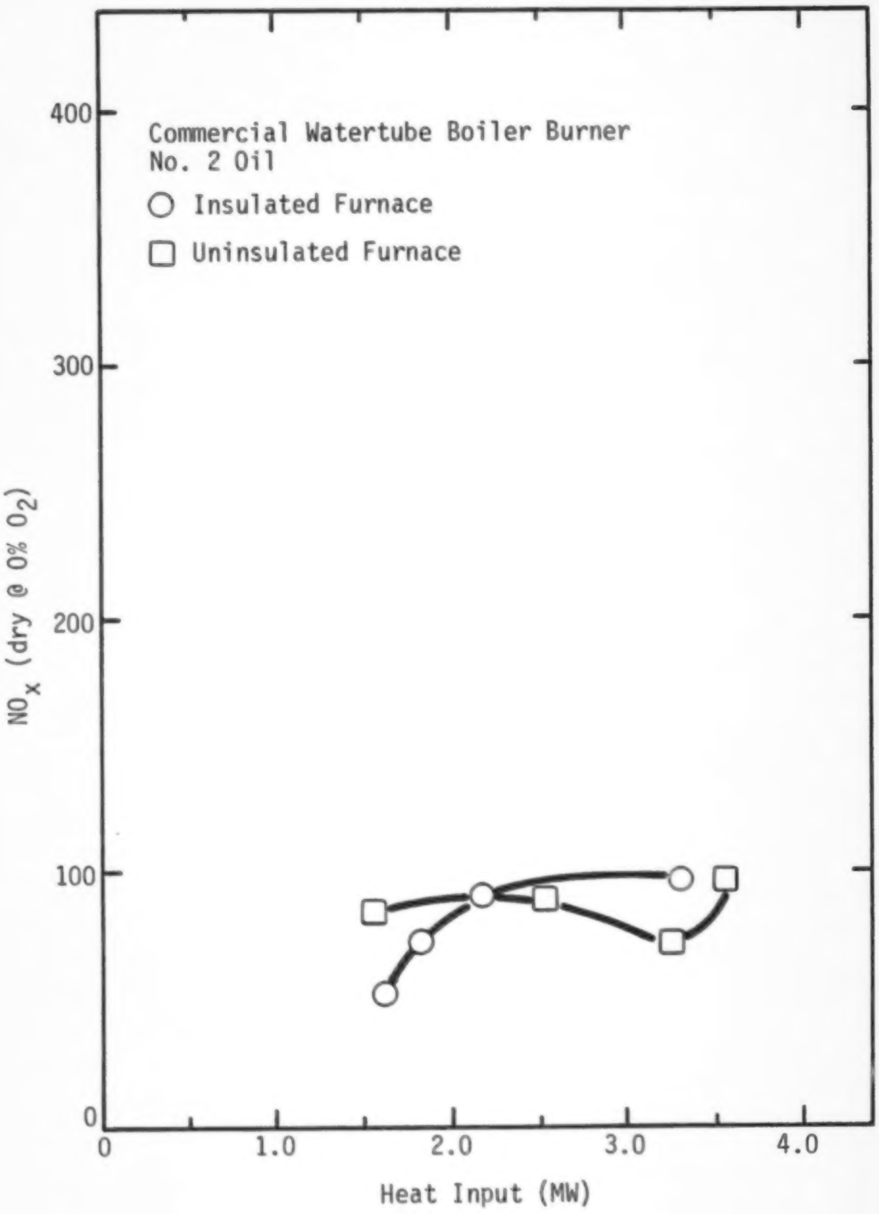

Figure 3-7. Commercial watertube burner--effect of load (No. 2 oil).

Figures 3-8 and 3-9 show similar results for No. 6 oil and residual shale oil. Again the trends were slightly different for the insulated and uninsulated furnace. NO_x emissions in the insulated furnace were consistently higher than in the uninsulated furnace throughout the load range. NO_x emissions with furnace insulation were higher at the minimum load investigated for both fuels, even though excess oxygen was approximately constant. NO_x emissions without insulation appeared to be slightly less sensitive to load.

Minimum excess oxygen levels were generally limited by the onset of CO and smoke emissions, indicating poor combustion efficiency. Those conditions which produced the lowest NO_x emissions typically produced high smoke emissions. Figure 3-10 shows the results of tests to minimize NO_x emissions from No. 6 oil by making burner adjustments. NO_x emissions are shown versus Bacharach smoke number. It can be seen that burner operating parameters influence NO_x significantly, and that the minimum NO_x level is limited by smoke emissions. Reducing excess O_2 at the optimum burner settings reduced NO_x but also increased smoke. Adding furnace insulation resulted in lower smoke numbers for similar NO_x levels, indicating improved burnout of soot and other cabonaceous particulate (e.g. cenospheres) formed in the flame.

Gas temperature measurements at the furnace exit (shown on Figure 3-5 and 3-6) were made to characterize the furnace environment. The actual gas temperature is probably higher than the measured temperature since only a bare thermocouple was used. This can result in significant radiation heat loss from the thermocouple since the exhaust duct is much cooler than the gas. It is estimated based on later data that these measurements are low by approximately 200 to 300°C. Estimated difference in exit temperature with and without furnace insulation is approximately 230°C at full load conditions.

Although increasing furnace temperature appears to increase NO_x emissions, it also decreases smoke emissions, allowing further burner optimization to decrease NO_x. The end result appears to be that slightly lower NO_x emissions are possible with higher furnace temperature because of increased

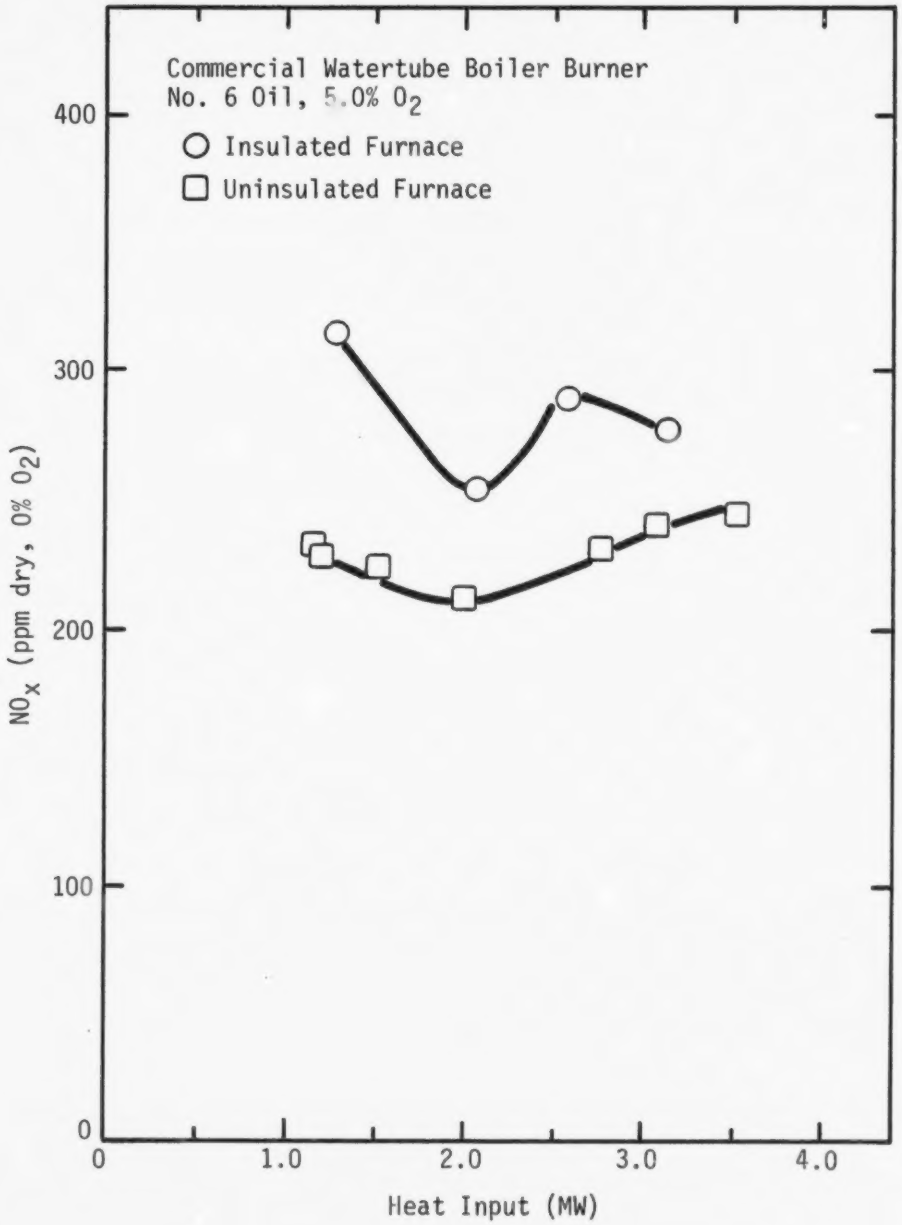

Figure 3-8. Commercial watertube burner--effect of load (No. 6 oil).

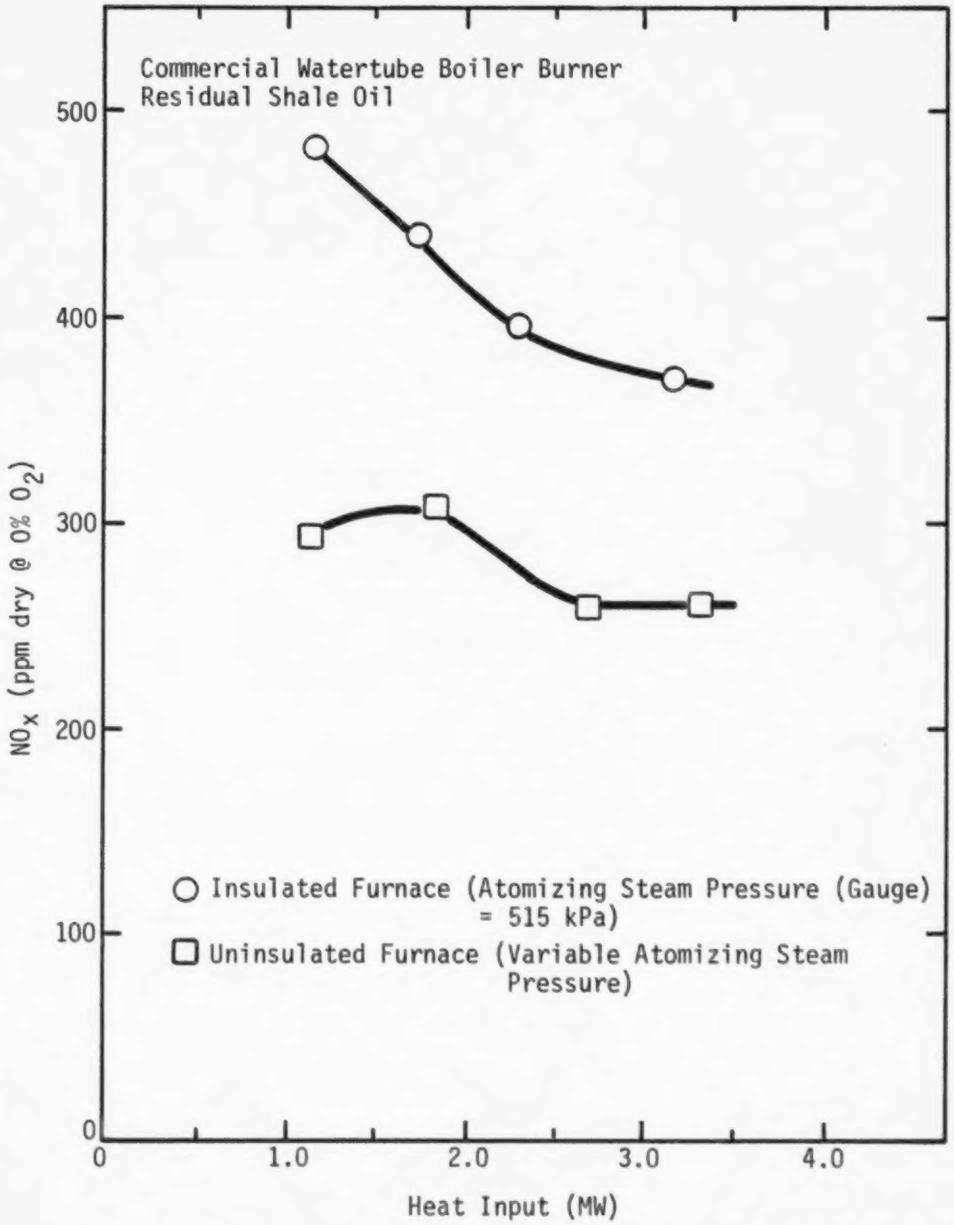

Figure 3-9. Commercial watertube burner--effect of load (residual shale oil).

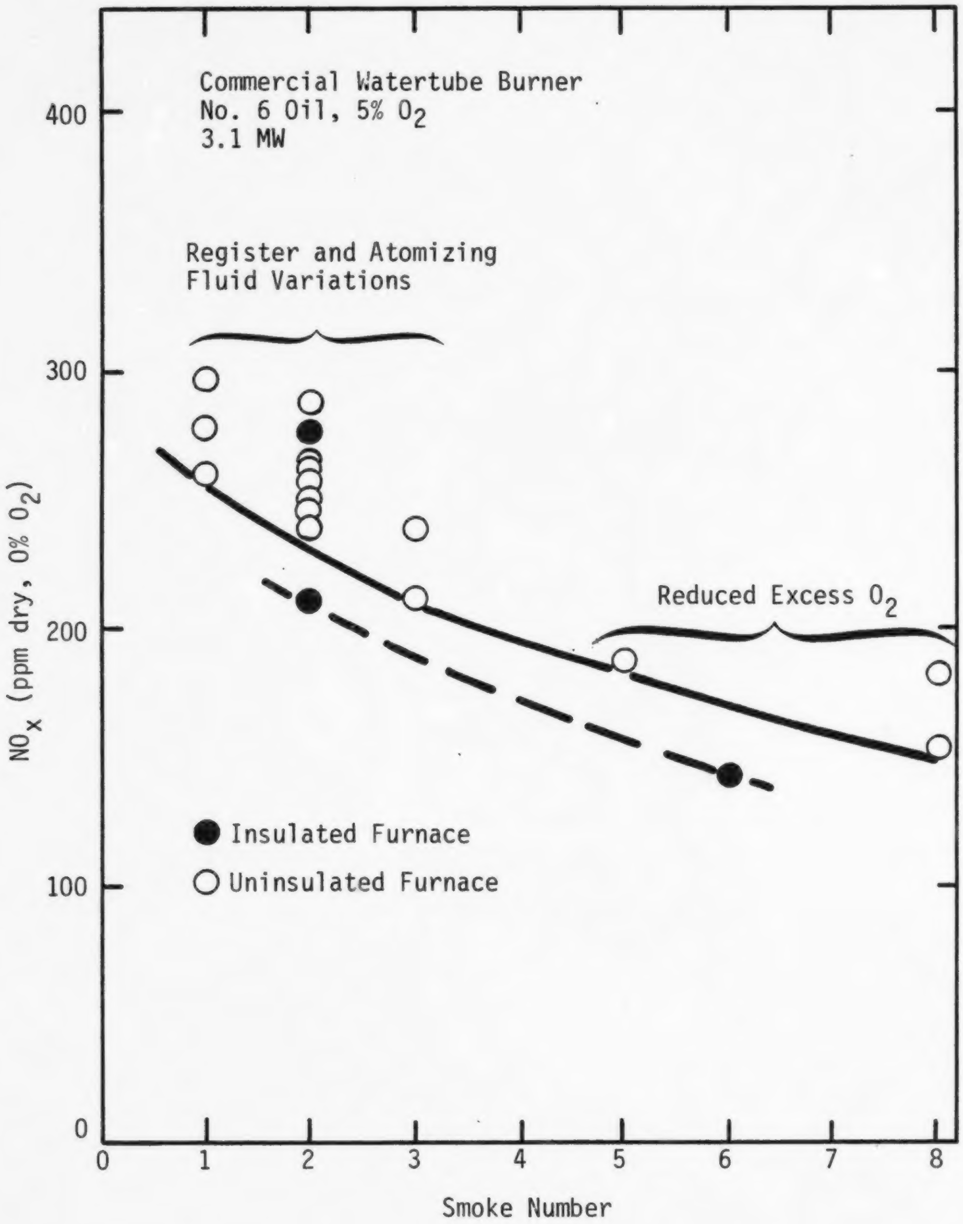

Figure 3-10. Commercial watertube burner--effect of register variations on NO_x vs. smoke emissions (No. 6 oil).

particulate burnout. This result is probably specific to this furnace/burner combination, and the effect of increasing furnace temperature with other configurations may result in a different tradeoff between decreased smoke emissions and increased thermal NO_x formation.

3.3 Distributed Mixing Burner Tests

A series of tests was conducted on the distributed mixing burner designed for coal firing under another EPA project. Tests were conducted with the California No. 6 oil only. The objective of these tests was to determine if external staging utilizing tertiary air ports outside the burner throat would yield substantially lower NO_x emissions compared to the commercial watertube burner. Extensive tests were not conducted to optimize all of the possible DMB burner parameters (i.e. swirl, air distribution).

The distributed mixing burner which was tested is illustrated in Figure 3-11. This burner was originally designed for coal-firing and was developed under EPA Contract 68-02-2667. For these tests, an oil atomizer was placed on the burner axis and only primary air was supplied through the coal nozzle.

Combustion air is divided into three passages within the burner throat and four external ports. Swirl and air flow is adjustable for each passage within the burner throat. The burner achieves low-NO_x emissions by delayed fuel/air mixing. The burner throat is designed to operate fuel-rich and the remaining combustion air is added through the four external tertiary air ports. Burner throat diameter is 0.32 meters. This results in an average air velocity at the throat of 11.5 meters per second with 135°C air preheat, 2.9 MW load and a burner zone stoichiometric ratio (SR_B) of 0.7. Air velocity through the tertiary ports is 8.1 meters per second with 16 percent excess air (3 percent excess oxygen). These velocities are lower than the original design point for coal firing primarily because available air preheat on the SWS facility (135°C) is much lower than the design point which is typical of full-scale systems (320°C).

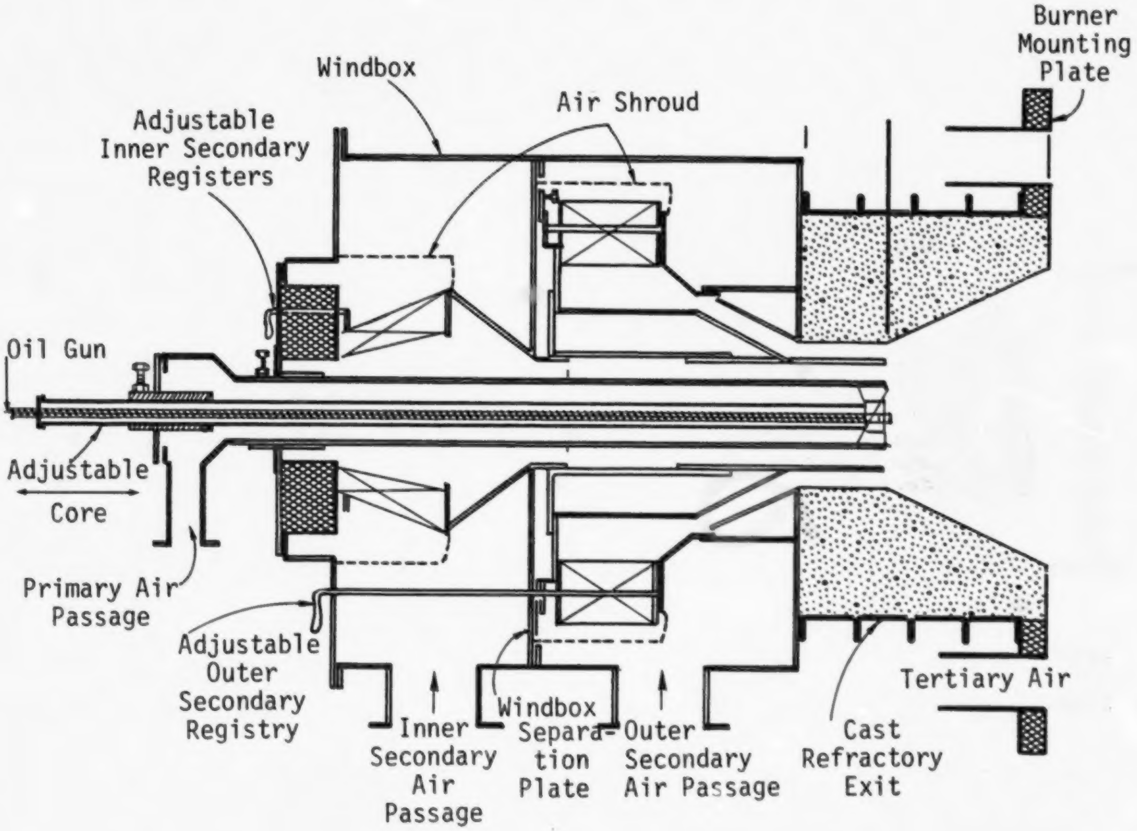
Burner Mounting Plate
Windbox
Air Shroud
Adjustable Inner Secondary Registers
Oil Gun
Adjustable Core
Primary Air Passage
Adjustable Outer Secondary Registry
Inner Secondary Air Passage
Windbox Separa-tion Plate
Outer Secondary Air Passage
Cast Refractory Exit
Tertiary Air

Figure 3-11. 2.9 MW distributed mixing burner.

Two commercial twin-fluid atomizers were used during the tests: the internal-mixing atomizer supplied with the commercial watertube boiler burner (Figure 3-4) and an ultrasonic atomizer similar to that used in the small pilot scale tests. The atomizer employs a central venturi-shaped passage for atomizing fluid with oil injected through holes in the divergent section. A hollow cup is suspended in front of the nozzle which, according to the manufacturer, causes the air stream to resonate and improves atomization fineness. Air was used as the atomizing fluid.

3.3.1 Experimental Results

NO_x emissions versus burner zone stoichiometric ratio (SR_B) are shown in Figure 3-12 for both atomizers. CO emissions are less than 100 ppm for all data shown in the figure. SR_B is defined as the fraction of stoichiometric air requirement supplied through the burner throat. NO_x emissions decreased as SR_B decreased. Minimum SR_B was approximately 0.63 with the ultrasonic nozzle before excessive smoke emissions occurred. The burner could be operated at lower SR_B (0.56) with the internal mixing nozzle; however, this did not result in lower NO_x emissions than with the ultrasonic nozzle. Air distribution within the burner throat was varied for some of the data shown in the figure. Nozzle position relative to the burner throat (beginning of the divergent quarl) appeared to have a greater impact on NO_x than air or swirl distribution within the burner throat. This is probably due to the effect of nozzle position on flame stability and early mixing at the base of the flame.

Figure 3-13 shows NO_x emissions plotted versus smoke number for all test conditions with the DMB. It can be seen that those conditions which gave highest NO_x emissions gave lowest smoke, and vice versa. Neither atomizer appeared to offer a distinct advantage in terms of smoke versus NO_x, although stable flames with moderate smoke emissions were more easily achievable with the internal mixing nozzle than with the ultrasonic nozzle. This was probably due to better matching of the fuel spray pattern with the combustion air flow field. Optimum NO_x emissions for smoke number of 6 were approximately 160 ppm (corrected to zero percent excess O_2).

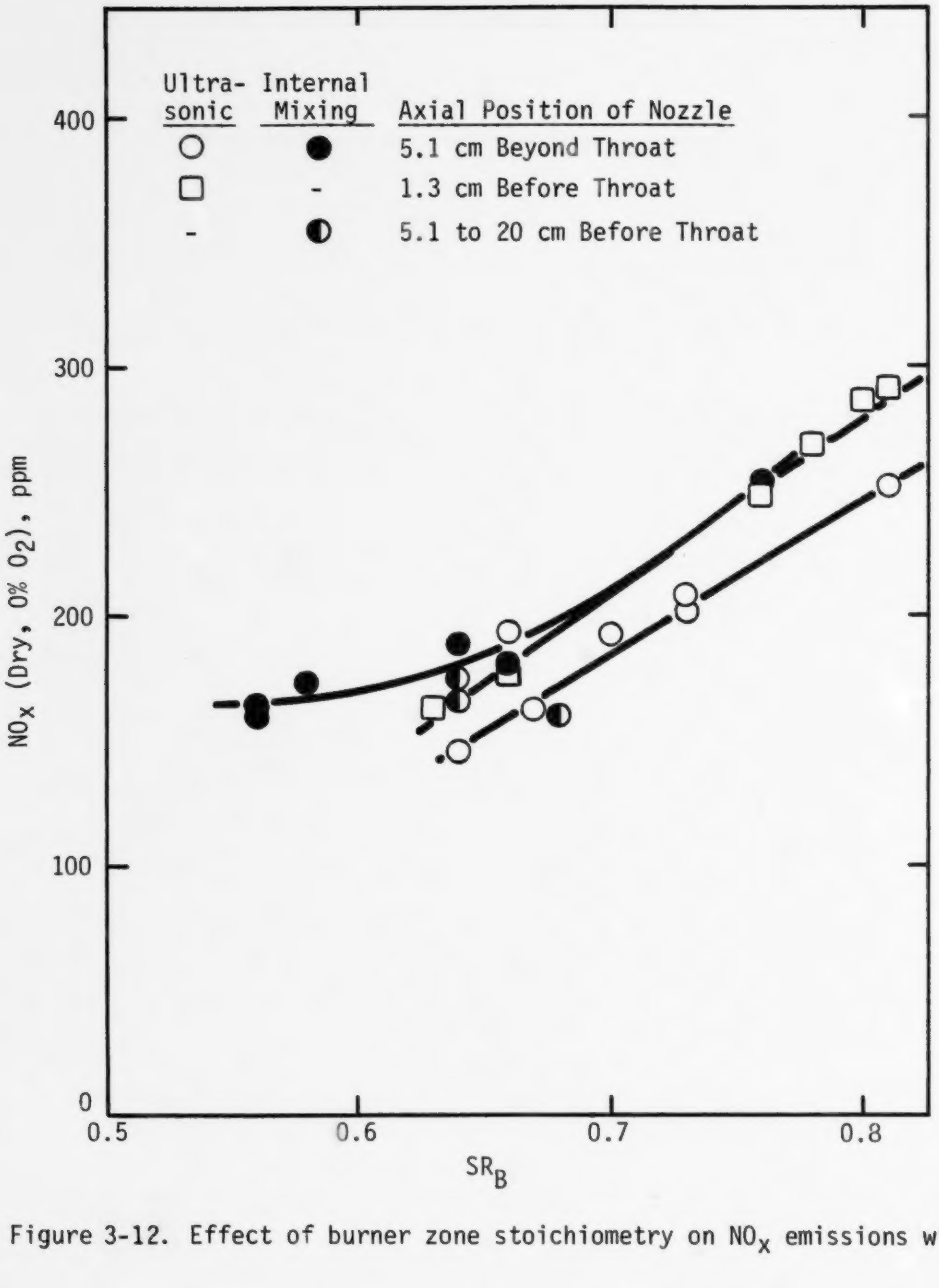

Figure 3-12. Effect of burner zone stoichiometry on NO_x emissions with DMB.

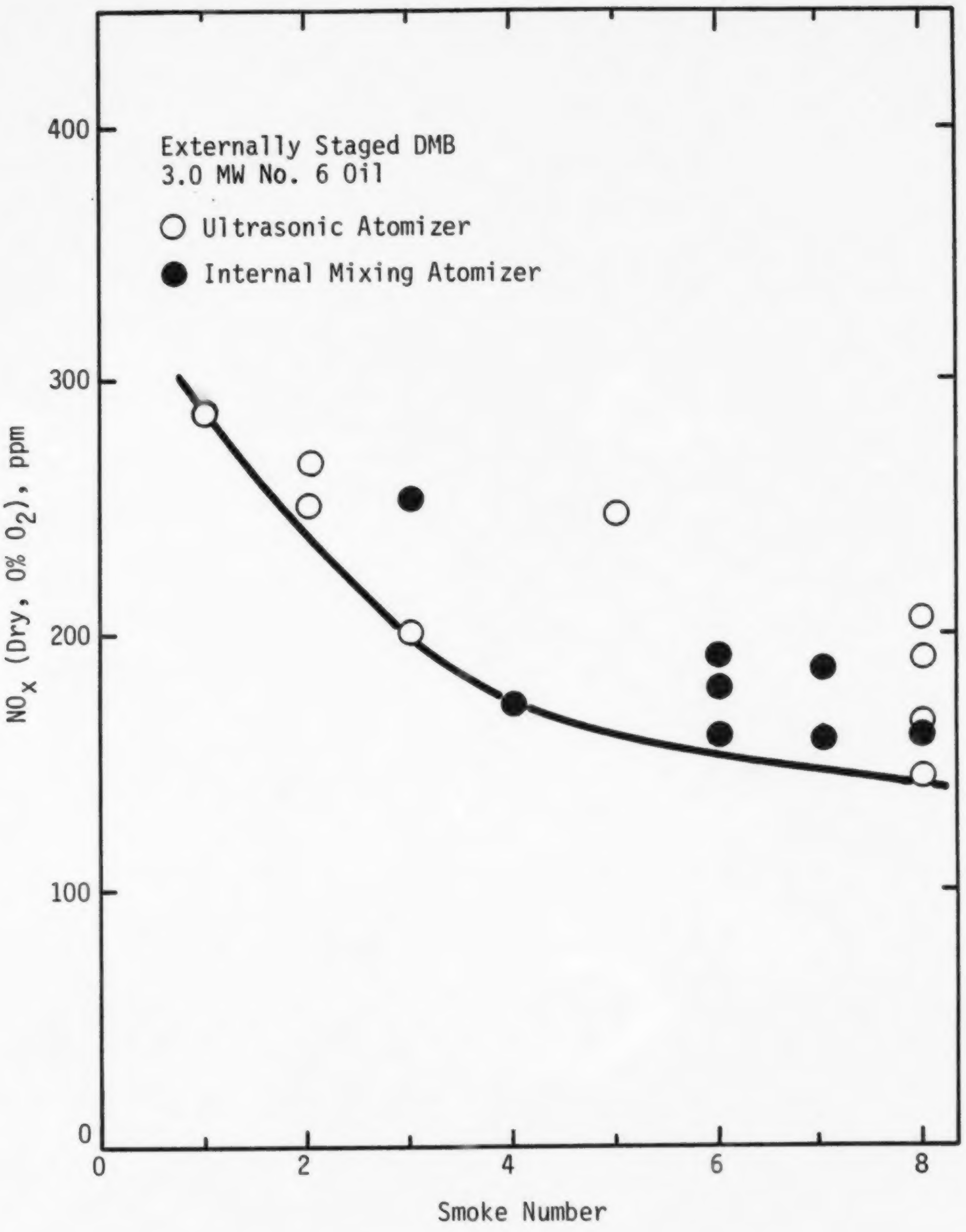

Figure 3-13. Optimum NO_x emissions from DMB.

3.4 Advanced Prototype Burner Tests

A 3.5 MW_{th} version of the experimental prototype burner developed in the small pilot scale studies was constructed and tested in the SWS in order to validate the conceptual low-NO_x design criteria and to investigate scaling effects. The burner was designed according to the same criteria presented earlier in Table 2-5. Additional flexibility was built into the secondary air register to permit variation of secondary air swirl level as a design parameter.

The burner is illustrated in Figure 3-14. As in the earlier design, it too is constructed of high-temperature insulating castable materials layered to minimize heat losses through the wall. The mean gas residence time in the primary zone was 410 milliseconds at $SR_1 = 0.7$ and 1540°C gas temperature. Primary air and fuel are premixed in a premix table similar to that used in the small pilot scale design. An ultrasonic atomizer was also used without the resonator cap. Fuel and primary air are admitted into the primary zone through an abrupt expansion (zero-angle quarl) entrance. The main primary zone chamber has $L/d = 2$ and five sample ports were included to permit temperature and species measurements. The main chamber diameter reduces from approximately 1.0 meter to 0.5 meter at the chamber exit to minimize heat loss from and backmixing into the primary zone. Secondary air is admitted into the SWS furnace through an annulus surrounding the primary zone exit. Combustion is completed in the SWS furnace.

The objectives of these tests were to obtain information on direct scaleup of the earlier burner design. An extensive test series was not conducted. The tests included variation of first-stage stoichiometry, thermal input (heat release), overall excess air, and secondary air swirl. Two levels of primary air preheat were investigated and all of the tests were conducted using a California residual oil similar to that described earlier in Section 3. Fuel nitrogen content was 0.68 percent by weight.

Figures 3-15 and 3-16 present NO_x and smoke emissions as a function of load and primary air preheat level. Secondary air was not preheated. At 2.9

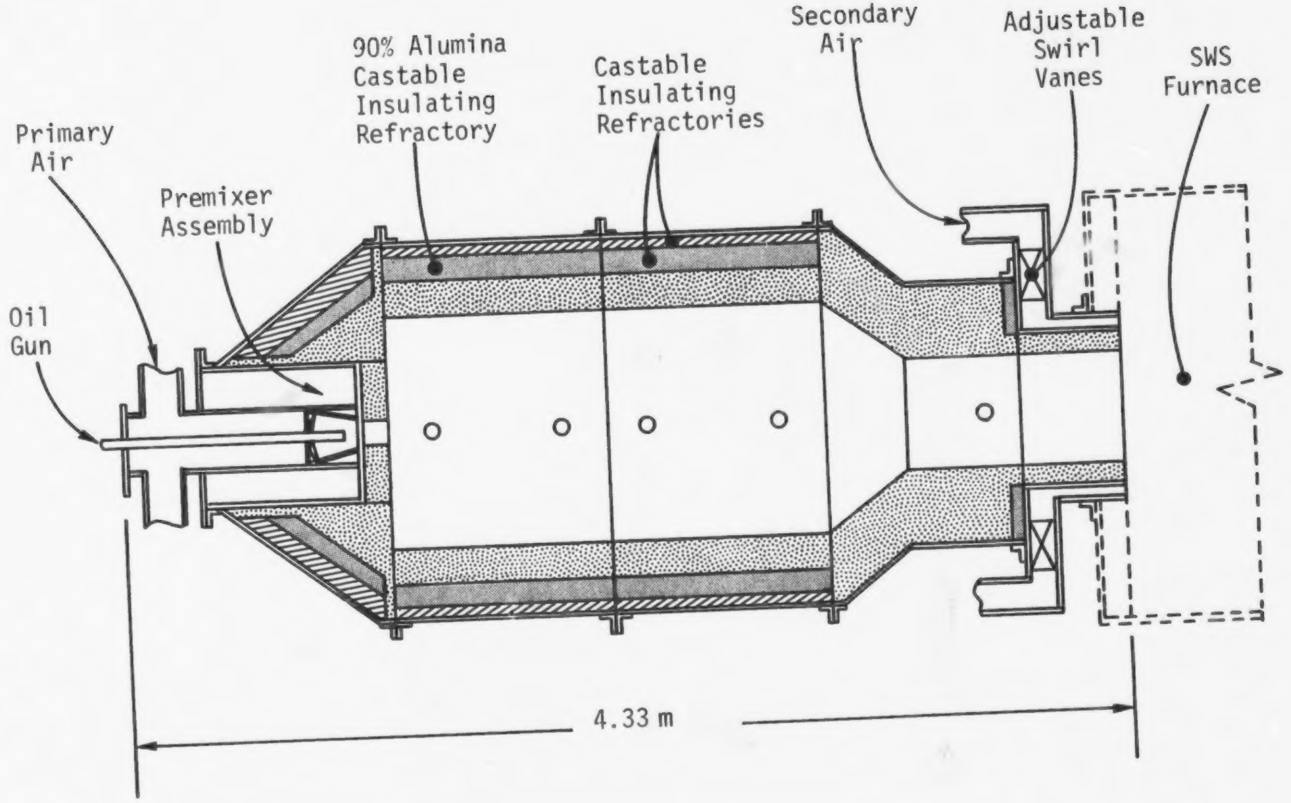
Primary Air
Premixer Assembly
90% Alumina Castable Insulating Refractory
Castable Insulating Refractories
Secondary Air
Adjustable Swirl Vanes
SWS Furnace
Oil Gun
4.33 m

Figure 3-14. 3.5 MW_{th} experimental prototype burner.

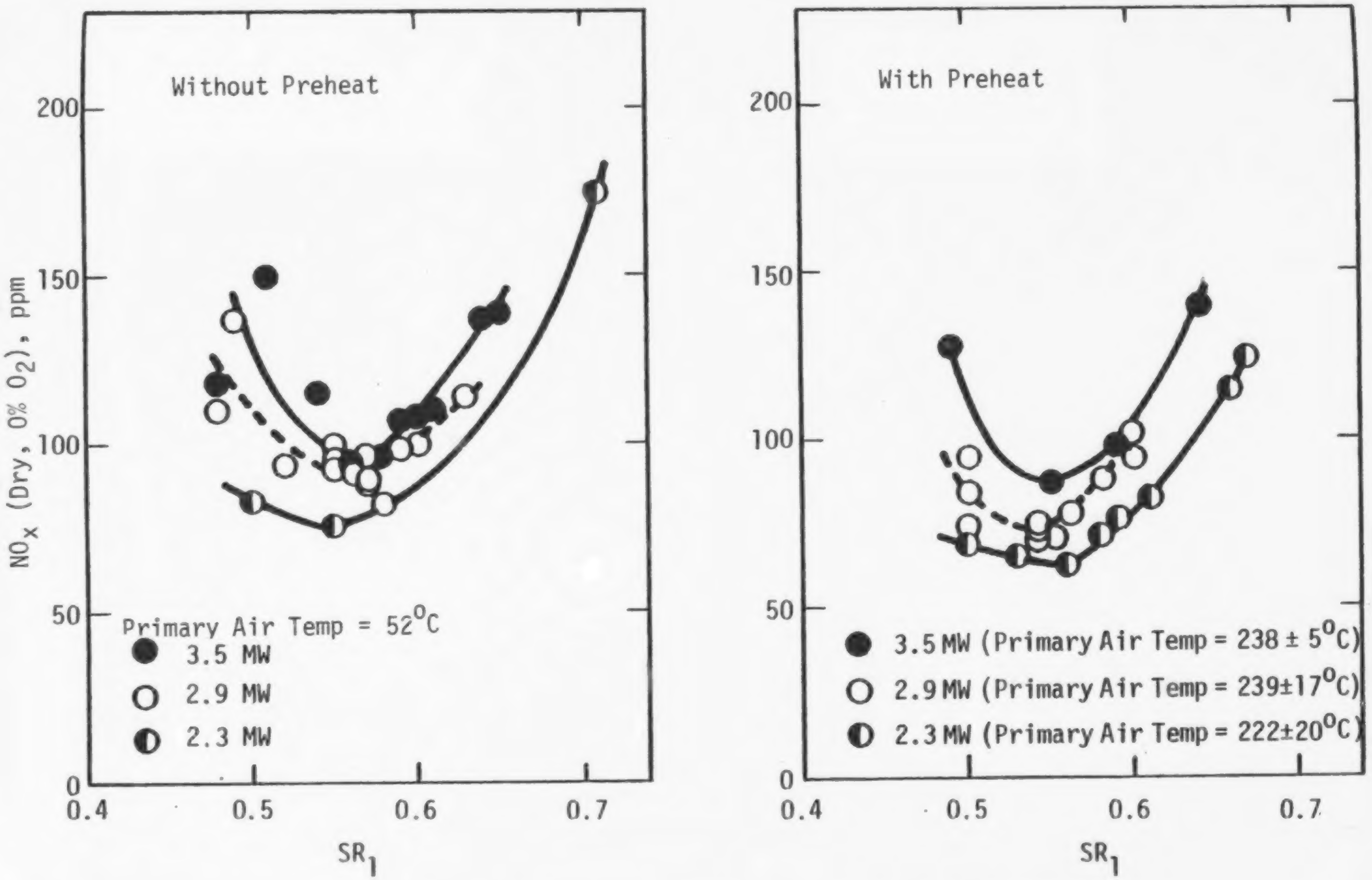

Figure 3-15. Effect of load and primary air preheat on NO$_x$ emissions.

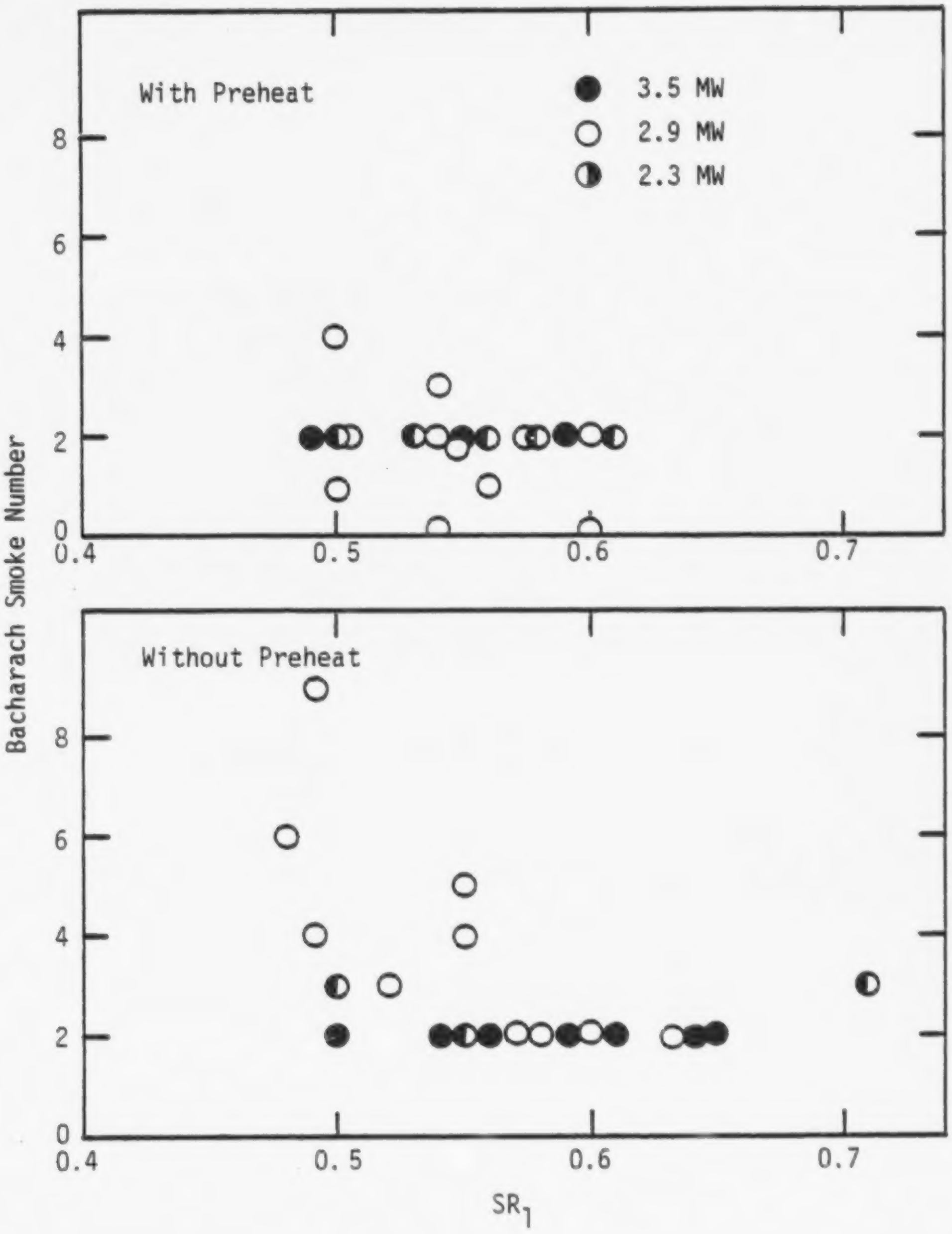

Figure 3-16. Effect of load and primary air preheat on smoke emissions.

MW, NO_x levels reached a minimum of approximately 92 ppm, corrected to zero percent oxygen (all data presented in this report are taken at near 3 percent overall excess oxygen and corrected to zero percent oxygen unless otherwise noted) with no first-stage air preheat. This corresponds to 79 ppm at 3 percent oxygen. Increasing first-stage air preheat to 239°C (± 17°C) but maintaining ambient temperature second-stage air decreased NO_x emissions to approximately 73 ppm (63 ppm at 3 percent oxygen). The optimum stoichiometric ratio decreased slightly with the increase in air temperature, from 0.56 to 0.54.

Smoke emissions were similar with and without primary air preheat (Figure 3-16). Smoke was generally low at the minimum NO_x condition (Bacharach smoke numbers 2 to 4) and increased sharply as stoichiometry was further reduced below optimum.

Minimum NO_x emissions increased with load, ranging from 95 ppm to 77 ppm at 3.5 to 2.3 MW load, respectively, without first-stage air preheat. With first-stage air preheat, minimum NO_x ranged from 88 to 63 ppm at the same loads, respectively. The optimum stoichiometry in the first-stage was not shifted significantly. Optimum SR_1 varied from 0.54 to 0.56 with preheat and from 0.55 to 0.57 without preheat. Smoke emissions were insensitive to load.

The effect of inducing swirl on the secondary air with the annular injector was small (Figure 3-17) producing a decrease in minimum NO_x of 10 ppm over the baseline condition. Although the swirl register was designed to yield a high swirl number for secondary air, the swirl induced to the total stream is much less. A very minor change in flame shape was observed with the addition of swirl. The importance of second-stage air on NO_x emissions was discovered when the annulus was distorted by heat during a series of tests, producing an unsymmetric air flow from the annulus. This maldistribution of air could be seen in the unsymmetric flame produced and in an upward shift in the baseline NO_x emissions (Figure 3-17). This also pointed out some of the practical difficulties associated with maintaining a narrow, uniform annular passage surrounding the burner exit.

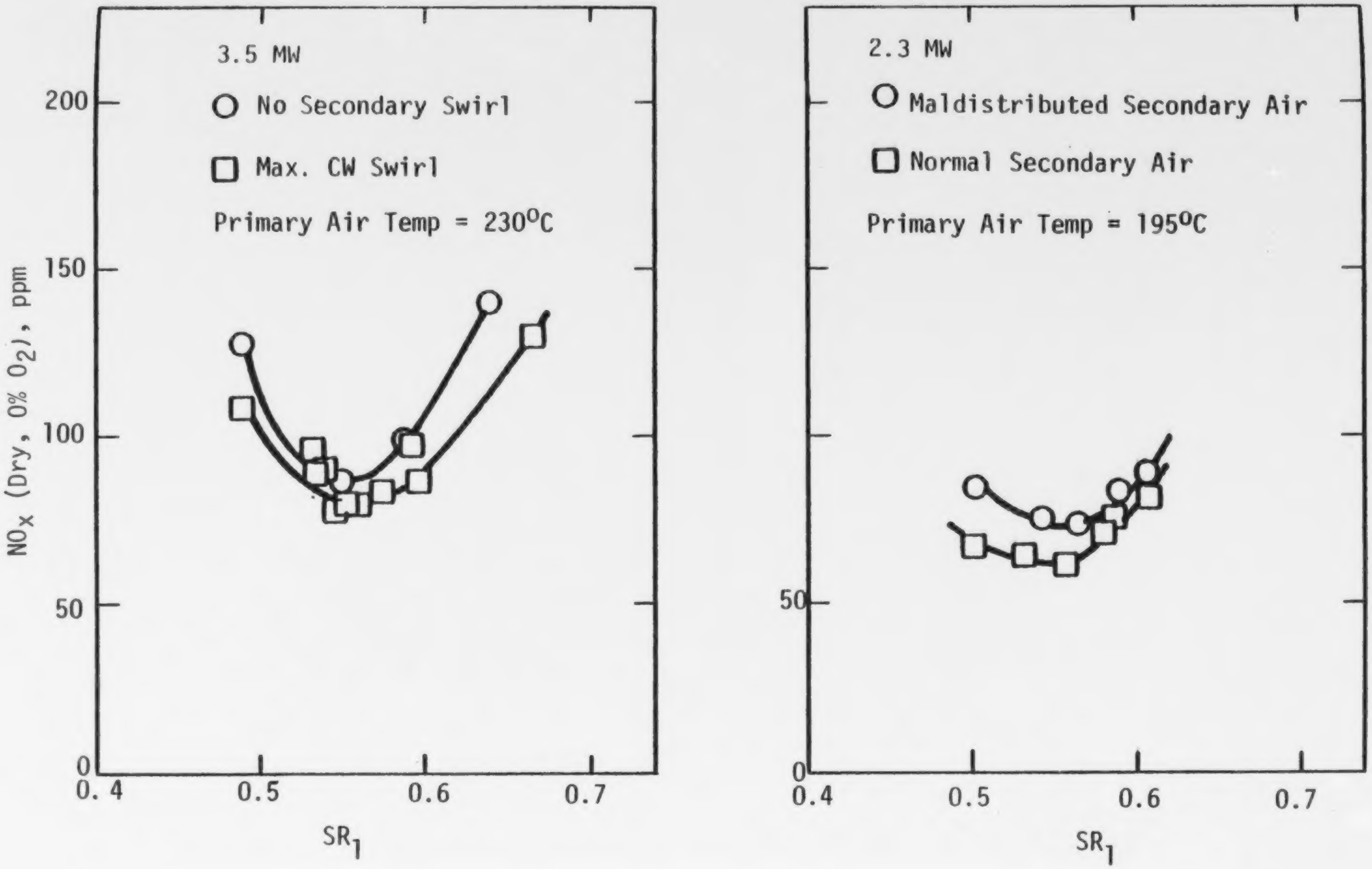

Figure 3-17. Effect of annular air swirl and air distribution.

Figure 3-18 illustrates the effect of overall excess O_2 on NO_x emissions. Overall excess O_2 was varied by changing secondary air flow while maintaining primary zone conditions constant. NO_x was relatively insensitive to excess O_2 regardless of load. Smoke emissions (not shown) were low with Bacharach smoke number less than 4 for all data shown on the figure except at 0.3 percent excess O_2. Since NO_x emissions were not strongly affected by excess O_2 level, this suggests that thermal NO_x formation in the second stage is not significant.

These data confirm that the design criteria established earlier were sufficient to permit successful scaleup of the low-NO_x concept. In addition, these tests confirmed the hypothesis that increased primary zone temperature in a primary air preheat is beneficial. The data also indicate that optimum SR_1 decreases with increasing scale, as shown in Figure 3-19. This can be attributed to increased primary zone temperature with increased load because lower surface-to-volume ratios lead to lower heat losses as scale increases. This effect can be expected to diminish with further increases in burner scale.

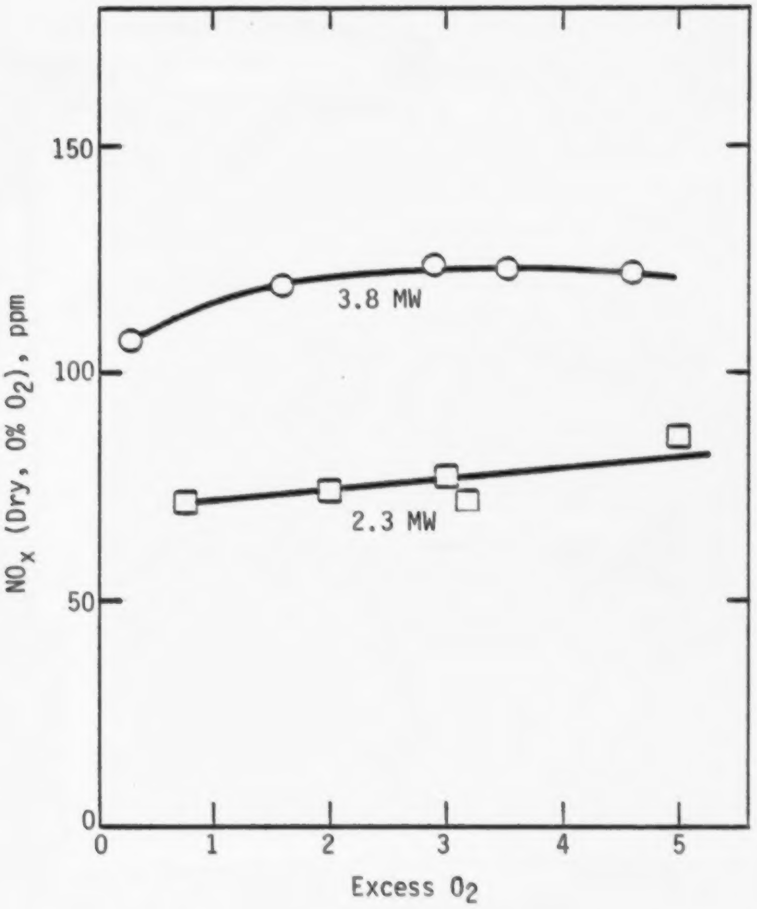

Figure 3-18. Influence of excess air on second-stage NO_x.

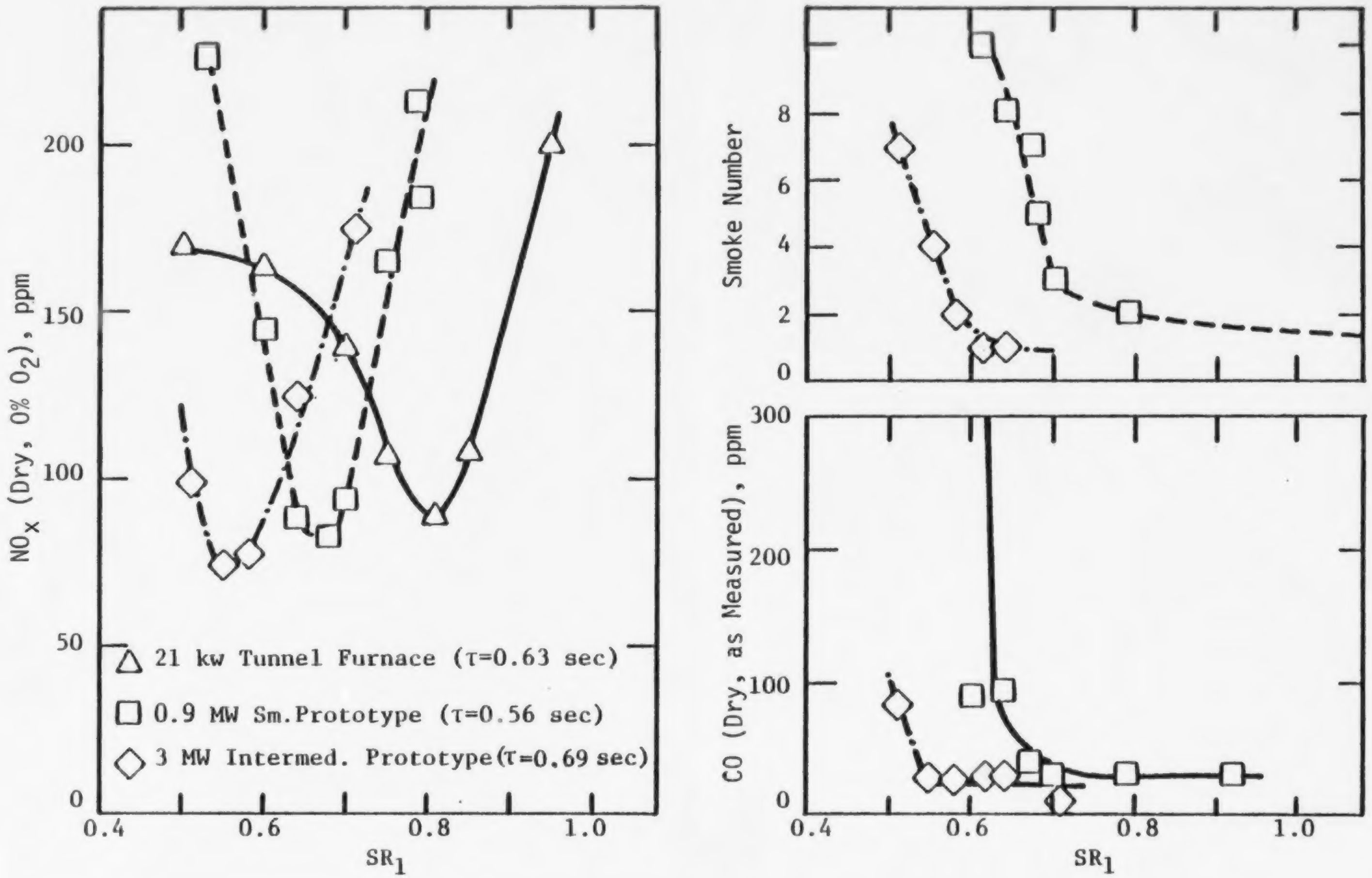

Figure 3-19. Influence of first-stage stoichiometry on NO$_x$, CO, and smoke emissions (bench scale and pilot scale, California residual fuel oil).

4.0 REFERENCES

1. England, G. C., et al., "Effects of Fuel Properties and Atomization Parameters on NO_x Control for Heavy Liquid Fuel Fired Package Boilers." EPA Report No. 600/7-82-029, April 1982.

2. Heap, M. P., et al., "Control of Pollutant Emissions from Oil-Fired Package Boilers." Proceedings of the Stationary Source Combustion Symposium, EPA 600/2-76-152b, June 1976.

3. Kramlich, J., M. P. Heap, W. R. Seeker, and T. J. Tyson, "Fundamental Combustion Research Applied to Pollution Control - Volume 1: Gas Phase Chemistry." Final Report, EPA Contract 68-02-2631, April 1981.

4. Muzio, L. J. and R. P. Wilson, Jr., "Experimental Combustor for Development of Package Boiler Emission Control Techniques--Phase I of III." EPA-R2-73-292a, 1973.

5. Perry, R. H. and C. H. Chilton, "Chemical Engineers' Handbook." Fifth edition, McGraw-Hill, New York, New York, 1973.

6. Pierce, R. M., S. A. Mosier, C. E. Smith, and B. S. Hinten, "Advanced Combustion Systems for Stationary Gas Turbine Engines: Volume II. Bench-Scale Evaluation." Final Report, EPA 600/7-80-017b, January 1980.

7. Sarofim, A. F., J. H. Pohl, and B. R. Taylor, "Mechanisms and Kinetics of NO_x Formation: Recent Developments." Paper presented at 69th Annual Meeting AIChE, Chicago, Illinois, November 1976.